International Atomic Energy Agency

INDC(BLR)-013
Distr. L

INDC INTERNATIONAL NUCLEAR DATA COMMITTEE

FISSION LEVEL DENSITY AND BARRIER PARAMETERS FOR ACTINIDE NEUTRON-INDUCED CROSS SECTION CALCULATIONS

Final Report of Research Contract 8832/RB

V.M. Maslov

Radiation Physics & Chemistry Problems Institute
220109, Minsk-Sosny, Belarus

October 1998

IAEA NUCLEAR DATA SECTION, WAGRAMERSTRASSE 5, A-1400 VIENNA

Reproduced by the IAEA in Austria

October 1998

INDC(BLR)-013
Distr. L

FISSION LEVEL DENSITY AND BARRIER PARAMETERS FOR ACTINIDE NEUTRON-INDUCED CROSS SECTION CALCULATIONS

Final Report of Research Contract 8832/RB

Time period covered: 15 December 1995 - 14 June 1998

V.M. Maslov

Radiation Physics & Chemistry Problems Institute
220109, Minsk-Sosny, Belarus

Abstract

Fission and total level densities modelling approach was developed. Neutron-induced fission cross section data for incident energies from 10 keV up to emissive fission threshold were employed to extract level density and fission barrier parameters. In particular, fission barrier parameters (inner barrier height, outer barrier height, curvatures) were extracted for altogether 49 isotopes of Th, Pa, U, Np, Pu, Am, Cm, Bk and Cf. The adopted level density modelling approach and fission barrier parametrization was supported by calculations of fission cross section data above the emissive fission threshold, up to 20 MeV neutron incident energy.

Summary

Adopted fission and total level densities modelling along with fission barrier parameters allowed to describe available neutron-induced fission cross section data for Th, Pa, U, Np, Pu, Am, Bk,Cm and Cf target nuclei. The data for incident neutron energies ~10 keV up to emissive fission threshold were analyzed. Saddle asymmetries relevant to SCM calculations influence fission barriers, extracted by cross section data analysis. The inner barrier was assumed axially symmetric in case of U, Np and Pu neutron-deficient nuclei. We have demonstrated that observed irregularities in neutron-induced fission cross section data could be attributed to the interplay of few-quasiparticle excitations in the level density of fissioning and residual nuclei. In case of Z-even, N-odd fissile targets the step-like irregularities in fission cross section data shapes are supposed to be due to interplay of two-quasiparticle excitations in the level density of even fissioning nucleus and one-quasiparticle excitation in odd residual nucleus. In case of the only available Z-odd, N-odd target ^{242m}Am the effect of Z-odd, N-even fissioning nucleus level density is evidenced as a step-like shape of fission cross section data below 1 MeV. In case of Z-even, N-even targets neutron-induced fission the step-like structures (U, Pu) and resonance-like structures (Cm) were interpreted to be due to interplay of one-quasiparticle excitations in the level density of odd fissioning nucleus and two-quasiparticle excitation in even residual nucleus. The sophistication of the level density modelling seems to be unavoidable, since it is backed by experimental data. That is the price to be paid for consistent modelling of fission cross section data behavior and extracting reasonable level density and fission barrier parameter values. Fission barrier parameters: inner(A) and outer(B) barrier heights $E_{fA(B)}$ and curvatures $\hbar\omega_{A(B)}$ are provided.

Level density modelling and fission barrier parameters were applied for fission data description up to 20 MeV incident neutron energy. Secondary neutron spectrum model was validated by ^{238}U neutron data description.

Contents

1 Introduction

Neutron-induced fission cross section data base for actinides (Th, Pa, U, Np, Pu, Am, Cm, Cf) provides a fair chance to develop a theoretical tools to predict competing reaction cross sections, like neutron inelastic scattering, radiative capture and (n,xn). In most cases fission data description serves as the only constraint for these reaction cross section estimation. At the other hand, theoretical calculations are desirable to fill the gaps for nuclei where fission cross section data are lacking. For this purpose theoretical parameter systematics are highly desirable for smooth interpolations. Fission barrier parameters and fissioning nucleus level densities are key ingredients involved in neutron-induced actinide fission cross section calculations. Confidence with which theoretical fission barrier parameters could be calculated from Strutinsky-type theory [1] (Shell Correction Method (SCM)) is not better than $\sim$1 MeV, which is completely unacceptable for fission cross section data prediction. Anyway, theoretical fission barrier parameter trends, especially for neutron-rich nuclei might be of some value. General trends inferred from SCM calculations [2] might be correlated with the behavior of fission cross sections. Fission level density might be considered to be in a worse shape than level density at equilibrium deformation, since there is no relevant direct measured data. Neutron-induced fission cross section data provide a sound basis to extract fission barrier parameters and elaborate level density modelling approach. We will analyze neutron induced fission data for fissile targets from $\sim$1 keV up to emissive fission threshold. For non-fissile nuclei in sub-threshold energy region we would not address the consequences of intermediate structure in fission cross sections and deal only with "gross shape" of fission cross section. Irregularities in fission cross sections in MeV incident neutron energy region would be investigated, to correlate them with theoretical fission barrier and level density parameter trends. The important point is that fission level density and barrier parameters are strongly interdependent. The level density of deformed nucleus depends on collective properties, pair correlations and shell structure of nucleus. These effects were introduced in SCM calculations of fission barriers and they should be "imbedded" into the level density model either at saddle and equilibrium deformations. These could be accomplished within framework of generalized superfluid model [3].

There exist a lot of experimental signatures which would be used to test the validity of the model and importance of collective, pairing and shell effects at equilibrium and saddle deformations. We will demonstrate that one needs the sophistication in level density modelling to enable correct

definition of parameters involved in actinide (Th-Cf) neutron-induced cross section calculations. It will be shown that observed irregularities in neutron-induced fission cross section data could be attributed to the interplay of few-quasiparticle excitations in the level density of fissioning and residual nuclei [4, 5].

The shell structure effects are usually introduced as level density $a-$parameter dependence on the excitation energy. The shell effects dumping affects the first chance fission cross section behavior at excitation energies above emissive fission threshold. The impact of collective, pair correlation and shell effects on calculated fission cross sections varies with increasing excitation energy [44], [45].

2 THE STATISTICAL MODEL

Average fission cross sections are treated within Hauser-Feshbach [7] theory, coupled channel optical model and double-humped fission barrier model [1]. In case of actinide fissioning compound nuclei produced by fast neutron interaction with target nuclei, the main competing channels against fission are neutron scattering and radiative neutron capture. Below there is a short outline of the statistical model employed.

2.1 Cross Section Formula

In the statistical theory of nuclear reactions the neutron-induced fission reaction cross section is given by

$$\sigma_{nf}(E) = \frac{\pi \lambda\!\!\!^{-2}}{2(2I+1)} \sum_{ljJ\pi} (2J+1) T_{lj}^{J\pi}(E) P_f^{J\pi}(E) S. \qquad (1)$$

Here, the fission probability of the compound nucleus with excitation energy U for given spin J and parity π, $P_f^{J\pi}(E)$, is

$$P_f^{J\pi}(E) = \frac{T_f^{J\pi}(U)}{T_f^{J\pi}(U) + T_n^{J\pi}(U) + T_\gamma^{J\pi}(U)}, \qquad (2)$$

where $U = B + E$ is the excitation energy of the compound nucleus, B is the neutron binding energy, E is the incident neutron energy, $T_{lj}^{J\pi}$ are the entrance neutron transmission coefficients for the channel $(ljJ\pi)$, $\overrightarrow{J} = \overrightarrow{I} + \overrightarrow{j}$, $\overrightarrow{j} = \overrightarrow{l} + \overrightarrow{s}$, I is the target nucleus spin, l an s are orbital momentum and spin of the neutron, $T_f^{J\pi}$, $T_n^{J\pi}(U)$ and $T_\gamma^{J\pi}(U)$ are the transmission coefficients of the fission, neutron scattering and radiative decay channels, and $S_{nf}^{ljJ\pi}$ denotes partial widths Porter-Thomas fluctuation factor. Below incident neutron energy equal to the cut-off energy of discrete level spectra the neutron cross sections were calculated within Hauser-Feshbach approach

with correction for width fluctuation [6]. For partial width fluctuation correction calculation only Porter-Thomas fluctuations are taken into account. Effective number of degrees of freedom for fission channel is defined at the higher fission barrier saddle as $\nu_f^{J\pi} = \mathrm{T}_f^{J\pi}/\mathrm{T}_{f\,\mathrm{max}}^{J\pi}$, where $\mathrm{T}_{f\,\mathrm{max}}^{J\pi}$ is the maximum value of the fission transmission coefficient $\mathrm{T}_f^{J\pi}$. At higher incident neutron energies approach by Tepel et al. [8] is employed.

2.2 Fission Channel

Analyzing neutron-induced fission data in a double humped fission barrier model, fission process can be viewed as a two-step process, i.e. a successive crossing over the inner hump A and over the outer hump B. Hence, the transmission coefficient of the fission channel $T_f^{J\pi}\ (U)$ can be represented as

$$T_f^{J\pi}(U) = \frac{T_{fA}^{J\pi}(U) T_{fB}^{J\pi}(U)}{(T_{fA}^{J\pi}(U) + T_{fB}^{J\pi}(U))}. \tag{3}$$

The transmission coefficient $T_{fi}^{J\pi}(U)$ is defined by the transition states and level density $\rho_{fi}(\epsilon, J, \pi)$ of the fissioning nucleus at the inner and outer humps (i = A,B, respectively):

$$\begin{aligned} T_{fi}^{J\pi}(U) &= \sum_{K=-J}^{J} T_{fi}^{JK\pi}(U) + \int_0^U \frac{\rho_{fi}(\epsilon, J, \pi) d\epsilon}{(1 + \exp(2\pi(E_{fi} + \epsilon - U)/h\omega_i))}, \\ T_{fi}^{JK\pi}(U) &= \frac{1}{(1 + \exp(2\pi(E_{fi} + \varepsilon_{fi}^{JK\pi} - U)/h\omega_i))}, \end{aligned} \tag{4}$$

where the first term denotes the contribution of low-lying collective or single-particle states $\varepsilon_{fi}^{JK\pi}$ and the second term that from the continuum levels at the saddle deformations, ϵ is the intrinsic excitation energy of fissioning nucleus. The first term contribution due to discrete transition states as well as the total level density $\rho_{fi}(\epsilon, J, \pi)$ of the fissioning nucleus are determined by the order of symmetry of nuclear saddle deformation [9]. Theoretical fission barrier height values and saddle order of symmetry are interdependent, the same is the case with our model parameters, i.e. inner and outer fission barrier heights and curvatures as well as level densities at both saddles.

According to shell correction method calculations for actinides by Howard and Möller [2] the following tendencies were anticipated. In case of the actinide nuclei of interest outer fission barrier retains axial symmetry while being mass asymmetric. Inner barrier of higher mass nuclides ($A > A_{tr}$) is triaxially asymmetric during fission process, as has first been noted by Pashkevich [10], while that of lower mass fissioning nuclides ($A \leq A_{tr}$) retains axial symmetry. The transition $A-$value A_{tr} depends on Z and N of fissioning nucleus. It was calculated by Howard and Möller [2] that axially

symmetric inner saddle becomes lower than the triaxially asymmetric one by ~1 MeV. This peculiarity would be probed for U, Np and Pu nuclei. The most explicit evidence of this peculiarity was encountered in case of ^{232}U(n,f) data analysis. This can explain the non-threshold behavior of measured data at low incident neutron energies [11].

2.2.1 Z-even, N-even fissioning nuclei transition spectra

The discrete transition spectra contribution $\sum_{K=-J}^{J} T_{fi}^{JK\pi}(U)$ to the fission transmission coefficient is dependent upon the order of symmetry for fissioning nucleus at inner and outer saddles. In case of axial symmetry at the inner saddle the band-heads spectra are similar to those at equilibrium deformation. In case of axial asymmetry at the inner saddle the $\gamma-$vibration $K^\pi = 2^+$ band-head is sufficiently lowered. The position of negative parity band $K^\pi = 0^-$ at outer saddle is lowered due to mass asymmetry and is almost degenerate with lowest state $K^\pi = 0^+$. In case of ^{234}U and ^{236}U fissioning nuclides the inner barrier of fissioning nuclides is lower than outer one, in case of Pu, Cm and Cf nuclei addressed here the higher barrier is the inner one. That means that we can fix basically the discrete transition spectra at outer saddle fitting ^{233}U(n,f) and ^{235}U(n,f) data. The discrete transition spectra at inner saddle could be fixed fitting ^{239,241}Pu(n,f), ^{243,245,247}Cm(n,f) and ^{249}Cf(n,f) measured data. Table 1 shows adopted band-heads of the transition spectra for inner and outer saddles, note the effect of axial asymmetry on $E_{2^-}^{nonax}$ position.

Table 1

Transition spectra band-heads of Z-even, N-even nuclei

inner saddle			outer saddle	
K^π	$E_{K^\pi}^{ax}$, MeV	$E_{K^\pi}^{nonax}$, MeV	K^π	E_{K^π}, MeV
0^+	0.0	0.0	0^+	0.0
2^+	0.5	0.1	2^+	0.5
0^-	0.4	0.4	0^-	0.2
1^-	0.4	0.4	1^-	0.5

2.2.2 Z-even, N-odd fissioning nuclei transition spectra

Each one-quasiparticle state in odd fissioning nucleus is assumed to have a rotational band built on it with a rotational constant, dependent upon the respective saddle deformation (see below). We construct the discrete transition spectra up to ~100 keV, using one-quasiparticle states by Bolsterli et al. [12] (see Table 2). Due to the axial asymmetry at the inner saddle

the number of rotational states increases and we additionally assume $(2J+1)$ rotational levels for each J value. The negative parity bands $K^\pi = 1/2^-, 3/2^-, 5/2^-$ ... at outer saddle are assumed to be doubly degenerate due to mass asymmetry. With transition state spectra thus defined the fission barrier parameters could be searched for. The $s-$wave fission widths $\Gamma_f^{1/2+}$ calculated at incident neutron energy of ~0.1 keV should be compatible with average fission width obtained from unresolved resonance region.

Table 2

Transition spectra band-heads Z-even, N-odd nuclei

inner saddle		outer saddle	
K^π	E_{K^π}, MeV	K^π	E_{K^π}, MeV
$1/2^+$	0.0	$1/2^+$	0.0
$5/2^+$	0.08	$1/2^-$	0.01
$1/2^-$	0.05	$3/2^+$	0.08
$3/2^-$	0.01	$3/2^-$	0.08
		$5/2^+$	0.01
		$5/2^-$	0.01

2.2.3 Z-odd, N-even fissioning nuclei transition spectra

We construct the discrete transition state spectra for $Z-$odd, $N-$even fissioning nuclei up to 200 keV, using one-quasiparticle states, predicted by Bolsterli et al.[12] in the same way as for $Z-$even, $N-$odd fissioning nuclei. The positive parity bands $K^\pi = 1/2^+, 3/2^+, 5/2^+$ ... at outer saddle are assumed to be doubly degenerate due to mass asymmetry [2]. With transition state spectra thus defined (see Table 3) the fission barrier parameters for ^{243}Am were obtained (see below). The fission widths $\Gamma_f^{9/2-} = 0.435$ eV and $\Gamma_f^{11/2-} = 0.349$ eV were calculated at incident neutron energy of 0.043 keV [13]. These values give average fission width $\langle\Gamma_f\rangle = 0.390$ meV, which is consistent with estimate, obtained from unresolved resonance region.

2.2.4 Z-odd, N-odd fissioning nuclei transition spectra

We will consider here one example of odd-odd nuclide ^{242}Am, since actual spectrum of K^π values much depends on specific nucleus, as distinct from other parity nuclei. In other respects the procedures are similar. The intrinsic two-quasiparticle state spectrum of odd-odd nuclide ^{242}Am at equilibrium deformation were modelled by Sood and Singh [15]. The expected location of still unobserved two-quasiparticle states was predicted. Using these intrinsic states as the band-head energies we have built the rotational bands,

i.e. transition state spectrum of fissioning nuclide ^{242}Am. Due to the axial asymmetry at the inner saddle [2] we additionally assume $(2J+1)$ rotational levels for each J value. The rotational band levels at outer saddle are assumed to be doubly degenerate due to mass asymmetry. With transition state spectra defined in the first 0.2 MeV excitation energy range the fission barrier parameters [14] (see below) were obtained by fitting fission data. The fission width for $s-$wave neutrons $\langle\Gamma_f\rangle$, calculated at incident neutron energy of 0.15 keV is consistent with average fission width value, obtained in unresolved resonance region.

Table 3

Transition spectra band-heads of Z-odd, N-even nuclei

inner saddle		outer saddle	
K^π	E_{K^π}, MeV	K^π	E_{K^π}, MeV
$3/2^-$	0.0	$5/2^+$	0.0
$5/2^+$	0.140	$5/2^-$	0.0
$7/2^-$	0.180	$3/2^+$	0.08
$5/2^-$	0.180	$3/2^-$	0.08
		$1/2^+$	0.04
		$1/2^-$	0.04
		$1/2^+$	0.05
		$1/2^-$	0.05

Table 4

Transition spectra band-heads of $Z-$odd, $N-$odd nuclei

inner saddle		outer saddle	
K^π	E_{K^π}, MeV	K^π	E_{K^π}, MeV
1^-	0.0	1^-	0.0
0^-	0.044	0^-	0.044
5^-	0.049	5^-	0.049
6^-	0.170	6^-	0.170
1^-	0.220	1^-	0.220
3^-	0.242	$3-$	0.242
2^-	0.288	2^-	0.288

2.3 Neutron Channel

The lumped transmission coefficient of the neutron scattering channel is given by

$$T_n^{J\pi}(U) = \sum_{l'j'q} T_{l'j'}^{J\pi}(E - E'_q) + \sum_{l'j'I'} \int_0^{U-U_c} T_{l'j'}^{J\pi}(E')\rho(U - E', I', \pi)dE', \quad (5)$$

where E'_q and $\rho(U - E', I', \pi)$ are discrete levels and level density of the residual nucleus, respectively. The entrance channel neutron transmission coefficients $T_{lj}^{J\pi}$ are calculated within a coupled channel approach.

The deformed optical potential is employed for actinide nuclei. For even-even target nuclei we employed optical potential parameters, defined by fitting total cross section data, angular distributions and $s-$wave strength function for ^{238}U [16]. The quadrupole β_2 and hexadecapole β_4 deformation parameter values were obtained by fitting respective $s-$wave neutron strength function $\langle S_o \rangle$ values for relevant nucleus, other parameter values being unchanged. Deformation parameter values influence the compound cross section values below $\sim$1 MeV, which is important for the correct extraction of fission barrier parameters both for fissile and non-fissile targets. Below follow the potential parameters values for ^{238}U target nucleus [16], coupling schema being 0^+ - 2^+ - 4^+ - 6^+:

$V_R = 46.29 - 0.3E, MeV, r_R = 1.26\ fm, a_R = 0.63\ fm$

$$W_D = \begin{cases} 2.92 + 0.4E, MeV, & E \leq 10 MeV, r_D = 1.26\ fm, a_D = 0.52\ fm \\ 6.92\ MeV, & E > 10\ MeV \end{cases}$$

$V_{SO} = 6.2\ MeV, r_{SO} = 1.12\ fm, a_{SO} = 0.47\ fm, \beta_2 = 0.2054, \beta_4 = 0.075$

In case of even-odd target nuclei deformed optical potential parameters, recommended by Young [17] were employed, in most cases 6 ground state band rotational levels were coupled. The direct excitation of ground state band levels strongly changes the compound nucleus formation cross section as compared with spherical optical model calculations. For the compound nucleus formation cross section calculation the cross sections of the direct excitation of ground state band levels were subtracted from the reaction cross section. The coupled channel calculations as well as the statistical model calculations were performed with the computer code STAT [18], respectively.

The exit neutron transmission coefficients $T_{l'j'}^{J\pi}(E')$ were calculated using the same deformed optical potential, as that for the entrance channel, but without coupling.

2.4 Level Density

Level density is the main ingredient of statistical model calculations. Level density of residual(target) and compound nuclei define transmission coefficients of neutron scattering and radiative decay channels. Fission level densities (or fissioning nucleus level densities at inner and outer saddle deformations) are required for fission transmission coefficient calculation.

Back-shifted Fermi-Gas Model (BFGM)[19], Constant Temperature Model (CTM)[20] and Generalized Superfluid Model (GSM)[3] are widely used for the description of level densities at stable deformations. These models provide approximately identical level density description at excitations close to the neutron binding energy, since they are normalized to reproduce neutron resonance spacing data. It is low excitation energies where they are discrepant, while this energy region is crucial for fission cross section calculations. A drawback of BFGM and traditional CTM approaches is that it is difficult to include in a consistent way pair correlations, collective effects and shell effects. Pair, shell and collective properties of nucleus do not diminish just to renormalization of main level density parameter a, but influence the energy dependence of level densities. The importance of these effects turns out to be more important because they seem to be dependent upon deformation, either equilibrium or saddle. These effects could be easily introduced within basically GSM approach [3].

In adiabatic approximation the total nuclear level density $\rho(U,J,\pi)$ could be represented as the factorized contribution of quasiparticle and collective states:

$$\rho(U,J,\pi) = K_{rot}(U,J)K_{vib}(U)\rho_{qp}(U,J,\pi), \tag{6}$$

where $\rho_{qp}(U,J,\pi)$ is the quasiparticle level density at excitation energy U,spin J and parity π, $K_{rot}(U,J)$ and $K_{vib}(U)$ are factors of rotational and vibrational enhancement of the level density. Equation (6) holds in an adiabatic approximation, when the intrinsic and collective states contributions to the total level density $\rho(U,J,\pi)$ factorize. Shell and pairing effects influence mainly quasiparticle level density. The collective contribution to the level density of deformed nucleus is defined by the nuclear deformation order of symmetry. The actinide nuclei equilibrium deformation is axially symmetric. The order of symmetry of nuclear shape at inner and outer saddles we adopted from SCM calculations by Howard & Möller [2].

For axially symmetric deformations, which are characteristic for equilibrium and outer saddle deformations of actinide nuclei

$$\begin{aligned} K_{rot}^{sym}(U) &= \sum_{K=-J}^{K=J} exp(-K^2/K_o^2) \approx \sigma_\perp^2 = F_\perp t, \\ K_o^2 &= (\sigma_\parallel^{-2} - \sigma_\perp^{-2})^{-1}, \end{aligned} \tag{7}$$

where $\sigma_\perp$ and $\sigma_\parallel$ are the angular momentum distribution parameters, K is the spin J projection on the symmetry axis, t is the thermodynamic temperature. The momentum of inertia $F_\perp$ (perpendicular to the symmetry axis), equals rigid body $F_\perp^{rig}$ value at high excitation energies $U \geq U_{cr}$, when pairing is destroyed,

$$F_{\perp}^{rig} = 2/5 m_o r_o^2 A^{5/3}(1 + 1/3\varepsilon), \tag{8}$$

where $r_o = 1.24$ fm, m_o - nucleon mass, ε– quadrupole deformation parameter. At "zero" temperature t, momentum of inertia $F_{\perp}$ equals experimental value F_o and is interpolated in between, using pairing model equations [3].

The mass asymmetry at outer saddle doubles the $K_{rot}^{sym}(U)$ factor as defined by Eq.7. For triaxially symmetric nuclei the rotational enhancement factor usually is represented as follows:

$$K_{rot}^{asym}(U) \simeq 2\sqrt{2\pi}\sigma_{\perp}^2\sigma_{\parallel}. \tag{9}$$

The factor of the vibrational enhancement of the total level density [3] is calculated as

$$K_{vib}(U) = exp(1.7(3m_oA/(4\pi\sigma_{LD})^{2/3}t^{4/3})), \tag{10}$$

where σ_{LD} denotes surface tension coefficient in a liquid drop model, normalized as $4\pi r_o^2\sigma_{LD} = 18\ MeV$.

The quasiparticle level density $\rho_{qp}(U, J, \pi)$ is defined as

$$\rho_{qp}(U, J, \pi) = \frac{(2J+1)\omega_{qp}(U)}{4\sqrt{2\pi}\sigma_{\perp}^2\sigma_{\parallel}} \exp\left(-\frac{J(J+1)}{2\sigma_{\perp}^2}\right), \tag{11}$$

here $\omega_{qp}(U)$ is the intrinsic quasiparticle state density.

The shell correction dependence of a–parameter is defined using the following equation [3]:

$$a(U) = \begin{cases} \tilde{a}(1+ \delta W f(U - E_{cond})/(U - E_{cond})), & U > U_{cr} = 0.47 a_{cr}\Delta^2 - m\Delta \\ a(U_{cr}) = a_{cr} & U \leq U_{cr} = 0.47 a_{cr}\Delta^2 - m\Delta, \end{cases} \tag{12}$$

here m =0, 1, 2 for even-even, odd-A and odd-odd nuclei, respectively; $f(x) = 1 - \exp(-0.064x)$, is the dimensionless function, defining the shell effects dumping; condensation energy $E_{cond} = 0.152 a_{cr}\Delta^2 - m\Delta$, where Δ is the correlation function. It equals $12/\sqrt{A}$ for ground state deformations, $\tilde{a}$ and a_{cr} are the main level density a-parameter values at high excitation energies and at critical energy $U = U_{cr}$, respectively.

The respective parameters for inner(outer) saddle and equilibrium deformations: shell correction δW, pairing correlation function Δ, quadrupole deformation ε, and momentum of inertia at zero temperature $F_o/\hbar^2$ are given in Table 5. Shell correction values at inner and outer saddle deformations $\delta W_f^{A(B)}$ are adopted following the comprehensive review by Bjornholm and Lynn [20]. For ground state deformations the shell corrections were calculated as $\delta W = M^{exp} - M^{MS}$, where M^{MS} denotes liquid drop mass (LDM), calculated with Myers-Swiatecki parameters [21], and M^{exp} is the

experimental nuclear mass. We assume that asymptotic value of main level density parameter $\tilde{a}$ is independent on the deformation of the nucleus, i.e. we use the same values for nuclei at saddle and equilibrium deformations. Note that shell correction is negative at ground state and positive at saddles, consequently a-parameter values at low excitation energies would be rather different.

The values of the main $a-$parameter of the model, $\tilde{a}$ and a_{cr}, at high excitations and at excitation energy $U = U_{cr}$, respectively, are defined by fitting neutron resonance spacing. The neutron resonance spacing $\langle D_{obs} \rangle$ as well as $s-$wave neutron strength function $\langle S_o \rangle$ values were generally adopted from Reference Input Parameter Library Starter File [22] and in some selected cases obtained using a method, which takes into account the correlation of weak resonance missing and resonance missing due to poor experimental resolution [23, 24]. The $A-$dependence of $\tilde{a}/A$ values is shown on Fig.1. The isotopic dependences of $\tilde{a}/A$ seems to be rather smooth for Th, U, Pu, Am and Cm nuclei. It is evident, that global systematics of over actinide region is hardly possible. On the contrary, the $\tilde{a}-$parameter local systematics $\tilde{a}/A = \alpha + \beta A$ for Th, U, Pu, Am and Cm seem to be suitable for interpolations (see [24]).

Table 5

Level density parameters of fissioning nucleus and residual nucleus

Parameter	inner saddle(A)	outer saddle(B)	neutron channel
δW, MeV	2.5*	0.6	LDM
Δ, MeV	$\Delta_o + \delta^{**}$	$\Delta_o + \delta^{**}$	Δ_o
ε	0.6	0.8	0.24
$F_0/\hbar^2$, MeV^{-1}	100	200	73

*) for axially asymmetric deformations, 1.5 MeV for axially symmetric deformations;

**)$\delta = \Delta_f - \Delta$ value is defined by fitting fission cross section in the plateau region.

Level density description at equilibrium deformations should reproduce both the average neutron resonance spacing $\langle D_{obs} \rangle$ and the observed cumulative number of levels $N^{exp}(U)$. The problem one faces in this respect is the fair description of the cumulative number of residual nuclide levels $N^{exp}(U)$ with the $N^{theor}(U)$, calculated cumulative number of levels. GSM model fails to describe the cumulative number of low-lying levels without introducing additional shift of the excitation energy δ_{shift}. To calculate the

residual nucleus level density in the low excitation energy, i.e. just above the last discrete level excitation energy where $N^{exp}(U) \sim N^{theor}(U)$, we employ a modified CTM approach. The constant temperature approximation of

$$\rho(U) = dN(U)/dU = T^{-1} \exp((U - U_o)/T), \tag{13}$$

is extrapolated to the matching point U_c to GSM model [3], with the condition

$$U_c = U_o - Tln(T\rho(U_c)). \tag{14}$$

In this approach $U_o = -n\Delta$, where Δ is the pairing correlation function, $\Delta = 12/\sqrt{A}$, A is mass number, $n = 0$ for even-even, 1 for odd and 2 for odd-odd nuclei, i.e. U_o has the meaning of the odd-even energy shift. The value of nuclear temperature parameter T is obtained by the matching conditions at the excitation energy U_c. We will illustrate description of cumulative number of levels with constant temperature approximation for various parity nuclides. The parameters of constant temperature model for selected nuclei are given in Table 6.

Table 6

Constant temperature model parameters

^{A}X	U_c, MeV	U_o, MeV	T, MeV
^{232}U	4.4	-.18277	0.39966
^{233}U	2.8	-.73554	0.38578
^{234}U	4.4	-.19143	0.40018
^{235}U	3.8	-1.0275	0.40314
^{236}U	4.4	-.19024	0.39320
^{237}U	2.6	-.68059	0.36704
^{238}U	4.0	-.06227	.37575
^{239}U	2.8	-.71107	0.36291
^{241}Am	3.6	-.97413	0.40495
^{242}Am*	2.4	-1.6457	0.39345

Figures 2 - 11 demonstrate the description of cumulative plots of low-lying levels for selected U and Am nuclei within current approach. Histogram plots were obtained using ENSDF [25] data, straight solid lines are model fits. Cumulative plots for even U nuclides ^{232}U, ^{234}U, ^{236}U and ^{238}U look very similar to each other. They could be fitted with U_c= 4.4 MeV, except for ^{238}U where U_c= 4.0 MeV is assumed. In case of ^{232}U, value of U_c= 4.4 MeV is accepted, main level density parameter $\tilde{a}$ being defined by systematics.

In case of odd U nuclei cumulative plot shapes are rather different, steepest cumulative plot is observed for ^{235}U nuclide. For ^{233}U and ^{237}U nuclides difference is only slight, so values of U_c = 2.8 MeV U_c = 2.6 MeV, respectively, are used . However, for ^{235}U nuclide we should increase U_c up to 3.8 MeV. For ^{239}U nuclide missing of levels starts at rather low excitation energy $U \sim 0.25$ MeV, which is predicted if value of U_c = 2.8 MeV is accepted.

The cumulative number of discrete excited levels in N-odd and Z-odd nuclide ^{241}Am is shown on Fig. 10. Above ~0.5 MeV excitation energy appreciable missing of levels occurs.

The ^{242}Am low-lying levels of scheme of Nuclear Data Sheets appears incomplete at rather low excitation energy (see Fig. 11). The experimental data on odd-odd ^{242}Am nuclide energy levels are supplemented by the results of the intrinsic level modelling by Sood & Singh [15]. The still unobserved doublet of two-quasiparticle bandheads $J = 6^-$ ($K^\pi = 6^-$) and $J = 1^-$ ($K^\pi = 6^-$) is predicted, the Gallagher-Moszkowski splitting energy being ~80 keV. Assuming $E^J_{K^\pi} = A[J(J+1) - K(K+1)]$, A =5.5 keV, we model a rotational level sequence. Nonetheless, appreciable missing of levels is observed at rather low excitation energies. The cumulative number of observed levels could be fitted easily decreasing U_o parameter to ~1 MeV. However, in this case the predicted number of levels of odd-even (even-odd) and odd-odd nuclei would be comparable, while the $N(U)$ for odd-odd nuclei should be appreciably higher. For other nuclides of the same odd-odd character the discrepancies are similar.

Constant temperature model description of fission level density might be adopted after following assumptions. The respective constant temperature parameters for fissioning nucleus, namely, nuclear temperature T_f and excitation energy shift U_{of}, are defined at the matching energy $U_{cf} = U_c$, which is adopted to be the same as for equilibrium deformation. That is a fair approximation because for ground state deformations the U_c value is not very much sensitive to the a—parameter value. After that the effects of non-axiality and mass asymmetry are included. At excitation energies above U_{cf} the continuum part of the transition state spectrum is represented with the GSM model [3].

We would call our constant temperature model approach "modified CTM approach", since constant temperature model is matched to the GSM model, instead of traditional Fermi-gas model. In our modified CTM approach the modelling of total level density

$$\rho(U) = K^{sym}_{rot}(U) K_{vib}(U) \frac{\omega_{qp}(U)}{\sqrt{2\pi}\sigma_{\|}} = T^{-1} \exp((U - U_o)/T) \qquad (15)$$

looks like a simple renormalization of quasiparticle state density $\omega_{qp}(U)$ at excitation energies $U < U_c$. Spin distribution parameter $\sigma_{\|}$ is defined as

$$\sigma_{\parallel}^2 = F_{\parallel} t = 6/\pi^2 \langle m^2 \rangle (1 - 2/3\varepsilon) t, \tag{16}$$

where $\langle m^2 \rangle = 0.24 A^{2/3}$ is the average value of the squared projection of the angular momentum of the single-particle states, and ε is quadrupole deformation parameter.

The closed-form expressions for thermodynamic temperature and other relevant equations which one needs to calculate level density $\rho(U, J, \pi)$ are provided by GSM model [3].

Few-quasiparticle effects which are due to pairing correlations are essential for state density calculation at low intrinsic excitation energies either for equilibrium or saddle deformations. An evidence of few-quasiparticle effects at stable deformations in neutron-induced reactions was revealed recently. The step-like structure in ^{239}Pu(n,2n) reaction cross section was shown to be a consequence of threshold excitation of two-quasiparticle configurations in residual even-even nuclide ^{238}Pu [26] above a pairing gap. The same effect is pronounced in ^{238}U(n,γ) data description through (n,γn') reaction competition [27]. The perturbations of the level density by pair correlations was directly evidenced in statistical $\gamma-$decay spectra of even rare-earth nuclei [28, 29].

The pair correlation effects in fission are well-known. In case of even-even fissioning nuclei step-like structure of the K_o^2 parameter, defining the angular anisotropy of fission fragments is interpreted to be due to few-quasiparticle excitations. Few-quasiparticle effects which are due to pairing correlations are essential for state density calculation at low intrinsic excitation energies. Structure evident in K_o^2 parameter is virtually insensitive to the detailed fission level density shape, as opposed to the fission cross section. Previously we have demonstrated that few-quasiparticle excitations in the level density of fissioning and residual nuclei [4, 5] are important for reasonable fitting of fission cross section data at low energies for selected nuclei, typically below $\sim$2 MeV incident neutron energy [4, 5, 30]. We will demonstrate below that observed irregularities in neutron-induced fission cross section data for actinide target nuclei with various parity of neutrons and protons, could be attributed to the interplay of few-quasiparticle excitations in the level density of fissioning and residual nuclei.

The partial $n-$quasiparticle state densities, which sum-up to intrinsic state density of quasiparticle excitations could be modelled using the Bose-gas model prescriptions [26, 31]. The intrinsic state density of quasiparticle excitations $\omega_{qp}(U)$ could be represented as a sum of $n-$quasiparticle state densities $\omega_{nqp}(U)$:

$$\omega_{qp}(U) = \sum_n \omega_{nqp}(U) = \sum_n \frac{g^n (U - U_n)^{n-1}}{((n/2)!)^2 (n-1)!}, \tag{17}$$

where $g = 6a_{cr}/\pi^2$ is a single-particle state density at the Fermi surface, n is the number of quasiparticles. This equation reproduces a step-like structure of state density at low excitation energies either for even and odd nuclei. Partial $n-$quasiparticle state densities $\omega_{nqp}(U)$ depend critically on the threshold values U_n for excitation of the n-quasiparticle configurations, $n = 1, 3...$ for odd-A nuclei and $n = 2, 4...$ for even-even or odd-odd nuclei. The discrete character of few-quasiparticle excitations is virtually unimportant only in case of odd-odd nuclei. The values of U_n are defined as follows from [31] :

$$U_n = \begin{cases} E_{cond}(3.23n/n_{cr} - 1.57n^2/n_{cr}^2), & \text{if } n < 0.446n_{cr} \\ E_{cond}(1 + 0.627n^2/n_{cr}^2), & \text{if } n \geq 0.446n_{cr}. \end{cases} \quad (18)$$

Here, $n_{cr} = 12/\pi^2(ln2)gt_{cr}$, critical temperature $t_{cr} = 0.571\Delta$, condensation energy $E_{cond} = 0.152a_{cr}\Delta^2 - m\Delta$, with m=0, 1, 2 for even-even, odd-A and odd-odd nuclides, respectively. This U_n value estimate embodies the energy dependence of the correlation function $\Delta(U)$ as well as a modified Pauli correction to the excitation energy. It depends also on shell correction values for saddle and stable deformations. The angular momentum distribution parameter $\sigma_{\|}^2$ could be represented as

$$\sigma_{\|}^2 = \sum_n n\langle m^2\rangle\omega_{nqp}(U) / \sum_n \omega_{nqp}(U). \quad (19)$$

We will illustrate few-quasiparticle effects in level density of actinide nuclei for ^{239}Pu fissioning nuclide and ^{238}Pu nuclide at stable deformations, which fit measured data for ^{238}Pu(n,f) reaction.

2.4.1 ^{239}Pu fission level density

In odd nuclei "blocking" of pairing by unpaired particle is roughly taken into account by excitation energy shift. The level density of the fissioning nuclide ^{239}Pu could be calculated with equations (6-19), introducing odd-even excitation energy shift: $\widetilde{U} = U + \Delta$, where Δ is the correlation function for the saddle point deformations, see Table 5. At lower energies the energy behavior of level density is strongly dependent on the number of excited quasiparticles. Pairing is weakened by excitation of few-quasiparticle states, virtually only lowest quasiparticle number states lead to pronounced structure in level density of actinide nuclei. In case of even-odd fissioning nuclide ^{239}Pu the partial contributions $\omega_{nqp}(U)$ of $n-$quasiparticle states to the total intrinsic state density $\omega_{qp}(U)$ produce "shoulder" below three-quasiparticle state excitation threshold. For the lowest number of quasiparticles n =1 intrinsic state density $\omega_1 \sim g$, there is no explicit excitation energy dependence within Bose-gas model approximation. One-quasiparticle state density defines the step-like trend of fission cross section up to the incident

neutron energy of $E_3 = U_3 + E_{fA} - B \simeq 1.25$ MeV, where B is the neutron binding energy, E_{fA} is the inner saddle height, which corresponds to three-quasiparticle state excitation threshold U_3 at the inner saddle deformation. At higher incident neutron energies the three-quasiparticle state excitations with intrinsic excitation state density $\omega_3 \sim g^3U^2$ came into play. Hence, the fission cross section starts to increase once again above three-quasiparticle state excitation threshold (see Fig. 12). To fit neutron-induced fission data of ^{238}Pu target nuclide we could just scale the intrinsic states densities by an empirical factor, i.e. $\widetilde{\omega_1} \sim 3\omega_1$ and $\widetilde{\omega_3} \sim 2\omega_3$. One should afford that this estimate of level density at low excitation energies depends on the fission barrier parameter values. nonetheless scaling factors seem to be rather large. Here we suppose that the ^{238}Pu(n,f) cross section magnitude is governed mainly by the inner fission barrier parameters. We believe that Bose-gas approximation of intrinsic state density as given by equation (17) gives only qualitatively correct description of level density at low excitation energies. At higher excitation energies it should be normalized to the smooth model with unconstrained number of quasiparticles [3]. However, we will approximate level densities at low energies in another way.

To avoid using Bose-gas equations for modelling intrinsic state density, we will model step-like behavior of $\omega_{qp}(U)$ at low excitation energies with empirical constant temperature model parameters. Level density of axially symmetric nucleus

$$\rho(U) = K_{rot}^{sym}(U) K_{vib}(U) \frac{\omega_{qp}(U)}{\sqrt{2\pi}\sigma_{\|}}, \tag{20}$$

could be calculated with equations (6-19). At the other hand level density of axially symmetric nucleus could be calculated within constant temperature approximation as

$$\rho(U) = T_f^{-1} \exp((U - U_o)/T_f). \tag{21}$$

where $U_o \simeq -m\Delta$, $m = 0$, 1, 2 for even, odd and odd-odd nuclei, respectively. The nuclear temperature T_f and excitation energy shift U_o are defined by matching constant temperature model to the pairing model with unconstrained number of quasiparticles [3] at the energy $U_c = 2.4$ MeV. At excitation energies $U \geq U_c$ the continuum part of the transition state spectrum is represented with the phenomenological GSM [3] model. Then the influence of triaxiality and mass asymmetry at respective saddle deformations is taken into account, as discussed above. In case of even-odd nuclei the nuclear level density $\rho(U)$ up to the three-quasiparticle excitation threshold depends on the excitation energy only weakly, since the intrinsic state density $\omega_1 \sim g$ is constant. In this excitation energy region we will model the level density as

$$\begin{aligned}\rho(U) &= T_f^{-1}(1+\delta_{10}(U-0.5U_3))\exp((U_3+\Delta_f-U_o-\delta_1)/T_f) \\ &\simeq T_f^{-1}\exp((\Delta_f-U_o)/T_f). \qquad (22)\end{aligned}$$

Using this equation we could fit measured fission cross section data trend using parameters $\delta_1 = 1.25$ MeV and $\delta_{10} = 2$ MeV. One- and three-quasiparticle states level density of even-odd fissioning nucleus ^{239}Pu defines the fission cross section shape at incident neutron energies below ~2.5 MeV (see Fig. 12). For excitation energies below five-quasiparticle and above three-quasiparticle states excitation threshold the level density is slightly increased as compared with constant temperature model approximation:

$$\rho(U) = T_f^{-1}\exp((U-U_o+\delta_3)/T_f), \qquad (23)$$

where parameter $\delta_3 = 0.145$ MeV was defined by fitting fission cross section data. Level density of fissioning nuclide ^{239}Pu at inner saddle, triaxiality effects being included, is shown on Fig. 13. Level density, calculated with equations (6-19) is compared with constant temperature approximation of equations (22) and (23) and "scaled" Bose-gas model. The arrows on the horizontal axis of Fig. 13 indicate the excitation thresholds of odd $n-$quasiparticle configurations.

2.4.2 ^{238}Pu level density

In case of even-even nuclides the partial contributions of $\omega_{nqp}(U)$ of $n-$quasiparticle states to the total intrinsic state density $\omega_{qp}(U)$ produce "jumps" only for $n = 2$ and $n = 4$ configurations (see Fig. 14). The arrows on the horizontal axis of Fig. 14 indicate the excitation thresholds of even $n-$quasiparticle configurations. The intrinsic state density $\omega_2(U)$ for the residual nuclide ^{238}Pu could be represented by equation, modifying Bose-gas approximation of $\omega_2(U) = g^2(U-U_2)$ with a Woods-Saxon expression at excitations below four-quasiparticle excitation threshold:

$$\omega_2(U) = g^2(U_4-U_2-0.35)(1+\exp((U_2-U+0.1)/0.1))^{-1}. \qquad (24)$$

This estimate of two-quasiparticle states $\omega_2(U)$ was obtained by modelling the structure of ^{238}Pu intrinsic state density to interpret the step-like structure in ^{239}Pu(n,2n) reaction data near threshold [26]. We model here the nuclear level density $\rho(U)$ in the same manner as for ^{239}Pu nuclide. Above the pairing gap U_2 up to the four-quasiparticle excitation threshold U_4 level density is approximated as

$$\rho(U) = \rho(U_4-\delta_2)/(1+\exp(U_2-U+\delta_a)/\delta_s), \qquad (25)$$

here $\delta_2 \sim 0.5(U_4 - U_2)$. Two-quasiparticle states level density of even-even residual nuclide ^{238}Pu influences the fission cross section shape at incident neutron energies above ~1.2 MeV. Parameters $\delta_2 = 0.25$ MeV, $\delta_a = \delta_s = 0.1$ MeV values were extracted by fitting measured fission data shape. Level density, calculated with equations (6-19) is compared with constant temperature approximation of equation (25) and "scaled" Bose-gas model (Eq. 17). Present and Bose-gas approximation are consistent at low excitation energies, while they start to be discrepant around 5 MeV excitation energy.

Below the pairing gap U_2 collective levels [25] were employed. The continuum level density above excitation energy U_4 and below $U_c = 3.6$ MeV is calculated with the constant temperature model, with parameters $U_o =$ -0.0002 MeV, nuclear temperature $T = 0.38454$ MeV, which fit cumulative number of observed levels. At higher excitation energies the GSM [3] model is used. Main level density model parameter a for residual nuclide ^{238}Pu is obtained by systematics, derived for Th-Cf nuclei [24].

3 Fission Cross Section Calculation

Approach adopted here to model level density at equilibrium and saddle deformations will be used to describe available neutron-induced fission cross section data for actinide nuclei, specifically: ^{232}Th, ^{231}Pa, $^{232-238}$U, ^{236,237}Np, $^{238-244}$Pu, $^{241-243}$Am, $^{242-248}$Cm, ^{249}Bk, ^{249}Cf target nuclides. Data for incident neutron energies up to emissive fission threshold would be reproduced. Above ~2.5 MeV incident neutron energy fission cross section data were fitted by slight increase of pairing correlation function value Δ_f. Actually the amount of this increase depends on the ratio of $a-$parameters at saddle and equilibrium deformations, which, in turn, is a function of $(\delta W_f^{A(B)} - \delta W)$. It might be anticipated that value of the parameter $\delta = (\Delta_f - \Delta)$ contains lumped effect of pairing and shell effects differences at saddle and equilibrium deformations, numerical values of δ are provided in Table 8.

The manifestation of few-quasiparticle effects in fission cross section depends on the fission barrier structure, i.e. on the relative heights of inner and outer fission barrier humps. The internal excitation energy at the saddle point corresponding to the higher barrier hump $E_{fA(B)}$ is important, basically the value of $(B_n + E - E_{fA(B)})$ matters. Here a further evidence of few-quasiparticle effects in level densities is presented. We argue that to probe fission level density at low intrinsic excitation energy neutron-induced fission cross section data at low energies for even-even and even-odd target nuclei, typically below ~2 MeV incident neutron energy, are of primary value.

3.1 Z-even, N-even fissioning nuclei

In case of Z-even, N-odd fissile targets the step-like irregularities in fission cross section data shapes are supposed to be due to interplay of two-quasiparticle excitations in the level density of even-even fissioning nucleus and one-quasiparticle excitation in odd residual nucleus. The collective levels of even fissioning nuclei (see Table 1), lying within pairing gap, define the fission cross section below incident neutron energy of $E \leq E_{fA(B)} + U_2 - B_n$, where $E_{fA(B)}$ is the higher of the barrier humps.

3.1.1 ^{233}U(n,f), ^{235}U(n,f)

In case of ^{233}U and ^{235}U target nuclides the inner barrier of fissioning nuclides is lower than outer one, in case of Pu and Cm nuclei addressed here the higher barrier is the inner one. That means that calculated fission cross section of ^{233}U(n,f) and ^{235}U(n,f) reactions is more sensitive to the discrete transition spectra at outer saddle fitting data. The discrete transition spectra at inner saddle are more important when fitting ^{239,241}Pu(n,f), ^{243,245,247}Cm(n,f) and ^{249}Cf(n,f) measured data.

At excitation energies $U > U_2$, i.e. above the pairing gap, level density of axially symmetric fissioning nucleus is calculated as described above. After that the effects of mass asymmetry at the outer saddle are included.

The most distinct evidence of pair correlation effects is observed in case of ^{233}U(n,f) (see Fig. 15) and ^{235}U(n,f) (see Fig. 16) reactions. SCM calculations by Howard & Möller [2] predicted that inner fission barrier for uranium nuclei with $A \leq 236$ is axially symmetric while $E_{fA} < E_{fB}$. The two-quasiparticle excitations in ^{234}U at the outer saddle deformations occur at intrinsic excitation energy, correspondent to $E \geq 0.1$ MeV, they explain the step-like behavior of ^{233}U(n,f) data shape above 0.1 MeV up to 2 MeV. In this section sensitivity of calculated fission cross section to two- and four-quasiparticle state density of fissioning nucleus was estimated by changing $|\delta_2|$ and $|\delta_4|$ by 0.2 MeV. Dashed and short-dashed curves on Fig. 15 show the sensitivity of calculated fission cross section to two-and four-quasiparticle excitations in fissioning nuclide ^{234}U. Above ~0.9 MeV incident neutron energy four-quasiparticle excitations occur (see Fig. 15), but calculated fission cross section is much less sensitive to relevant state density variation. Fission level density of even-even nuclide ^{234}U was calculated here using equation (25), relevant δ_2 parameter values are given in Table 7, δ_a and δ_s parameter values are assumed to be the same as for equilibrium deformations. At intrinsic excitation energies higher than four-quasiparticle excitation threshold U_4 level density $\rho(U)$ was estimated as

$$\rho(U) = T_f^{-1} \exp((U_6 - U_o - \delta_4)/T_f), \qquad (26)$$

where U_6 is six-quasiparticle excitation threshold. Fission level density of ^{234}U is shown on Fig. 17. The arrows on the horizontal axis of Fig. 17 indicate the excitation thresholds of even $n-$quasiparticle configurations.

Table 7
Level density parameters

Nuclide	δ_1^n	δ_1^f	δ_{10}^f	δ_3^f	δ_2^n	δ_2^f	δ_4^f
^{232}Th					0.3		
^{233}Th		1.65	3.0	0.05			
^{232}U					0.5		
^{233}U	1.075	1.275	2.0	0.15			
^{234}U					0.4	0.55	0.2
^{235}U	1.075	1.35	2.0	0.15			
^{236}U					0.4	0.6	0.05
^{237}U	1.075	1.30	3.0	0.15			
^{238}U					0.3	0.6	0.05
^{239}U		1.22	2.5	0.075			

Table 7 (continued)
Level density parameters

Nuclide	δ_1^n	δ_1^f	δ_{10}^f	δ_3^f	δ_2^n	δ_2^f	δ_4^f
^{236}Pu					0.25		
^{237}Pu		1.25	2.0	0.145			
^{238}Pu					0.25		
^{239}Pu	1.075	1.275	2.0	0.145			
^{240}Pu					0.50	0.60	0.2
^{241}Pu	1.075	1.45	2.0	0.07			
^{242}Pu					0.5	0.50	0.2
^{243}Pu	1.075	1.50	2.0	0.0			
^{244}Pu					0.6	0.5	0.2
^{245}Pu	1.075	1.45	3.0	0.0			
^{242}Cm					0.0		
^{243}Cm	1.075	1.35	1.5	0.05			
^{244}Cm					0.0	0.5	0.05
^{245}Cm	1.075	1.25	1.5	0.05			
^{246}Cm					0.0	0.5	0.05
^{247}Cm	1.075	1.45	1.5	0.1			
^{248}Cm					0.25	0.6	0.05
^{249}Cm		1.40	1.5	0.05			
^{249}Cf	1.075						
^{250}Cf						0.7	0.25

In case of ^{235}U(n,f) cross section two-quasiparticle states at outer saddle of ^{236}U fissioning nuclide are excited at higher incident neutron energies, as compared with respective excitation threshold in ^{233}U(n,f) reaction. It corresponds to $E \geq 0.6$ MeV, here also a step-like behavior of data shape is observed [4] (see Fig. 17). Above ~1.4 MeV incident neutron energy four-quasiparticle excitations occur (see Fig. 16), calculated fission cross section here is more sensitive to relevant four-quasiparticle state density variation. That is due to higher fission threshold of ^{236}U as compared with fission threshold of ^{234}U. Figure 18 shows neutron-induced fission cross section of ^{237}U(n,f). We have not tried to fit measured data by McNally et al.[32] because of their strange shape in MeV-energy range. Fission barrier parameters of ^{238}U were obtained with the aid of ^{238}U(n,f) measured fission data description above emissive fission threshold (see below). Fission threshold of ^{238}U corresponds to the inner fission barrier, it is higher on the neutron energy scale than those of ^{234}U and ^{236}U.

Values of δ_2 and δ_4 parameter values are provided in Table 7, they fluctuate only slightly for various U, Pu and Cm nuclei. Adopting structureless constant temperature approximation of fission level density one fails to describe fission cross section of Z-even, N-odd fissile targets exactly in the neutron energy range up to ~2-3 MeV incident neutron energy. Evidence on few-quasiparticle excitation depends on the fission barrier value in the neutron energy scale. At intrinsic excitation energies $U \geq U_6$ fission level density is almost perfectly smooth.

3.1.2 ^{239}Pu(n,f), ^{241}Pu(n,f), ^{243}Cm(n,f), ^{245}Cm(n,f), ^{247}Cm(n,f)

In case of fissile Pu and Cm target nuclei covered in current analysis the inner saddle is axially asymmetric and inner barrier is higher than outer one ($E_{fA(B)} > E_{fA(B)}$). The interchange of roles of the inner and outer barriers occurs, as compared with lighter U nuclei. For ^{239}Pu(n,f) and ^{241}Pu(n,f) reactions value of $E_2 = E_{fA} + U_2 - B_n$, corresponding to excitation of two-quasiparticle states is rather high. There is less distinct evidence of step-like structures in fission cross sections below ~2 MeV, as compared with uranium fissile targets. However, there is still distinct dependence of calculated fission cross section on the two- and four-quasiparticle state density at the inner fission barrier. In case of ^{239}Pu(n,f) reaction there is a noticeable sensitivity of calculated fission cross section to the two-quasiparticle state density above ~0.5 MeV incident neutron energy and that of four-quasiparticle state density above ~1 MeV. Shapes of ^{239}Pu(n,f) and ^{241}Pu(n,f) fission cross sections are different below ~0.5 MeV incident neutron energy: fission cross section of ^{239}Pu(n,f) is almost flat, while that of ^{241}Pu(n,f) exhibit a steep rise with neutron energy decrease. Above ~2 MeV ^{239}Pu(n,f) fission cross section is systematically higher than that of ^{241}Pu(n,f) reaction. This

peculiarity is reflected in decreased height of inner fission barrier of ^{242}Pu fissioning nuclide (see Table 8). Calculated fission cross section is sensitive to two– and four-quasiparticle fission state density in 0.4-1.2 and 1.2-3 MeV neutron energy range, respectively.

Adopting structureless constant temperature approximation of level density one fails to describe the fission cross section from 10 keV up to 2 MeV incident neutron energy, which corresponds to excitation of six-quasiparticle states at the inner saddle. The comparison of calculated cross section with measured data is shown on Figs. 19 and 20.

Data base for ^{243}Cm(n,f), ^{245}Cm(n,f), ^{247}Cm(n,f) reaction cross sections expanded extensively when data by Fursov et al.[33] become available.

Two-quasiparticle state excitations might be pronounced in calculated fission cross section of ^{243}Cm(n,f) reaction at incident neutron energies as low as 0.1 MeV. It follows from the fission barrier parameters estimate based on measured data in MeV-energy region. Unfortunately, there is no appropriate measured data to support or discard this peculiarity (see Fig. 21). Four-quasiparticle state density influences calculated fission cross section above $\sim$1 MeV and up to $\sim$3 MeV incident neutron energy. Fission cross sections of ^{245}Cm and ^{247}Cm target nuclides were calculated in the same way (see Figs. 13,14). The most disturbing is measured data discrepancy for ^{247}Cm(n,f). The data by Fursov et al. [33] above 0.1 MeV seem to be discrepant with data by Danon et al. [34] below 0.1 MeV. We suppose that the data by Fursov et al. [33] in the energy range 0.1-1 MeV and data by Danon et al. [34] can not be fitted simultaneously. They assume almost the same step-like structure above 0.1 MeV, as in case of ^{233}U(n,f) reaction. However, two-quasiparticle state excitation threshold corresponds to $\sim$0.1 MeV incident neutron energy and can not be correlated with this measured fission data irregularity. In other respects, calculated fission cross section behaves much in the same way as in case of Pu fissile targets. Neutron-induced fission cross section data for ^{249}Cf could be described in the same way (see Fig. 24).

Once again, adopting structureless constant temperature approximation of level density one fails to describe the fission cross section below $\sim$2 MeV incident neutron energy, that is the energy range where excitation of few-quasiparticle states at the inner saddle is of primary importance.

Figure 25 shows values of $E_{fA(B)} + U_2 - B_n$, two-quasiparticle excitation threshold in neutron energy scale as a function fissioning nucleus mass A. They are correlated with evidence of two-quasiparticle effects in neutron-induced fission cross sections. That is a condensed illustration of the above discussion.

3.2 Z-even, N-odd fissioning nuclei

In case of Z-even, N-even targets fission cross section data for U ($A \geq 234$), Pu ($A \geq 238$) and Cm target nuclei exhibit almost classic threshold shape. In case of ^{232}U and ^{236}Pu target nuclides there is a nonthreshold behavior in contrast with other N-even isotopes. In case of other plutonium and curium targets neutron-induced fission the step-like and resonance-like structures, respectively, are observed above fission threshold, actually in a region traditionally called 'first plateau'. They are supposed to be due to interplay of one-quasiparticle excitations in the level density of odd fissioning nucleus and two-quasiparticle excitation in even residual nucleus [5].

SCM calculations by Howard & Möller [2] predicted axial symmetry of inner fission barrier, while $E_{fA} < E_{fB}$, for neutron-deficient odd uranium and plutonium nuclei with $A \leq 235$ and $A \leq 237$, respectively. The different behavior of level densities of even-odd and even-even nuclei at low excitation energies could be taken into account as described above. The one-quasiparticle neutron states of even-odd fissioning nuclide, lying below the three-quasiparticle states excitation threshold define the shape of fission cross section below incident neutron energy of $E \leq E_{fA(B)} + U_3 - B_n$. At higher excitation energies three-quasiparticle states are excited. Two-quasiparticle states in even residual nucleus could be excited at incident neutron energies $E > U_2$. Relative position of U_3 and U_2 excitation thresholds in fissioning and residual nuclei, respectively, might influence fission cross section shape below ~3 MeV incident neutron energy.

3.2.1 ^{232}U(n,f), ^{234}U(n,f), ^{236}U(n,f), ^{238}U(n,f)

Fission cross section data of ^{238}U exhibits almost classic threshold shape, since vibrational resonance at ~1.15 MeV is rather weak. Figure 26 shows that "cusp" in fission cross section around 3.3 MeV incident neutron energy might be correlated with excitation of three-quasiparticle states in fissioning nuclide ^{239}U above 2.4 MeV. At this high energy influence of one-quasiparticle states on calculated fission cross section starts to diminish. There are some peculiarities in fission cross section data of ^{236}U and ^{234}U below ~2 MeV incident neutron energies, besides strong vibrational resonances at ~0.93 MeV in ^{236}U(n,f) and 0.78 MeV in ^{234}U(n,f). Adopted level density description allows to fit subthreshold cross section shape of ^{236}U(n,f) (see Fig. 27) and ^{234}U(n,f) (see Fig. 28). Note that for ^{237}U and ^{239}U fissioning nuclides $E_{fA} > E_{fB}$, while for ^{235}U and ^{233}U $E_{fA} < E_{fB}$. Incident neutron energies $E_3 = U_3 + E_{fA(B)} - B$ correspondent to excitation of three-quasiparticle states are: ~ 2.3 MeV for ^{238}U(n,f), ~1.8 MeV for ^{236}U(n,f), ~1.2 MeV for ^{234}U(n,f) and ~0.7 MeV for ^{232}U(n,f). Approximately at these energies abrupt changes in cross section shapes are observed (see Figs. 26,

27, 28, 29). At lower energies fission cross section shape is controlled by one-quasiparticle state density.

The most exotic cross section shape is encountered in case of ^{232}U(n,f) data (see Fig. 29). We can explain the non-threshold behavior of measured data at low incident neutron energies [11], assuming $E_{fA} < E_{fB}$. In this case the cross section is governed by the outer barrier E_{fB} value, which is $\sim$1 MeV lower than the neutron binding energy of the compound nucleus ^{233}U. The change of observed cross section shape around $\sim$1 MeV is qualitatively reproduced, while below 3 MeV it can not be reproduced within constant temperature approach (see Fig. 29). Below $\sim$0.3 MeV fission cross section ^{232}U(n,f) is rather sensitive to the discrete level spectra at the outer saddle. Other uranium non-fissile target cross sections are not so sensitive to the discrete level spectra at the higher barrier. Because the deformation is axially symmetric at both saddles in this case, the band-head positions were supposed to be analogous to those of ^{233}U at the ground state deformation. Then the transition state spectra were constructed using $F_0/\hbar^2$ at the inner and outer saddles shown in Table 5. Each positive parity band state is accompanied by the negative parity state. The cutoff energy for fission transition spectra was assumed to be 0.4 MeV. Because both barrier humps are below the neutron binding energy, the exact positions are not very important; it is their number that counts.

In this section sensitivity of calculated fission cross section to one- and three-quasiparticle state density of fissioning nucleus was estimated by changing values of $|\delta_1|$ and $|\delta_3|$ by 0.1 MeV. Dashed and short-dashed curves on Figs. 26, 27, 28 and 29 show the sensitivity of calculated fission cross section to one– and three-quasiparticle excitations in fissioning nuclide. In case of ^{238}U(n,f) reaction above $\sim$2.2 MeV incident neutron energy three-quasiparticle excitations occur (see Fig. 26), but calculated fission cross section is much more sensitive to one–quasiparticle state density variation in fissioning nuclide ^{239}U. Fission level density of even-odd nuclide ^{239}U was calculated here using equations (22) and (23) in the same way as for ^{239}Pu (see above), relevant δ_1, δ_{10} and δ_3 parameter values are given in Table 7.

Adopting structureless constant temperature approximation of level density one could describe the fission cross section data only above 3-4 MeV incident neutron energy and deep below fission threshold, when fission transmission coefficient is defined mainly by discrete fission transition states. At intermediate incident neutron energy, that is the energy range where excitation of few-quasiparticle states at the inner saddle is of primary importance, structureless constant temperature approximation fails.

3.2.2 ^{238}Pu(n,f), ^{240}Pu(n,f), ^{242}Pu(n,f), ^{244}Pu(n,f)

Excitation of three-quasiparticle states in fissioning nucleus is more pronounced for neutron-induced reactions on Pu target nuclei. Dashed and dot-dashed curves of Fig. 12 show the sensitivity of calculated fission cross section to the level density of ^{239}Pu fissioning nuclide at excitation energies lower than three-quasiparticle excitation threshold. For dashed curve, in fact, one-quasiparticle state density is varied, i.e. level density $\rho(U)$ is calculated with $\delta_3 = 1.35$ MeV (see equation (16), respectively, while for solid curve $\delta_3 = 1.25$ MeV. Calculated fission cross section appears to be slightly sensitive to one-quasiparticle state density below 1 MeV incident neutron energy, while it is very sensitive above 1 MeV up to 3 MeV.

Fission cross section of ^{240}Pu also exhibits step-like irregularity above ~1 MeV incident neutron energy (see Fig. 30). Incident neutron energies $E_3 = U_3 + E_{fA} - B$ correspondent to excitation of three-quasiparticle states is ~1.5 MeV for ^{240}Pu(n,f), for other plutonium targets they are: ~ 1.25 MeV for ^{238}Pu(n,f), ~1.6 MeV for ^{242}Pu(n,f) and ~1.7 MeV for ^{244}Pu(n,f) (see Figs. 13, 31 and 32, respectively). At lower energies fission cross section shape is controlled by one-quasiparticle state density. Figs. 13a, 30a, 31a and 32a demonstrate fits of threshold behavior of fission cross sections for ^{238}Pu, ^{242}Pu, ^{240}Pu and ^{244}Pu, respectively. Fission cross section of ^{236}Pu nuclide looks much the same as that of 232U, it is shown on Fig. 33 (see discussion above).

Calculated fission cross section appears also rather sensitive to the fission barrier parameter values, we could estimate their uncertainties for ^{239}Pu at rather low level: $\delta E_{fA} = 0.05$ MeV, $\delta E_{fB} = 0.10$ MeV, $\delta\hbar\omega_A = 0.03$ MeV, except curvature of outer fission barrier hump, where $\delta\hbar\omega_B = 0.4$ MeV, uncertainties for other nuclei are provided in Table 8. These uncertainties were defined as uncorrelated sensitivity of calculated fission cross section to the respective parameter variation, as compared with measured data base.

3.2.3 ^{242}Cm(n,f), ^{244}Cm(n,f), ^{246}Cm(n,f), ^{248}Cm(n,f)

Quasi-resonance structure is evident in fission cross section data by Fursov et al. [33], Moore et al. [35] and Fomushkin et al. [36, 37] for ^{244}Cm(n,f), ^{246}Cm(n,f), ^{248}Cm(n,f) reaction cross sections, although there are a systematic discrepancies evident in data sets as regards either data shapes and absolute values.

Broad quasi-resonance structure around 1.2 MeV neutron energy, evident in measured data by Moore et al. [35] and by Fomushkin et al.[36] for ^{244}Cm(n,f) reaction (see Fig. 34). Data by Fursov et al.[33] for ^{244}Cm(n,f) appear to be shifted to higher values, however there is also quasi-resonance structure around 1 MeV. These data could be described in the same man-

ner as those for Pu even-even target nuclei. Figure 34 shows the sensitivity of calculated fission cross section to one- and three-quasiparticle state density. Fission cross section shape up to 2.5 MeV neutron energy is controlled mainly by one-quasiparticle state density, while three-quasiparticle state density is important in the energy range of 2-3.5 MeV. It seems that data by Fursov et al.[33] are incompatible with deep-subthreshold data by Maguire et al.[38] (see Fig. 33a). Figure 33 shows fits of data by Fursov et al.[33], which were obtained by decreasing inner and outer fission barrier humps by 0.1 MeV and 0.25 MeV, respectively, so that one obtains E_{fA} = 6.325 MeV and E_{fA} = 5.35 MeV, other fission barrier and level density parameters being unchanged.

In case of ^{246}Cm(n,f) reaction measured data are more compatible, than in case of ^{244}Cm(n,f) fission data (see Fig. 35). Here, in case of even-odd fissioning nuclide ^{247}Cm partial contributions $\omega_{nqp}(U)$ of $n-$quasi-particle states to the total intrinsic state density $\omega_{qp}(U)$ produce "jumps" only for n =1 and n =3 (see Fig. 13). We suppose that ^{242,244,246,248}Cm target cross section magnitude are governed by the inner fission barrier, parameters of which are fixed by fission data fit for incident neutron energy above ~10 keV. Figs. 34, 35, 36 and 37 show the comparison of deep subthreshold data by Maguire et al. [38] measured with linac and bomb-shot data by Fomushkin et al.[36], [37], Moore et al. [35] and Fursov et al. [33]. One-quasiparticle state excitation define the decreasing trend of fission cross section above fission barrier up to the incident neutron energy of $E_3 = U_3 + E_{fA} - B$. Above incident neutron energy E_3 three-quasiparticle state excitations with intrinsic excitation state density came into play. Hence, the fission cross section starts to increase once again.

In case of ^{248}Cm(n,f) reaction there is a systematic discrepancy between data by Fomushkin et al. [37], Moore et al. [35] and data by Fursov et al. [33]. Structure in fission cross section data above ~1 MeV is much less pronounced than in case of ^{244}Cm(n,f) and ^{246}Cm(n,f) reactions. Data by Fursov et al. [33] could be described consistently with deep sub-threshold data by Maguire et al. [38] decreasing inner and outer fission barrier heights and inner barrier curvature (E_{fA} = 5.85 MeV, E_{fB} = 5.3 MeV, $\hbar\omega_A$ = 0.9 MeV), as compared with those, fitting data by Fomushkin et al. [37], Moore et al. [35].

Figure 37 shows comparison of calculated fission cross section of ^{242}Cm(n,f) reaction with neutron data by Alam et al. [39] and data inferred from transfer reaction [40]. The latter data seem to be incompatible with smooth increase of fission cross section for neutron deficient curium targets. Broad quasi-resonance structure is predicted above 1 MeV incident neutron energy, it might be noticed in data inferred from transfer reaction [40] as well.

The modelling of the intrinsic state density structure of fissioning and

residual nuclei has enabled the qualitative analysis of the quasi-resonance structure in ^{244}Cm(n,f), ^{246}Cm(n,f), ^{248}Cm(n,f) measured data well-above fission threshold. This irregularity is the consequence of threshold excitation of three-quasiparticle configurations. The excitation threshold is consistent with measured data below fission threshold.

Fission barrier structure for Th nuclei is much more complex. It is supposed to be triple-humped, deep sub-barrier neutron energy region being dominated by splitted barrier at deformations, correspondent to outer saddle deformations for U, Pu and Cm nuclei [20]. However, it seems reasonable to obtain double-humped fission barrier parameter estimates for ^{233}Th by analysis of ^{232}Th(n,f) reaction data above ~2 MeV incident neutron energies. We assume that there is no splitting of outer barrier humps, in other respects the fission model is the same as that, say, for ^{234}U(n,f) reaction. Figure 38 shows the sensitivity of calculated fission cross section to one– and three-quasiparticle excitations in fissioning nuclide ^{233}Th. Three-quasiparticle excitations influence on calculated fission cross section at incident neutron energies as high as ~3.4 MeV, however there is some structure evident in measured data, which might be correlated with them.

Figure 39 shows values of $E_{fA(B)}+U_3-B_n$, three-quasiparticle excitation threshold in neutron energy scale as a function fissioning nucleus mass A. They are correlated with evidence of two-quasiparticle effects in U, Pu and Cm neutron-induced fission cross sections. That is a condensed illustration of the above discussion

3.3 Z-odd, N-odd fissioning nuclei

3.3.1 ^{241}Am, ^{243}Am, ^{237}Np, ^{249}Bk, ^{231}Pa

In case of Z-odd, N-even targets ^{241}Am, ^{243}Am and ^{237}Np fission cross section exhibit classic threshold shape. The discrete character of few-quasiparticle excitations is virtually unimportant for level density modelling in case of odd-odd ^{242}Am fissioning nuclide. We will model the level density of $Z-$odd, $N-$odd fissioning nucleus above 0.2 MeV as follows. The respective parameters, nuclear temperature T_f and excitation energy shift U_o are defined at the matching energy U_c =2.4 MeV. The respective parameters: shell correction at saddles δW, pairing correlation function Δ, quadrupole deformation ε, and momentum of inertia at zero temperature $F_0/\hbar^2$ are given in Table 5. Figures 39, 40, 41 and 42 show measured data description for ^{241}Am, ^{243}Am ^{237}Np and ^{249}Bk target nuclides.

Fission barrier structure of ^{232}Pa nuclide is similar to that of ^{233}Th. We applied the same simplified approach to the data description of ^{231}Pa(n,f), as in case of ^{232}Th(n,f). There are evident the same deficiencies as in previous case (see Fig. 43).

3.4 Z-odd, N-even fissioning nuclei

3.4.1 ^{242m}Am, ^{236}Np

In case of the only available Z-odd, N-odd target ^{242m}Am the effect of Z-odd, N-even fissioning nucleus level density is evidenced as a step-like shape of fission cross section data. The one-quasiparticle neutron states of odd-even ^{243}Am fissioning nuclide define the shape of ^{242m}Am(n,f) fission cross section below incident neutron energy of ~1 MeV. Specifically, the step-like shape of fission cross section around 0.1 - 0.4 MeV. At higher incident neutron energies three-quasiparticle states could be excited in fissioning nucleus ^{243}Am at deformations of inner fission barrier hump. They define the fission cross section shape around 1 - 2.5 MeV incident neutron energy. There is virtually no step-wise structure in level density of odd-odd residual nuclide ^{242}Am. Calculated fission cross section appears to be less sensitive to one-quasiparticle state density, than fission cross section of Z-even, N-even targets, because of high fissility of ^{243}Am nuclide. In this excitation energy region we will model the level density with Eqs. (22) and (23), while δ_1= 1.425 MeV, δ_{10}= 0, δ_3= 0.1 MeV. Fig. 44 shows the comparison of measured data with calculated cross section. Dashed curve shows the drawbacks due to using constant temperature approximation.

In case of long-lived ^{236l}Np target there are neutron-induced fission data below 20 keV by Valskij et al.[41], besides simulated data [40], derived using fission probability data obtained in ^{236}U(^{3}He,df) reaction. Figure 45 shows neutron-induced fission cross section of ^{236l}Np ($J^\pi = 6^-$) target nuclide from 0.5 keV up to 5.5 MeV. Once again, the "shoulder" is predicted in calculated fission cross section below 0.5 MeV incident neutron energy. Fission barrier parameters of ^{237}Np fissioning nuclide were extracted by analysis of ^{237}Np(n,f) fission data above (n,nf) emissive fission threshold (see below). Consistency of calculated ^{236l}Np(n,f) fission cross section with simulated fission data in MeV-energy region and neutron-induced fission data in keV-energy region might be considered as an indirect validation of the approach employed here for ^{238}Np(n,f) fission cross section prediction (see Fig.46), for which only simulated fission data in MeV-energy region [40] are available.

4 Cross sections above emissive fission threshold

4.1 Fission cross section

At higher incident neutron energies when fission reaction of $A, A-1$ and $A-2$ compound nuclides is possible after emission of 1, 2 or 3 neutrons, the observed fission cross section is a superposition of non-emissive or first chance fission of nucleus A and xth-chance fission contributions. These

contributions are weighted with a probability of x neutrons emission before fission. In case of neutron-induced fission of ^{238}U target nuclide, for fixed statistical model parameters of residual nuclei ^{238}U, ^{237}U or ^{236}U, fissioning in (n,nf), $(n,2nf)$ or $(n,3nf)$ reactions, the behavior of the first-chance fission cross section σ_{f1} should make it possible to reproduce the measured fission cross section σ_f of ^{238}U. this approach is realized in a STAPRE [42] code, which was used for present calculations. A consistent description of the most complete set of measured data on the (n,f), $(n,2n)$, $(n,3n)$ and $(n,4n)$ reaction cross sections for the ^{238}U target nuclide up to 20 MeV enables one to consider the estimates of σ_{f1} and fission probability $P_{f1}$of the initial compound nuclei ^{239}U as fairly realistic.

Fission cross section of ^{238}U, shown on the Fig. 47 demonstrates a step-like structure, relevant to contribution of (n,xnf) reactions to total fission cross sections for $x = 1, 2, 3$. Contribution of first-chance fission appears to be sensitive to level density of residual nuclide ^{238}U. Contribution of second-chance fission of ^{238}U compound nuclide is sensitive to level density of fissioning nuclide ^{238}U. Estimate of ^{237}U $\langle D_{obs} \rangle = 2.973 \pm 0.416$ eV, obtained by analysis of resolved resonance parameters [24] is consistent with preequilibrium contribution into first neutron spectrum [43] and subsequent sharing of $\sigma_r = \sigma_{n,f1} + \sigma_{n,nx}$ reaction cross section into first-chance fission and neutron emission cross sections. To get a consistent fit of measured cross sections up to 20 MeV we decreased $\tilde{a}_f$ of fissioning nuclide ^{238}U by 10%. Cross section of ^{237}U(n,f) reaction is shown on Fig. 18, it corresponds to (n,nf) fission contribution to measured fission cross section ^{238}U(n,f) (see Fig. 47). Contributions of (n,2nf) and (n,3nf) reactions correspond to neutron-induced fission cross sections of ^{236}U and ^{235}U. Neutron-induced fission cross sections of ^{236}U and ^{235}U are shown on Figs. 27 and 16.

4.2 (n,xn) reaction cross sections

Estimates of (n,2n) and (n,3n) reaction cross sections for ^{238}U are presented on Figs. 48 and 49. Shape of calculated cross section, especially it's high-energy tail, is strongly correlated with secondary neutron spectrum shape.

Cross section of (n,3n) reaction is less sensitive to pre-equilibrium neutron emission contribution. Calculated curve, shown on the Fig. 49 is just the result of fitting fission and (n,2n) reaction cross sections.

4.3 Shell effects in first chance fission cross section

The behavior of the first-chance fission cross section σ_{f1} is obviously related with the energy dependence of the first-chance fission probability of the $A+1$ nucleus P_{f1}:

$$\sigma_{f1} = \sigma_r(1 - q(E))P_{f1}. \quad (27)$$

Once the contribution of first neutron pre-equilibrium emission $q(E)$ is fixed, the first-chance fission probability P_{f1} of the ^{239}U compound nuclide depends only on the level density parameters of fissioning and residual nuclei. That is, actually it depends on the ratio of shell correction values $\delta W_{fA(B)}$ and δW_n. The results of different theoretical calculations of the shell corrections as well as of the fission barriers vary by $1 \sim 2$ MeV. The same is true for the experimental shell corrections, which are obtained with a smooth component of potential energy calculated according to the liquid-drop or droplet model. However the isotopic changes of $\delta W_{fA(B)}$ and δW_n [20] are such that P_{f1} viewed as a function of the difference $(\delta W_{fA(B)} - \delta W_n)$ is virtually independent on the choice of smooth component of potential energy. In addition, existing calculations of the shell corrections do not allow for the influence of the asymmetric deformations on the smooth component of potential energy. Therefore, we shall consider the adopted $\delta W_{fA(B)}$ estimates (see Table 5) to be effective, provided that δW_n are obtained with the liquid drop model. The trend of the first-chance fission cross section σ_{f1} shown in Fig. 47 could be treated as a manifestation of the shell effects in first-chance fission probability. So it can be stated that we have got effective estimate of σ_{f1} which corresponds to consistent fit of $(n, 2n)$, $(n, 3n)$ and $(n, 4n)$ reaction cross section data.

Figures 51-57 show the description of measured neutron-induced fission data up to 20 MeV incident neutron energies for target nuclei with various fissilities and parities of protons Z and neutrons N. It seems that present estimates of fission barrier parameters and fission level density modelling provide a consistent description of available data up to 20 MeV.

5 Fission barriers

The collective contribution to the level density of deformed nucleus is determined by the order of symmetry of nuclear shape deformation at saddles [3]. The collective effects are manifested as drastic sensitivity to the inclusion of inner saddle point triaxiallity of both experimental and theoretical fission barrier parameters. The theoretical SCM fission barriers depend on elongation as well as axially symmetric and asymmetric coordinates. Introducing or abandoning saddle asymmetries relevant to SCM calculations we observe that fission barriers, extracted by cross section data analysis also exhibit strong (Z, N)-dependence [44, 45]. Once again, the non-threshold energy dependence of the ^{232}U(n,f) cross section is interpreted in a double-humped fission barrier model [11], the inner barrier of fissioning nucleus ^{233}U being

$\sim$ 1 MeV lower than the outer one, as anticipated with the SCM calculation [2]. The inner barrier was assumed axially symmetric in case of U compound systems with $A \leq 236$ and asymmetric for $A > 236$.

Table 8

Fission barrier parameters

Nuclide	E_{fA}	δE_{fA}	Sym_A	E_{fB}	δE_{fB}	Sym_B	$\hbar\omega_A$	$\delta\hbar\omega_A$	$\hbar\omega_B$	$\delta\hbar\omega_B$	δ
^{230}Th	6.1		S	6.8		MA	0.9		0.6		0.04
^{231}Th	6.0		S	6.7		MA	0.7		0.5		0.06
^{232}Th	5.8		S	6.7		MA	0.9		0.6		0.04
^{233}Th	5.35		S	6.60		MA	0.7		0.5		0.06
^{230}Pa	5.6		S	5.8		MA	0.6		0.4		0.18
^{231}Pa	5.5		S	5.5		MA	1.0		0.5		0.02
^{232}Pa	5.0		S	6.2		MA	0.6		0.4		0.18
^{233}Pa	5.7		S	5.8		MA	1.0		0.5		0.02
^{234}Pa	6.3		S	6.15		MA	0.6		0.4		0.18
^{231}U	4.4		S	5.5		MA	0.7		0.5		0.10
^{232}U	4.9		S	5.4		MA	0.9		0.6		0.05
^{233}U	4.15	0.7	S	5.85	0.05	MA	0.8	0.5	0.5	0.3	0.10
^{234}U	4.80	0.1	S	5.6	0.05	MA	0.9	0.5	0.6	0.2	0.05
^{235}U	5.45	0.3	S	5.90	0.05	MA	0.7	0.3	0.5	0.3	0.02
^{236}U	5.0	0.1	S	5.62	0.05	MA	0.9	0.5	0.6	0.2	0.07
^{237}U	6.4	0.05	GA	6.10	0.10	MA	0.75	0.03	0.5	0.4	0.01
^{238}U	5.80	0.05	GA	5.50	0.05	MA	0.90	0.5	0.6	0.2	0.12
^{239}U	6.45	0.05	GA	5.95	0.10	MA	0.68	0.03	0.5	0.4	0.02
^{235}Np	5.1		S	5.5		MA	1.0		0.5		0.0
^{236}Np	5.0		S	5.4		MA	0.6		0.4		0.08
^{237}Np	5.2		S	5.4		MA	1.0		0.5		0.00
^{238}Np	6.1	0.1	GA	5.95	0.05	MA	0.6	0.05	0.4	0.2	0.08
^{239}Np	6.1		GA	5.3		MA	0.7		0.5		0.03

Fission barrier parameters: inner(A) and outer(B) barrier heights $E_{fA(B)}$ and curvatures $\hbar\omega_{A(B)}$ are given in Table 8. The symbol 'Sym'$_{A(B)}$ denotes the symmetry of saddle point deformation. The correlation function $\Delta_f = \Delta_o + \delta$ at saddles depends, actually, on a_f/a_n ratio, which is a function of $(\delta W_f - \delta W_n)$. The comparison of obtained U, Np, Pu, Am, Cm fission barriers with SCM fission barriers and fission barriers provided by Smirenkin[46] is shown on Figs. 58-67. For uraniums the agreement is rather good for outer fission barrier. As regards the inner barrier the isotopic dependences

of present barriers and those predicted by Smirenkin[46] are similar. For plutonium and americium nuclei the agreement would be also good, if not the americium outer barrier for neutron-deficient nuclei. However, we extracted these barrier values by analysis of emissive fission contribution for the reaction ^{241}Am(n,f) [14]. Most disturbing might be the discrepancy in case of curium outer barrier values (see Fig. 66), measured data base have changed extensively during recent years and this is reflected in present fission barrier parameters.

Table 8 (continued)
Fission barrier parameters

Nuclide	E_{fA}	δE_{fA}	Sym$_A$	E_{fB}	δE_{fB}	Sym$_B$	$\hbar\omega_A$	$\delta\hbar\omega_A$	$\hbar\omega_B$	$\delta\hbar\omega_B$	δ
^{237}Pu	4.15		S	5.25		MA	0.7		0.6		0.08
^{238}Pu	5.6		S	5.1		MA	0.9		0.6		0.07
^{239}Pu	6.325	0.05	GA	5.70	0.10	MA	0.7	0.03	0.5	0.4	0.08
^{240}Pu	5.95	0.05	GA	5.15	0.05	MA	0.8	0.05	0.6	0.5	0.075
^{241}Pu	6.15	0.05	GA	5.50	0.10	MA	0.7	0.03	0.5	0.4	0.10
^{242}Pu	5.55	0.05	GA	5.15	0.05	MA	0.9	0.05	0.6	0.5	0.08
^{243}Pu	6.05	0.05	GA	5.45	0.1	MA	0.73	0.03	0.52	0.4	0.13
^{244}Pu	5.7		GA	4.85		MA	0.9		0.6		0.08
^{245}Pu	5.75	0.05	GA	5.40	0.1	MA	0.7	0.03	0.5	0.4	0.09
^{239}Am	6.00		GA	5.40		MA	0.8		0.5		0.00
^{240}Am	6.10		GA	6.00		MA	0.6		0.4		0.00
^{241}Am	6.00		GA	5.35		MA	0.8		0.5		0.00
^{242}Am	6.32	0.10	GA	5.78	0.05	MA	0.6	0.05	0.4	0.2	0.11
^{243}Am	6.40	0.05	GA	5.05	0.05	MA	1.0	0.3	0.5	0.50	0.00
^{244}Am	6.25	0.10	GA	5.9	0.05	MA	0.7	0.05	0.53	0.2	0.04
^{241}Cm	7.15		GA	5.5		MA	0.7		0.5		0.04
^{242}Cm	6.65		GA	5.0		MA	0.9		0.6		0.10
^{243}Cm	6.42	0.05	GA	5.4	0.1	MA	0.7	0.1	0.5	0.4	0.04
^{244}Cm	5.78	0.05	GA	4.80	0.1	MA	0.9	0.1	0.6	0.4	0.10
^{245}Cm	6.43	0.05	GA	5.60	0.1	MA	0.7	0.03	0.5	0.4	0.08
^{246}Cm	5.65	0.05	GA	5.40	0.1	MA	0.9	0.1	0.6	0.4	0.035
^{247}Cm	6.15	0.05	GA	5.35	0.1	MA	0.7	0.03	0.5	0.4	0.08
^{248}Cm	5.55	0.05	GA	4.85	0.1	MA	0.9	0.1	0.6	0.4	0.07
^{249}Cm	5.70	0.05	GA	5.10	0.1	MA	0.7	0.1	0.5	0.4	0.08
^{250}Bk	6.00	0.10	GA	5.40	0.05	MA	0.6	0.1	0.4	0.2	0.07
^{250}Cf	5.90	0.05	GA	5.45	0.1	MA	0.9	0.1	0.6	0.4	0.03

S - symmetric saddle point, GA - axially asymmetric saddle point, MA - mass asymmetric saddle point.

6 Conclusions

The sophistication of the level density model, as compared with various options of Fermi-gas closed-form expressions, although it still remains rather crude, seems to be unavoidable, since it is backed by a lot of experimental data. That is the shortest way to consistent modelling of fission cross section data behavior and extracting reasonable level density and fission barrier parameter values. Staying within a framework of Fermi-gas level density model one ignores direct experimental and theoretical evidence of pairing and collective effects in level densities and fission barriers.

The most important input items for statistical theory calculations of neutron-induced reactions are neutron resonance spacings $\langle D_{obs} \rangle$, $s-$wave neutron strength functions $\langle S_o \rangle$, shell corrections δW and coupled channel potential parameters, for these Reference Input Parameter Library (RIPL) Starter File recommendations [22] were extensively used.

It is shown that the modelling of the fission transition states and level densities at inner and outer saddle deformations provides a consistent set of actinide fission barrier and level density parameters. That is the price to be paid to interpret the features observed in measured fission cross section data as well as those predicted in shell correction method calculations of fission barriers. Fission barrier parameters and level density modelling were successively used for fission cross section calculation up to 20 MeV incident neutron energy.

References

[1]Strutinsky V.M. Nucl. Phys. A95, 420 (1967).

[2]Howard W.M., Möller P. Atomic Data and Nuclear Data Tables,25, 219 (1980).

[3]Ignatjuk A.V., Istekov K.K., Smirenkin G.N. Sov. J. Nucl. Phys. 29, 450 (1979).

[4]Ignatyuk A.V., Maslov V.M. Sov. J. Nucl. Phys., 54, 392 (1991).

[5]Maslov V.M. IV International Seminar on Interaction of Neutrons with Nuclei, Dubna, Russia, April 27-30, 1996, p. 65, 1996.

[6]Moldauer P.A., Rev. Mod. Phys. Phys. 36, 1079 (1964).

[7]Hauser W. and Feshbach H., Phys. Rev. 87, 366 (1952).

[8]Tepel J.W., Hoffman H.M., Weidenmuller H.A. Phys. Lett. 49, 1 (1974).

[9]Bohr A. and Mottelson B., Nuclear Structure, vol. 2, (Benjamin, New-York, 1975).

[10]Pashkevich V.V., Nucl. Phys. A133, 400 (1969).

[11]Maslov V.M., Kikuchi Y. Nucl. Sci. Eng 124, 492 (1996).

[12]Bolsterli M., Fiset E.O., Nix J.R., Norton J.L. Phys.Rev., C 5, 1050 (1972).

[13]Maslov V.M., Porodzinskij Yu.V., Sukhovitskij E.Sh., Morogovskij G.B., INDC(BLR)-7, Vienna, 1997.

[14]Maslov V.M., Porodzinskij Yu.V., Sukhovitskij E.Sh., Klepatskij A.B. and Morogovskij G.B., INDC(BLR)-5, Vienna, 1996.

[15]Sood P.C., Singh R.N. Nucl. Phys. A373, 519 (1982).

[16]Maslov V.M., Porodzinskij Yu.V., Hasegawa A. and Shibata K., JAERI-Research, 1998 (in print).

[17]Young P.G. In: INDC(NDS)-335, 1995, p.109.

[18]Maslov V.M, Porodzinskij Yu.V., Sukhovitskij E.Sh., Proc. Int. Conf. Nucl. Data for Sci. and Technology, Trieste, Italy, May 19-23, 1997, p. 1332.

[19]Dilg W., Shantl W., Vonach H. and Uhl M. Nucl. Phys. 217, 269 (1973).

[20]S. Bjornholm and J.E. Lynn, Rev. Mod. Phys. 52 (1980) 725.

[21]Myers W.O., Swiatecky W.J., Ark. Fyzik, 36, 243 (1967).

[22]Reference Input Parameter Library, IAEA-TECDOC, IAEA, Vienna, 1998, in print.

[23]Porodzinskij Yu.V., Sukhovitskij E.Sh., Maslov V.M. Proc. of International Conference on Nuclear Data for Science and Technology. Trieste, Italy, 19-24 May 1997, p.937.

[24]Maslov V.M. and Porodzinskij Yu.V. JAERI-Research, 1998 (in print).

[25]Evaluated Nuclear Structure Data File, 1997.

[26]Maslov V.M. Zeit. Phys. A, Hadrons & Nuclei, 347, 211 (1994).

[27]Maslov V.M., Proc. Ninth Int. Symp. Capture Gamma-Ray Spectroscopy and Related Topics, Budapest, Hungary, October 8-12, 1996, p.676.

[28]Dossing T., Khoo T.I., Lauritsen T. et al., Phys. Rev. Lett., 75, 1276 (1995).

[29]Khitrov V.A., Sukhovoj A.M., Voinov A.V., IV International Seminar on Interaction of Neutrons with Nuclei, Dubna, Russia, April 27-30, 1996, p. 45, 1996.

[30]Maslov V.M , Proc. of International Conference on Nuclear Data for Science and Technology, Trieste, Italy, 19-24 May 1997, p.1320.

[31]Fu C. Nucl. Sci. Engng. 86, 344 (1984).

[32]Mcnally J.H., Barnes J.W., Dropesky B.J., et al., Phys. Rev. C9, 717 (1974)..

[33]Fursov B.I., Polynov V.N., Samylin B.F., Shorin V.S., Proc. of International Conference on Nuclear Data for Science and Technology, Trieste, Italy, 19-24 May 1997. p.488.

[34]Danon Y., Slovacek R.E., Block R.C., et al., Nucl. Sci. Eng., 109, 341 (1991).

[35]Moore M.S., Keyworth G.A. Phys. Rev. C, 3, 1656 (1971).

[36]Fomushkin E.F., Novoselov G.F., Vinogradov Yu.I., Gavrilov G.F., Zherebtsov Sov. J. Nucl. Phys. 31, 19 (1980).

[37]Fomushkin E.F., Novoselov G.F., Vinogradov Yu.I., Gavrilov G.F., Zherebtsov Sov. J. Nucl. Phys. 36, 338 (1982).

[38]Maguire Jr.H.T.,Stopa C.R.S., Block R.C. et al. Nucl. Sci. Eng. 89, 293 (1985).

[39]Alam B., Block R.C., Slovacek R.E., Hoff R.W. Nucl. Sci. Eng. 99, 267 (1988).

[40]Britt H.C., Wilhelmy J.B. Nucl. Sci. Eng. 72, 222 (1979).

[41]Valskij G.V., Gromova E.A., Danichev V.V. et al. Proc. Int. Conf. on Neutron Physics, 14-18 Sept., Kiev, USSR.

[42]Uhl M. and Strohmaier B., IRK-76/01, IRK, Vienna (1976).

[43]Boykov G.S., Dmitriev V.D., Kudyaev G.A., Maslov V.M., et al., Ann. Nucl. Energy, 10, 585 (1994).

[44]Ignatjuk A.V., Maslov V.M., Proc. Int. Symp. Nuclear Data Evaluation Methodology, Brookhaven,USA, October 12-16, 1992, p.440, World Scientific, 1993.

[45]Maslov V.M., Kikuchi Y., JAERI-Research 96-030, 1996.

[46]Smirenkin G.N., INDC(CCP)-359, Vienna, 1993.

7 Figure captions

Fig. 1 Main level density parameter $\tilde{a}/A$ as a function of atomic mass A.
Fig. 2 Cumulative number of levels of ^{232}U.
Fig. 3 Cumulative number of levels of ^{233}U.
Fig. 4 Cumulative number of levels of ^{234}U.
Fig. 5 Cumulative number of levels of ^{235}U.
Fig. 6 Cumulative number of levels of ^{236}U.
Fig. 7 Cumulative number of levels of ^{237}U.
Fig. 8 Cumulative number of levels of ^{238}U.
Fig. 9 Cumulative number of levels of ^{239}U.
Fig. 10 Cumulative number of levels of ^{241}Am.
Fig. 11 Cumulative number of levels of ^{242}Am.
Fig. 12 Fission cross section of ^{238}Pu.
Fig. 13 Level density of fissioning nuclide ^{239}Pu.
Fig. 14 Level density of ^{238}Pu.
Fig. 15 Fission cross section of ^{233}U.
Fig. 16 Fission cross section of ^{235}U.
Fig. 17Level density of fissioning nuclide ^{234}U.
Fig. 18 Fission cross section of ^{237}U.
Fig. 19 Fission cross section of ^{239}Pu.
Fig. 20 Fission cross section of ^{241}Pu.
Fig. 21 Fission cross section of ^{243}Cm.
Fig. 22 Fission cross section of ^{245}Cm.
Fig. 23 Fission cross section of ^{247}Cm.
Fig. 24 Fission cross section of ^{249}Cf.
Fig. 25 Two-quasiparticle excitation threshold in neutron energy scale as a function fissioning nucleus mass A.
Fig. 26, 26a Fission cross section of ^{238}U.
Fig. 27, 27a Fission cross section of ^{236}U.
Fig. 28, 28a Fission cross section of ^{234}U.
Fig.29 Fission cross section of ^{232}U.
Fig. 30, 30a Fission cross section of ^{240}Pu.
Fig. 31, 31a Fission cross section of ^{242}Pu.
Fig. 32, 32a Fission cross section of ^{244}Pu.
Fig. 33 Fission cross section of ^{236}Pu.
Fig. 34,34a Fission cross section of ^{244}Cm.
Fig. 35, 35a Fission cross section of ^{246}Cm.
Fig. 36, 36a Fission cross section of ^{248}Cm.
Fig. 37, 37a Fission cross section of ^{242}Cm.

Fig. 38 Fission cross section of ^{232}Th.
Fig. 39 Three-quasiparticle excitation threshold in neutron energy scale as a function fissioning nucleus mass A.
Fig. 40, 40a Fission cross section of ^{241}Am.
Fig. 41, 41a Fission cross section of ^{243}Am.
Fig. 42, 42a Fission cross section of ^{237}Np.
Fig. 43 Fission cross section of ^{249}Bk.
Fig. 44 Fission cross section of ^{231}Pa.
Fig. 45 Fission cross section of ^{242m}Am.
Fig. 46 Fission cross section of ^{236l}Np.
Fig. 47 Fission cross section of ^{238}Np.
Fig. 48 Fission cross section of ^{238}U.
Fig. 49 ^{238}U(n,2n) reaction cross section.
Fig. 50 ^{238}U(n,3n) reaction cross section.
Fig. 51 Fission cross section of ^{235}U.
Fig. 52 Fission cross section of ^{242}Pu.
Fig. 53 Fission cross section of ^{237}Np.
Fig. 54 Fission cross section of ^{234}U.
Fig. 55 Fission cross section of ^{241}Am.
Fig. 56 Fission cross section of ^{243}Am.
Fig. 57 Fission cross section of ^{242m}Am.
Fig. 58 Inner fission barrier of U
Fig. 59 Outer fission barrier of U.
Fig. 60 Inner fission barrier of Np.
Fig. 61 Outer fission barrier of Np.
Fig. 62 Inner fission barrier of Pu.
Fig. 63 Outer fission barrier of Pu.
Fig. 64 Inner fission barrier of Am.
Fig. 65 Outer fission barrier of Am.
Fig. 66 Inner fission barrier of Cm.
Fig. 67 Outer fission barrier of Cm.

Citation of periodicals, reporting work done under this contract

1. Maslov V.M. "Above-threshold Structure in ^{244}Cm Neutron-induced Fission Cross Section", IV International Seminar on Interaction of Neutrons with Nuclei, Dubna, Russia, April 27-30, 1996, p. 65, 1996.
2. Maslov V.M. "Evidence of Pair Correlations in Actinide Neutron-Induced Fission Cross Sections", Proc.International Conference Nuclear Data for Science and Technology, Trieste, Italy, May 19-24, 1997, p. .
3. Maslov V.M. Contribution to final Report of CRP "Development of Reference Input Parameter Library for Nuclear Model Calculations of Nuclear Data", (in print), 1998.
4. Maslov V.M., Porodzinskij Yu.V., Sukhovitskij E.Sh. " Evaluation of Neutron data for Neptunium-238", INDC(BLR)-011, 1998.
5. Maslov V.M., Sukhovitskij E.Sh., Porodzinskij Yu.V. G.B. Morogovskij, " Evaluation of Neutron data for Americium-241,-242,-242m,-243", Proc. of International Conference on Nuclear Data for Science and Technology, Trieste, Italy, 19-24 May 1997, p.1317.
6. Maslov V.M., Porodzinskij Yu.V., Sukhovitskij E. Sh."238-U Inelastic Neutron Scattering" Proc. of International Conference on Nuclear Data for Science and Technology, Trieste, Italy, 19-24 May 1997, p.1332.
7. Maslov V.M., Porodzinskij Yu.V., Hasegawa A., Shibata K., "Neutron Data Evaluation of ^{238}U ", JAERI Research, 1998 (in print)
8. Maslov V.M., Proc. Ninth Int. Symp. Capture Gamma-Ray Spectroscopy and Related Topics, Budapest, Hungary, October 8-12, 1996, p.676.

Other relevant literature references

1. Maslov V.M. and Kikuchi Y. JAERI-Research, 96-030, 1996.
2. Maslov V.M. and Kikuchi Y. Nucl. Sci. Engng., 1996.
3. Maslov V.M., Porodzinskij Yu.V., Sukhovitskij E.Sh., Klepatskij A.B., Morogovskij G.B. "Evaluation of Neutron Data for Curium-243", INDC(BLR)-2, 1995.
4. Maslov V.M., Porodzinskij Yu.V., Sukhovitskij E.Sh., Klepatskij A.B., Morogovskij G.B. "Evaluation of Neutron Data for Curium-245", INDC(BLR)-3, 1995.
5. Maslov V.M., Porodzinskij Yu.V., Sukhovitskij E.Sh., Klepatskij A.B., Morogovskij G.B. "Evaluation of Neutron Data for Curium-246", INDC(BLR)-4, 1996.
6. Maslov V.M., Porodzinskij Yu.V., Sukhovitskij E.Sh., Klepatskij A.B., Morogovskij G.B. "Evaluation of Neutron Data for Americium-241", INDC(BLR)-5, 1996.
7. Maslov V.M., Porodzinskij Yu.V., Sukhovitskij E.Sh., Klepatskij A.B., Morogovskij G.B. "Evaluation of Neutron Data for Americium-243", INDC(BLR)-6, 1996.

8. Maslov V.M., Porodzinskij Yu.V., Sukhovitskij E.Sh., Morogovskij G.B. "Evaluation of Neutron Data for Americium-242m", INDC(BLR)-7, 1997.
9. Maslov V.M., Porodzinskij Yu.V., Sukhovitskij E.Sh., "Evaluation of Neutron Data for Americium-242g", INDC(BLR)-8, 1997.
10. Maslov V.M., Porodzinskij Yu.V., Sukhovitskij E.Sh., Morogovskij G.B. "Evaluation of Neutron Data for Plutonium-238", INDC(BLR)-9, 1997.
11. Maslov V.M., Porodzinskij Yu.V., Sukhovitskij E.Sh., Morogovskij G.B. "Evaluation of Neutron Data for Plutonium-242", INDC(BLR)-10, 1997
12. Maslov V.M., Porodzinskij Yu.V., Sukhovitskij E.Sh., Klepatskij A.B., Morogovskij G.B.Proc. Int. Conf. on the Physics of Reactors, September 16-21, 1996, Mito, Japan,1996, V. 3, p. F1.

Results obtained

Adopted fission and total level densities modelling along with fission barrier parameters allowed to describe available neutron-induced fission cross section data for Th, Pa, U, Np, Pu, Am, Bk,Cm and Cf target nuclei. The data for incident neutron energies ~10 keV up to emissive fission threshold were analyzed. Saddle asymmetries relevant to SCM calculations influence fission barriers, extracted by cross section data analysis. The inner barrier was assumed axially symmetric in case of U, Np and Pu neutron-deficient nuclei. We have demonstrated that observed irregularities in neutron-induced fission cross section data could be attributed to the interplay of few-quasiparticle excitations in the level density of fissioning and residual nuclei. In case of Z-even, N-odd fissile targets the step-like irregularities in fission cross section data shapes are supposed to be due to interplay of two-quasiparticle excitations in the level density of even fissioning nucleus and one-quasiparticle excitation in odd residual nucleus. In case of the only available Z-odd, N-odd target ^{242m}Am the effect of Z-odd, N-even fissioning nucleus level density is evidenced as a step-like shape of fission cross section data below 1 MeV. In case of Z-even, N-even targets neutron-induced fission the step-like structures (U, Pu) and resonance-like structures (Cm) were interpreted to be due to interplay of one-quasiparticle excitations in the level density of odd fissioning nucleus and two-quasiparticle excitation in even residual nucleus. The sophistication of the level density modelling seems to be unavoidable, since it is backed by experimental data. That is the price to be paid for consistent modelling of fission cross section data behavior and extracting reasonable level density and fission barrier parameter values. Fission barrier parameters: inner(A) and outer(B) barrier heights $E_{fA(B)}$ and curvatures $\hbar\omega_{A(B)}$ are provided.

Level density modelling and fission barrier parameters were applied for fission data description up to 20 MeV incident neutron energy. Secondary neutron spectrum model was validated by ^{238}U neutron data description. Contribution of emissive (second chance) and non-emissive (first chance) fission to the measured fission cross section of ^{238}U was investigated. The sensitivity of the fit to the ratio of main level density parameters of fissioning nuclide ^{239}U and residual nuclide ^{238}U, a_f and a_n, respectively, was revealed. Pre-equilibrium first neutron emission contribution is defined by high-energy tail of ^{238}U(n,2n) reaction cross section. The sensitivity of the modelling to coupled optical potential, used for reaction cross section calculation was investigated. The sum of ^{238}U(n,2n), ^{238}U(n,3n) and ^{238}U(n,f) reaction cross sections around 20 MeV defines actually reaction cross section value. That means we could define the sharing of total cross section to reaction and shape elastic scattering cross section. We argue that there is almost no need in additional volume absorption term in coupled channel optical potential

for ^{238}U.

Conclusions drawn

Adopting fission and total level densities modelling and extracted fission barrier parameters we described available neutron-induced fission cross section data for Th, Pa, U, Np, Pu, Am, Cm, Bk and Cf targets up to emissive fission threshold. The sophistication of the level density modelling seems to be unavoidable, since it is backed by experimental data. That is the price to be paid for consistent modelling of fission cross section data behavior. Staying within a framework of Fermi-gas level density model one ignores direct experimental and theoretical evidence of shell and collective effects in level densities and fission barriers.

Fission barrier parameters: inner(A) and outer(B) barrier heights $E_{fA(B)}$ and curvatures $\hbar\omega_{A(B)}$ are provided for some exotic nuclides like ^{238}U, for which there is no reliable ^{237}U(n,f) fission data.

Level density modelling and fission barrier parameters could be successively employed for fission data description up to 20 MeV incident neutron energy.

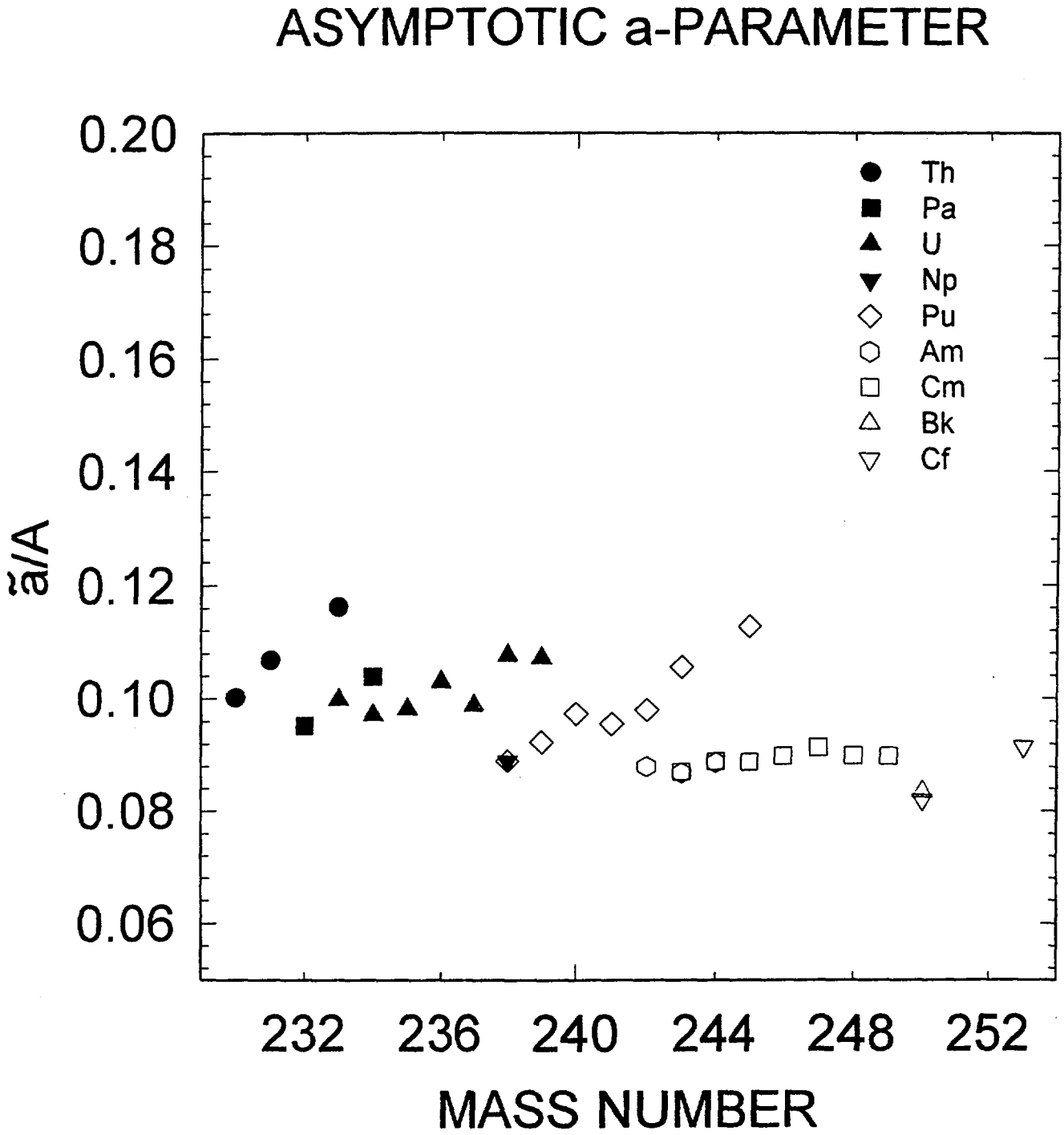
ASYMPTOTIC a-PARAMETER
0.20
0.18
0.16
0.14
0.12
0.10
0.08
0.06
ã/A
232
236
240
244
248
252
MASS NUMBER
Th
Pa
U
Np
Pu
Am
Cm
Bk
Cf

FIG. 1

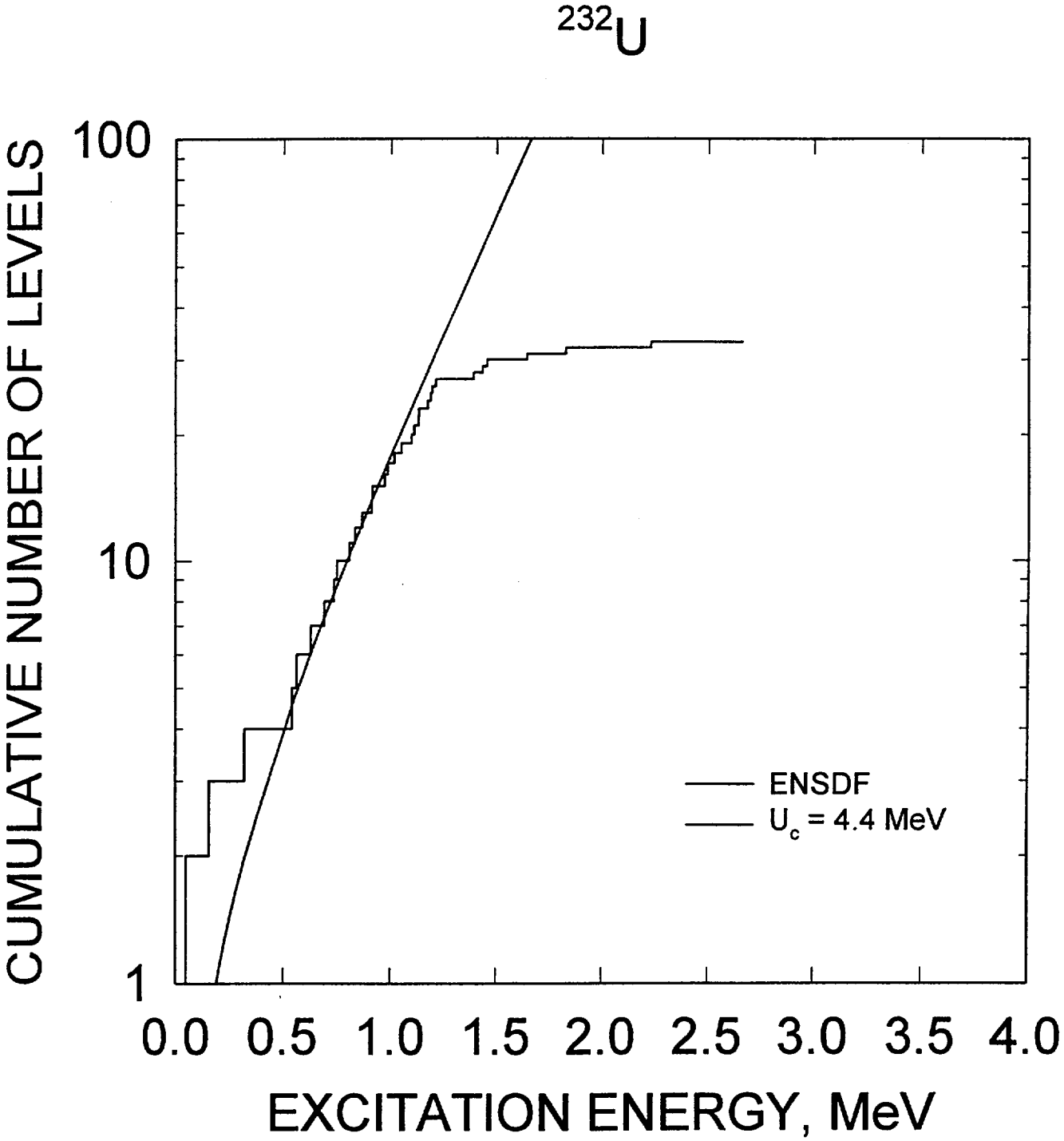
^{232}U
CUMULATIVE NUMBER OF LEVELS
100
10
1
0.0
0.5
1.0
1.5
2.0
2.5
3.0
3.5
4.0
EXCITATION ENERGY, MeV
ENSDF
U_c = 4.4 MeV

FIG. 2

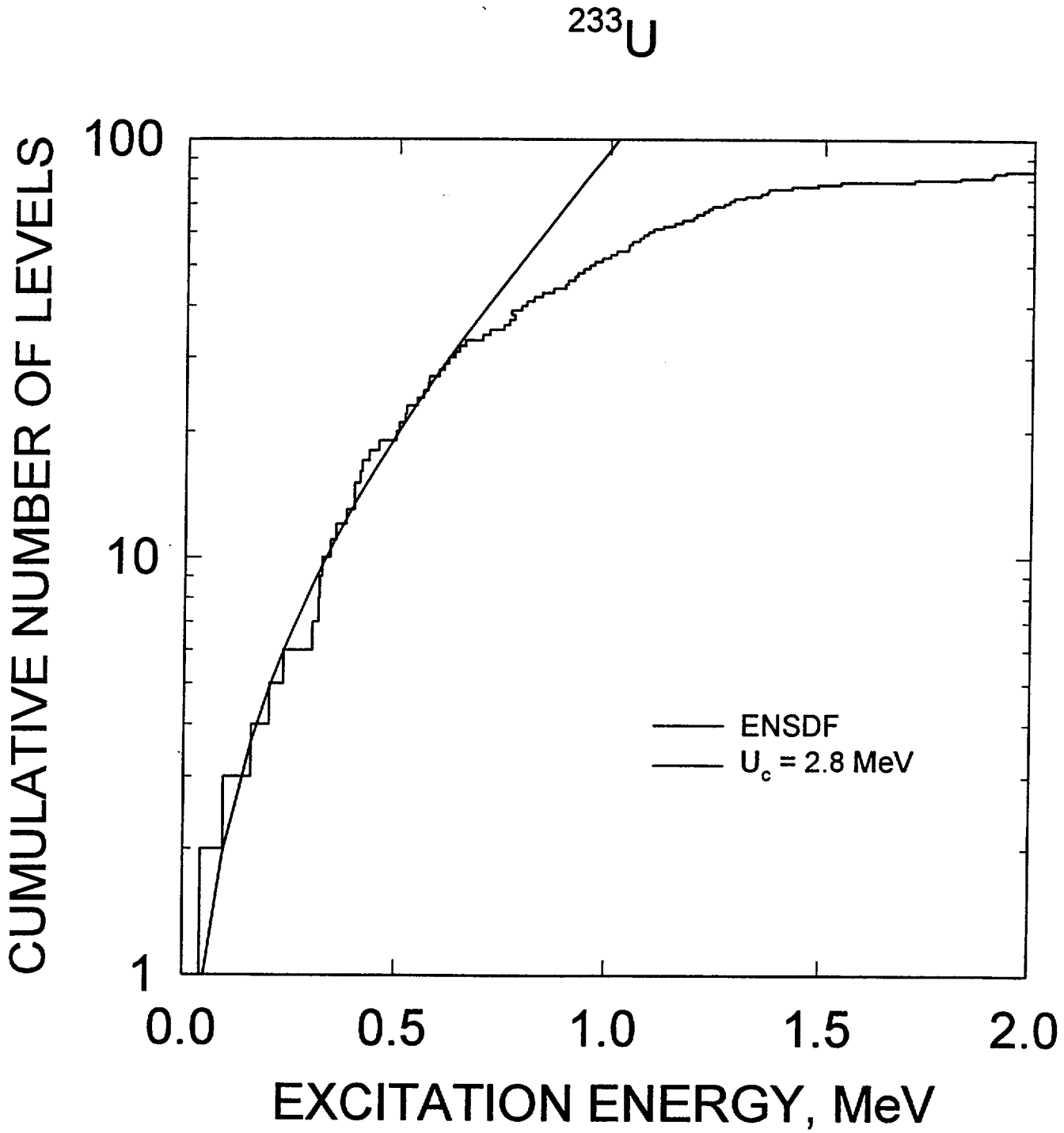
^{233}U
CUMULATIVE NUMBER OF LEVELS
100
10
1
0.0
0.5
1.0
1.5
2.0
EXCITATION ENERGY, MeV
ENSDF
U_c = 2.8 MeV

FIG. 3

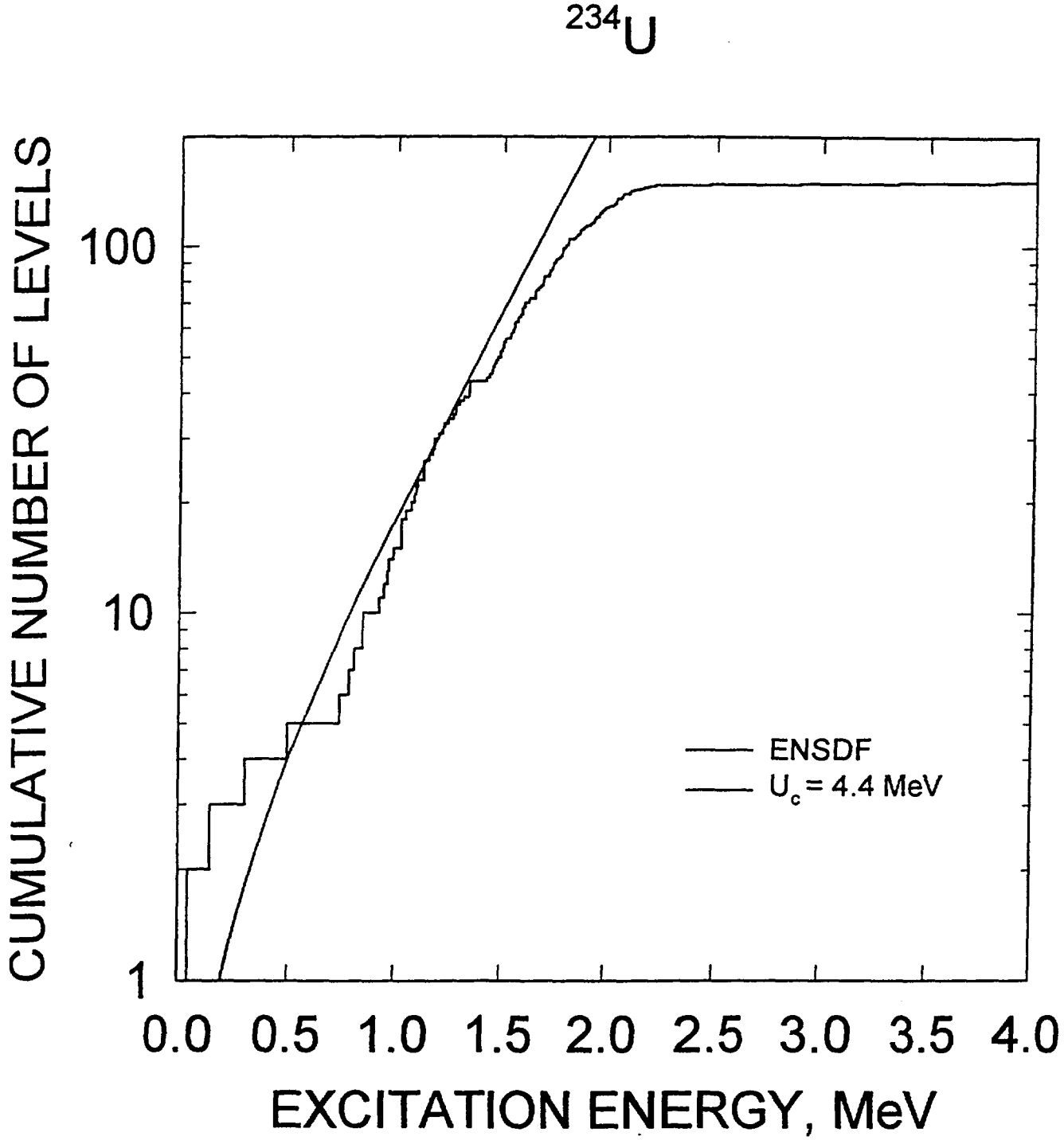
^{234}U
CUMULATIVE NUMBER OF LEVELS
100
10
1
0.0
0.5
1.0
1.5
2.0
2.5
3.0
3.5
4.0
EXCITATION ENERGY, MeV
ENSDF
U_c = 4.4 MeV

FIG. 4

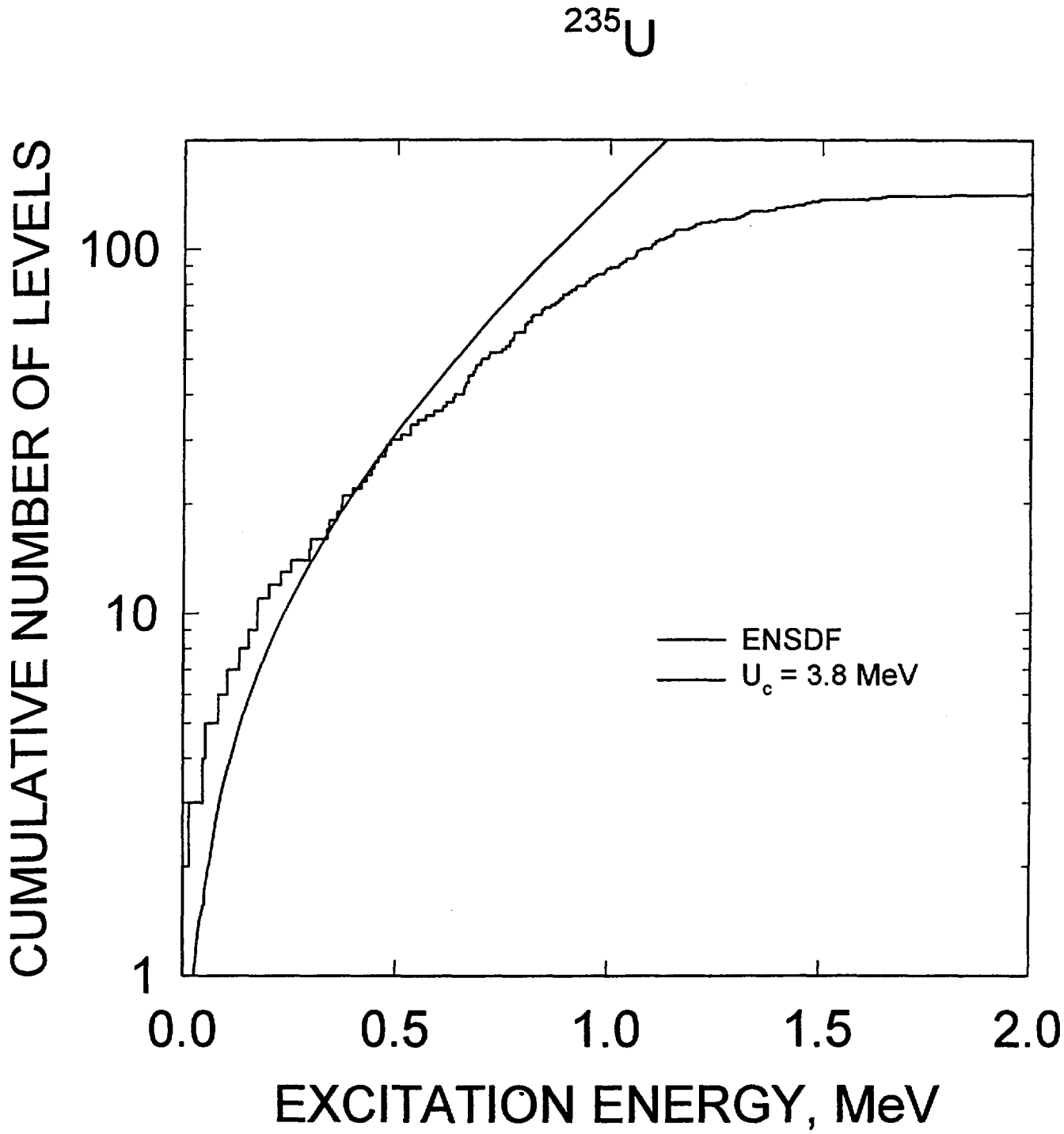
^{235}U
CUMULATIVE NUMBER OF LEVELS
100
10
1
0.0
0.5
1.0
1.5
2.0
EXCITATION ENERGY, MeV
ENSDF
U_c = 3.8 MeV

FIG. 5

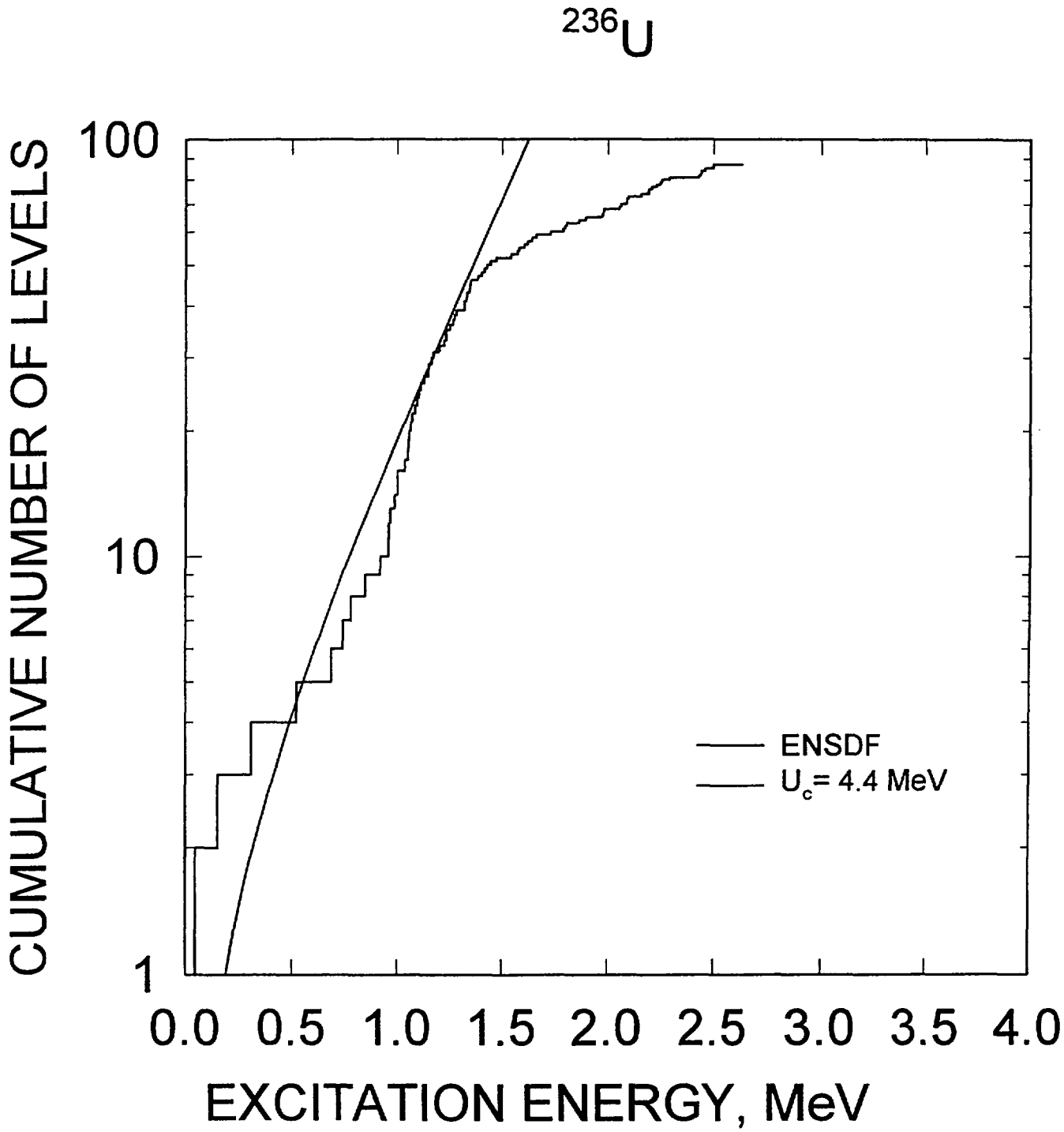
^{236}U
CUMULATIVE NUMBER OF LEVELS
100
10
1
0.0
0.5
1.0
1.5
2.0
2.5
3.0
3.5
4.0
EXCITATION ENERGY, MeV
ENSDF
U_c= 4.4 MeV

FIG. 6

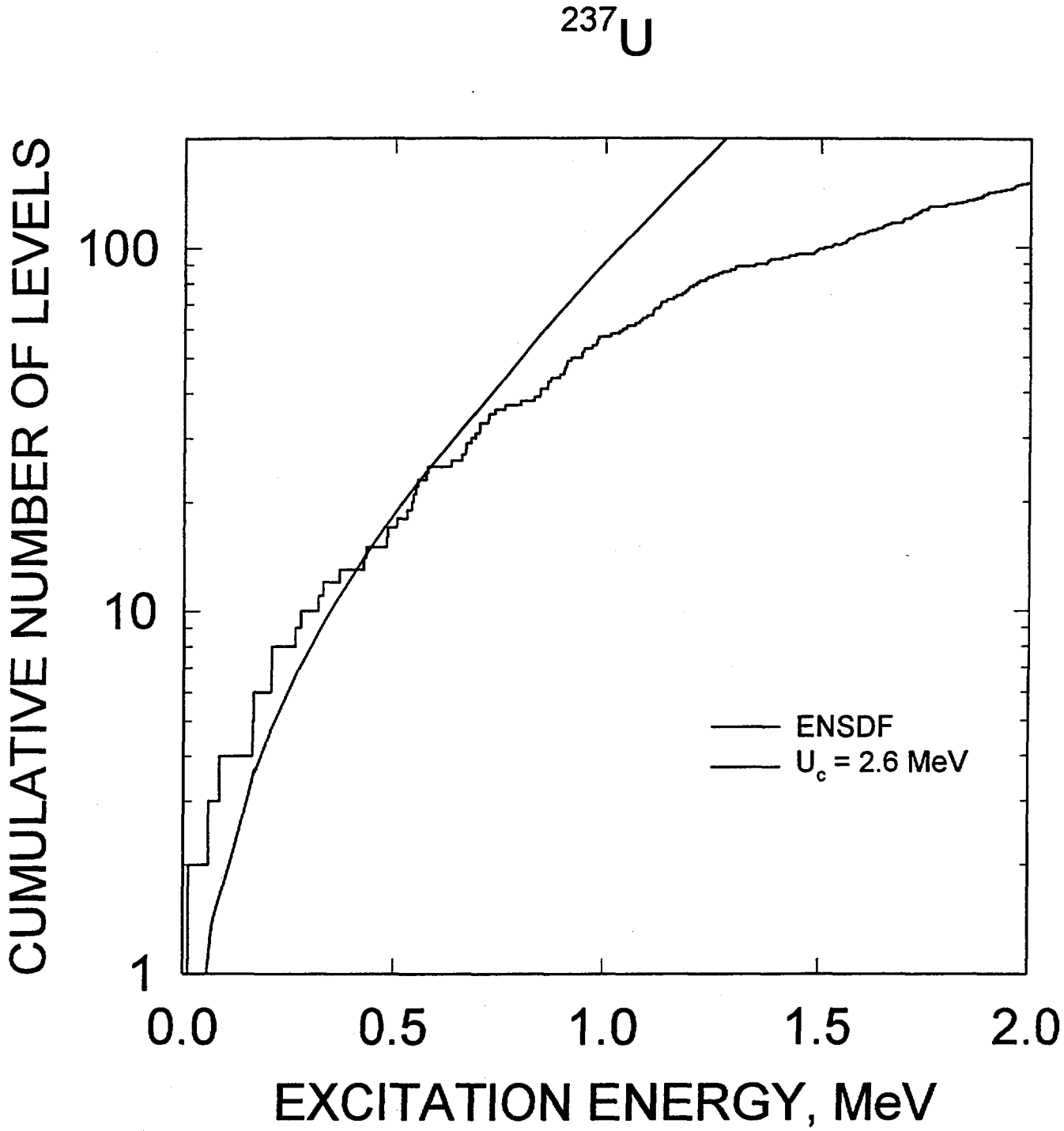
^{237}U
CUMULATIVE NUMBER OF LEVELS
100
10
1
0.0
0.5
1.0
1.5
2.0
EXCITATION ENERGY, MeV
ENSDF
U_c = 2.6 MeV

FIG. 7

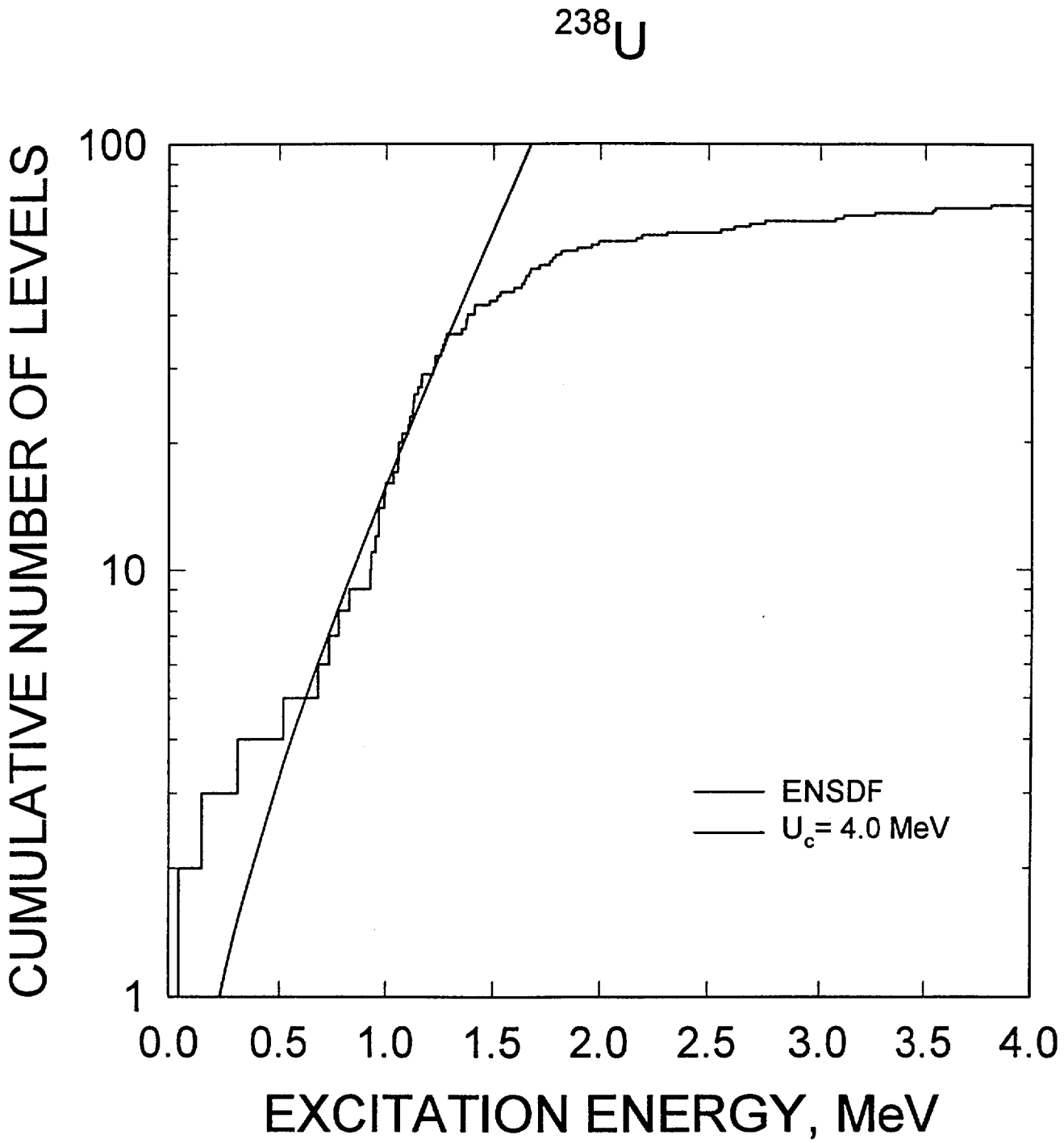
^{238}U
CUMULATIVE NUMBER OF LEVELS
100
10
1
0.0
0.5
1.0
1.5
2.0
2.5
3.0
3.5
4.0
EXCITATION ENERGY, MeV
ENSDF
U_c= 4.0 MeV

FIG. 8

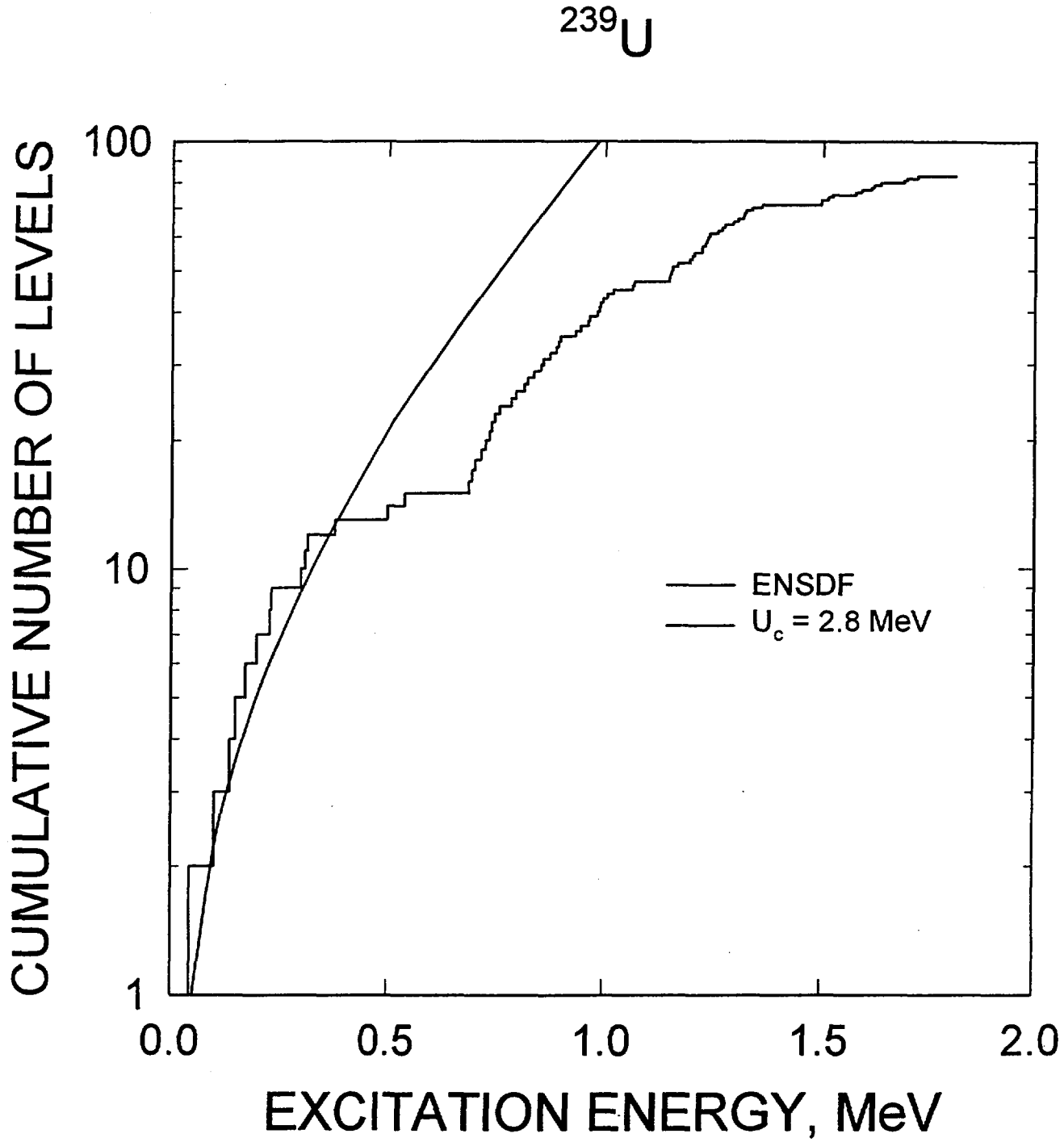
^{239}U
CUMULATIVE NUMBER OF LEVELS
100
10
1
0.0
0.5
1.0
1.5
2.0
EXCITATION ENERGY, MeV
ENSDF
U_c = 2.8 MeV

FIG. 9

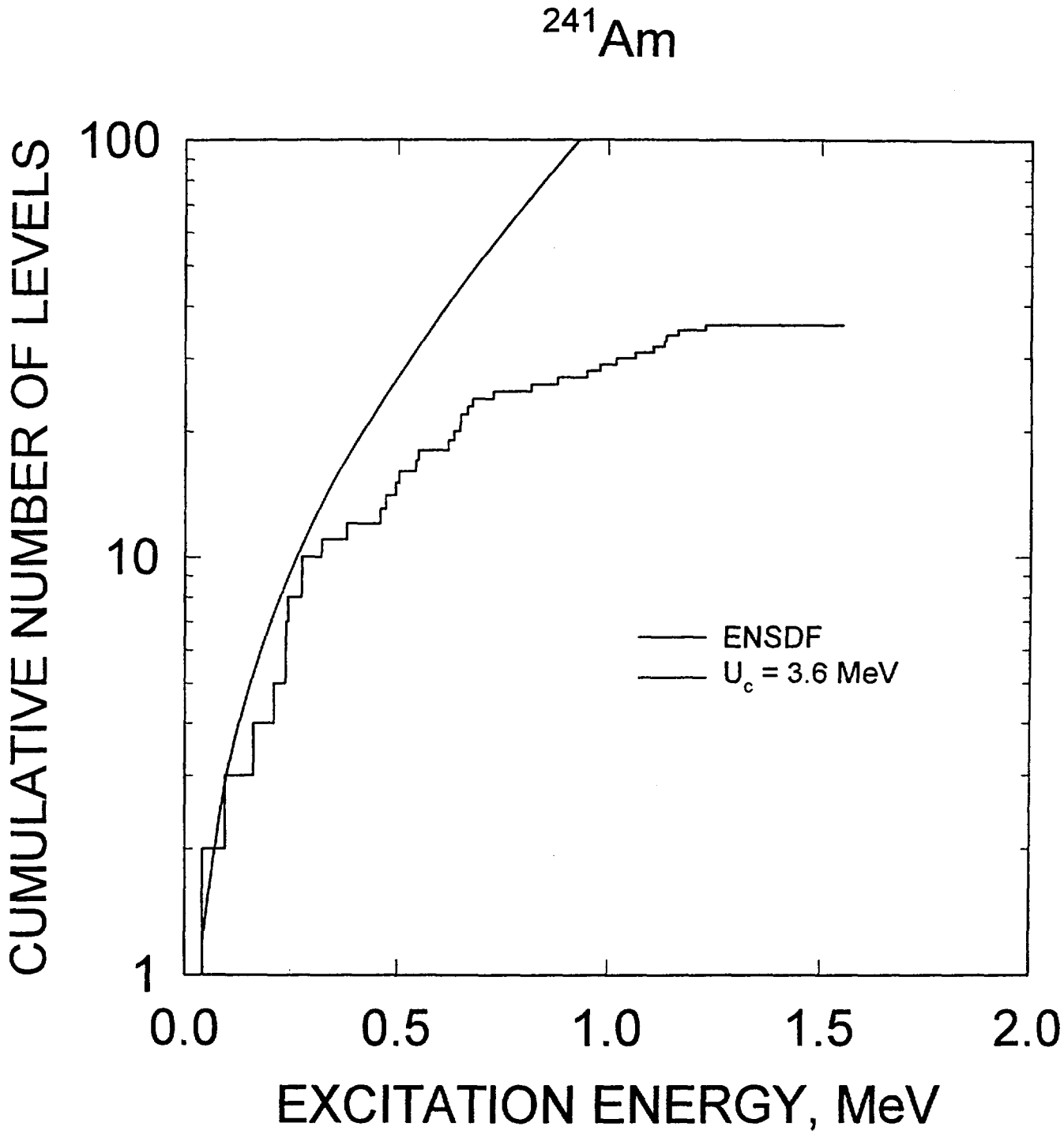
^{241}Am
CUMULATIVE NUMBER OF LEVELS
100
10
1
0.0
0.5
1.0
1.5
2.0
EXCITATION ENERGY, MeV
ENSDF
U_c = 3.6 MeV

FIG. 10

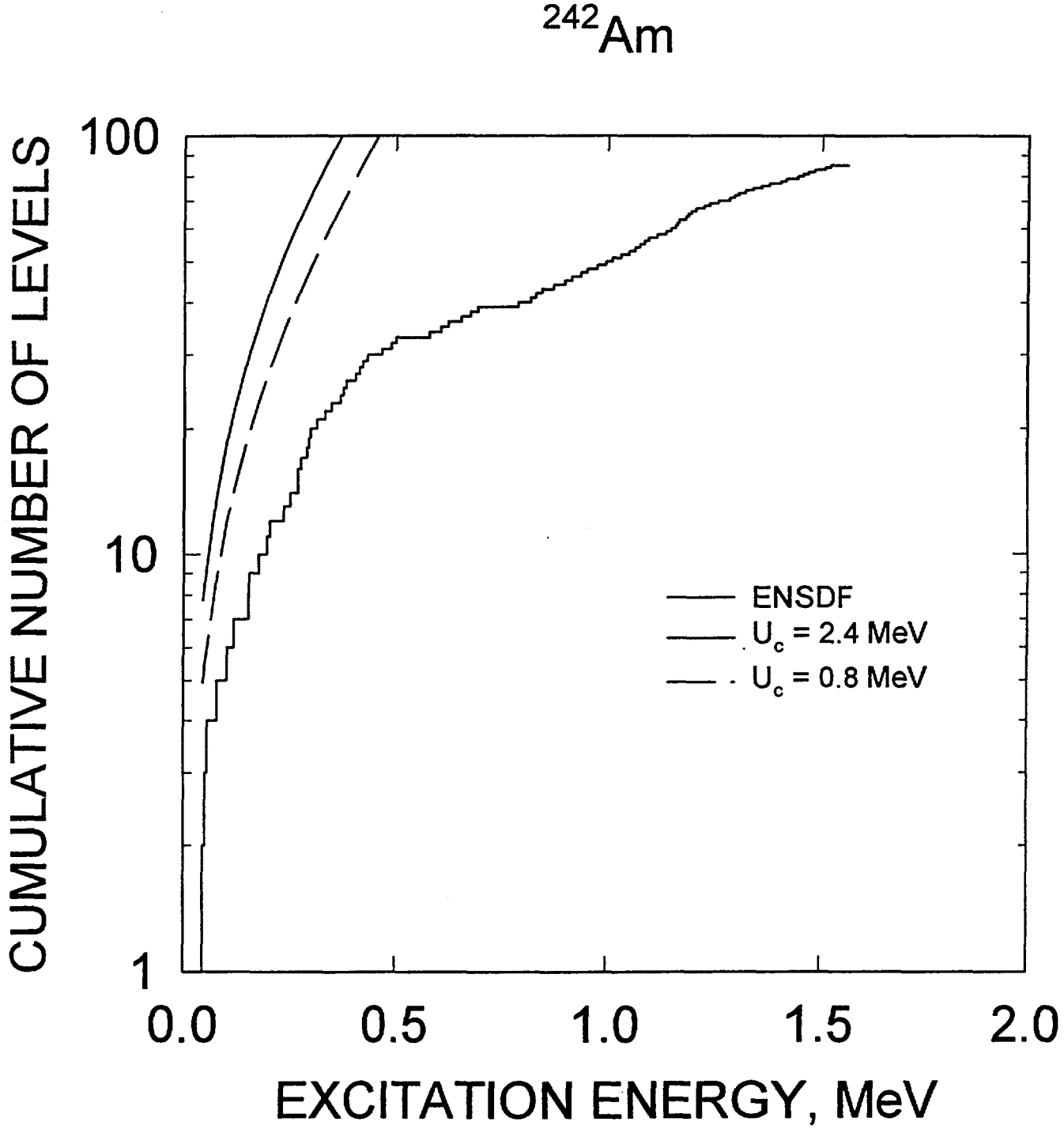
^{242}Am
CUMULATIVE NUMBER OF LEVELS
100
10
1
0.0
0.5
1.0
1.5
2.0
EXCITATION ENERGY, MeV
ENSDF
U_c = 2.4 MeV
U_c = 0.8 MeV

FIG. 11

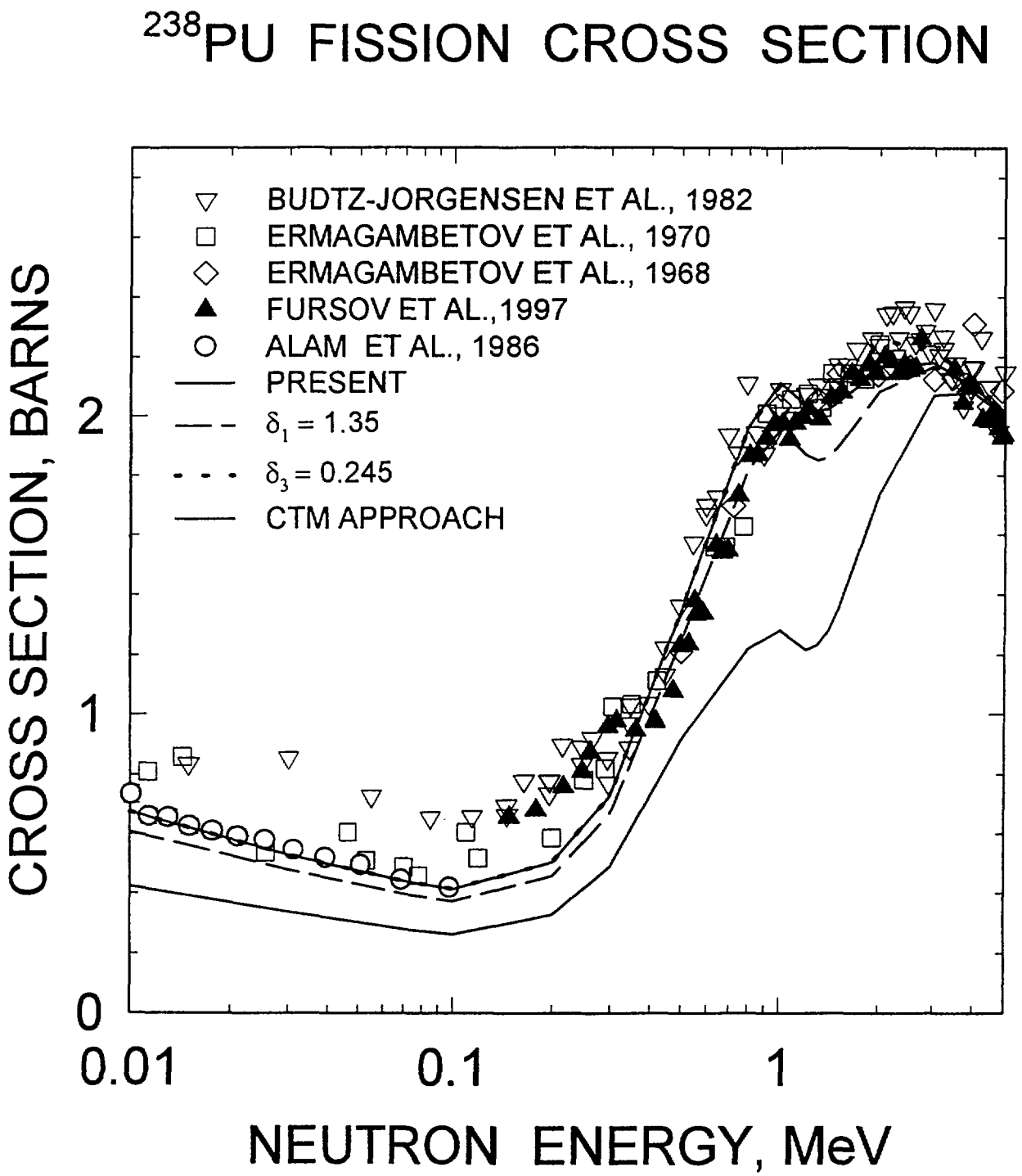
^{238}PU FISSION CROSS SECTION
BUDTZ-JORGENSEN ET AL., 1982
ERMAGAMBETOV ET AL., 1970
ERMAGAMBETOV ET AL., 1968
FURSOV ET AL.,1997
ALAM ET AL., 1986
PRESENT
$\delta_1 = 1.35$
$\delta_3 = 0.245$
CTM APPROACH
CROSS SECTION, BARNS
0
1
2
0.01
0.1
1
NEUTRON ENERGY, MeV

FIG. 12

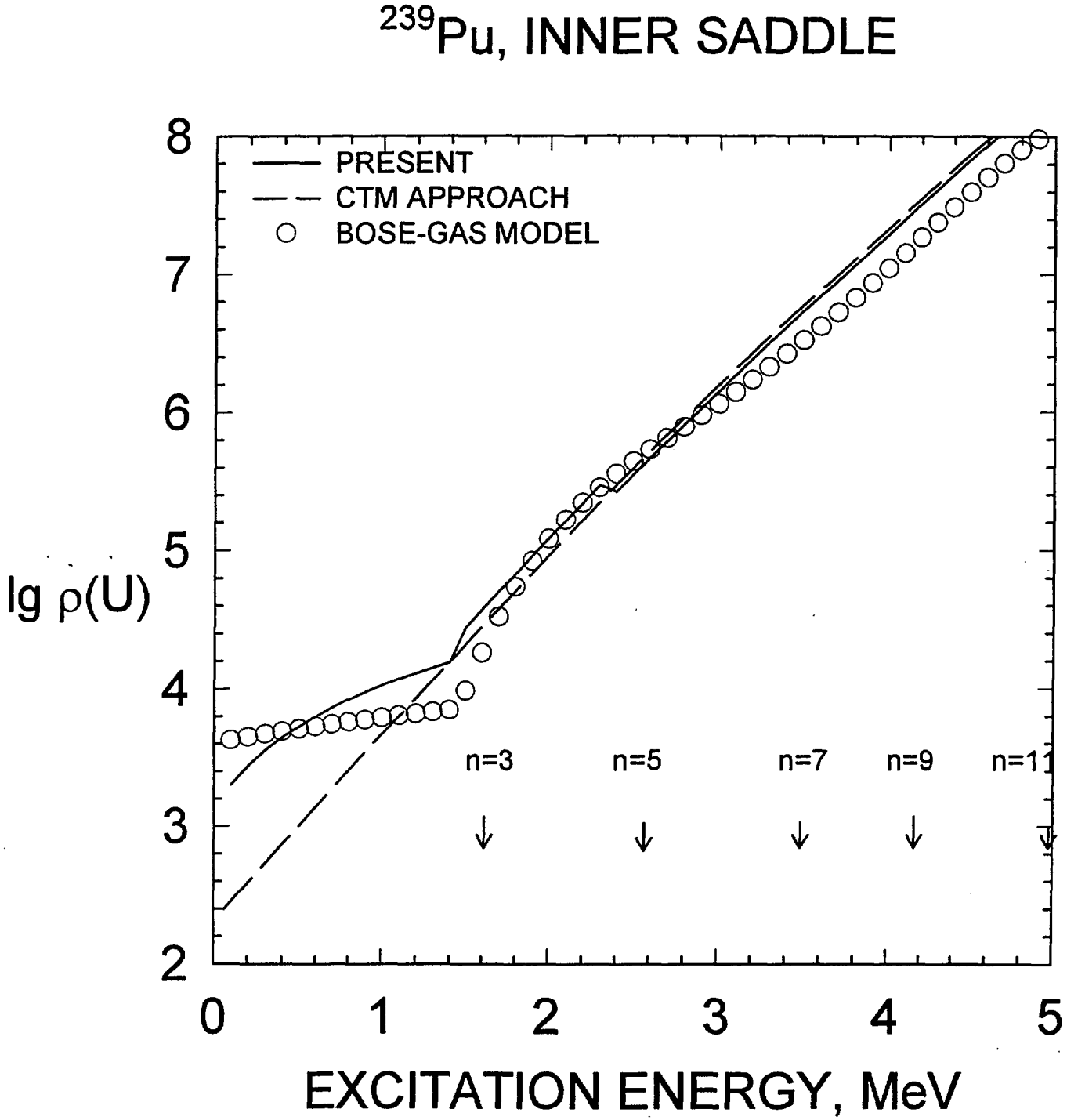
^{239}Pu, INNER SADDLE
PRESENT
CTM APPROACH
BOSE-GAS MODEL
lg ρ(U)
8
7
6
5
4
3
2
n=3
n=5
n=7
n=9
n=11
0
1
2
3
4
5
EXCITATION ENERGY, MeV

FIG. 13

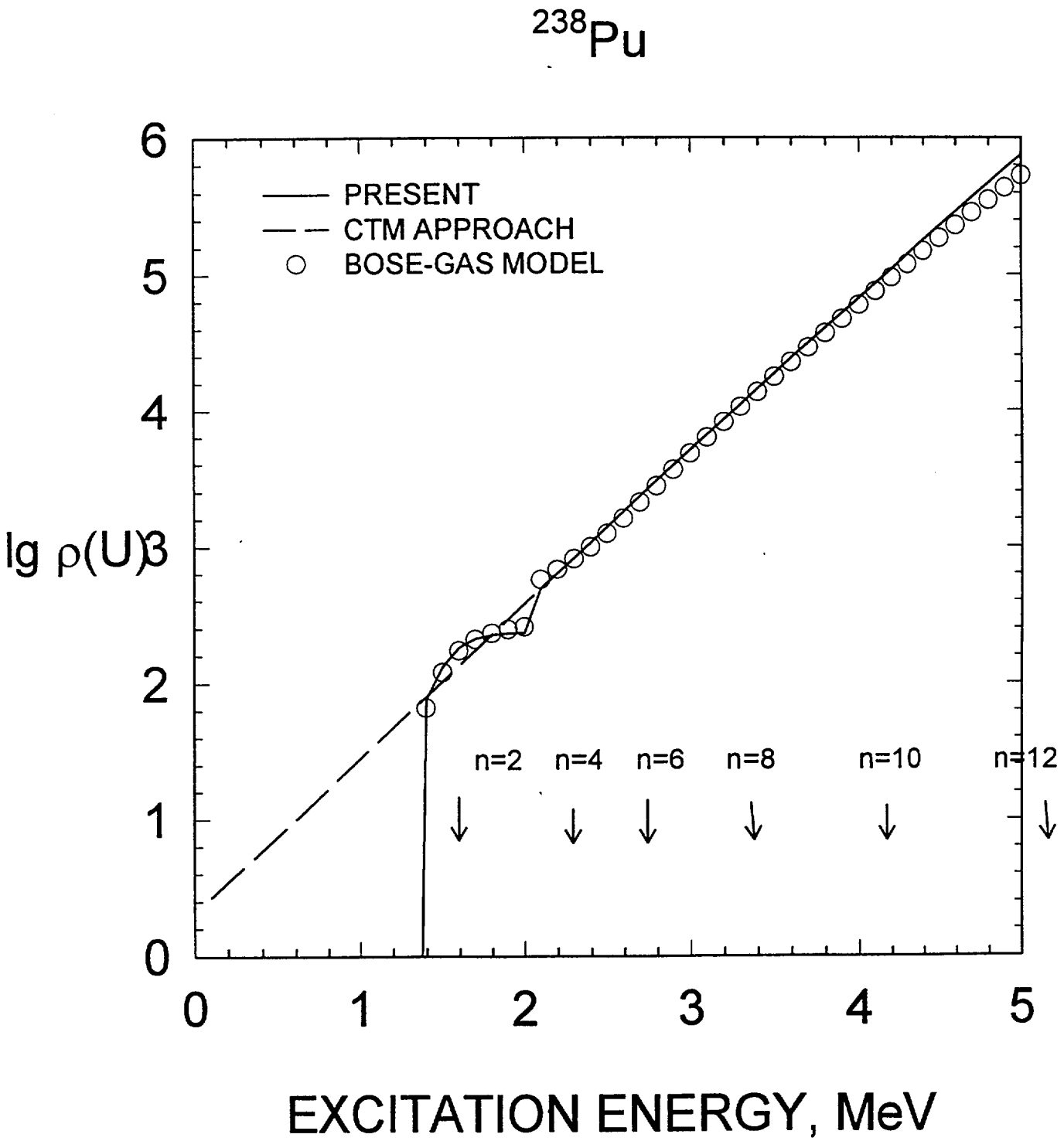
^{238}Pu
PRESENT
CTM APPROACH
BOSE-GAS MODEL
lg ρ(U)3
n=2
n=4
n=6
n=8
n=10
n=12
0
1
2
3
4
5
6
EXCITATION ENERGY, MeV

FIG. 14

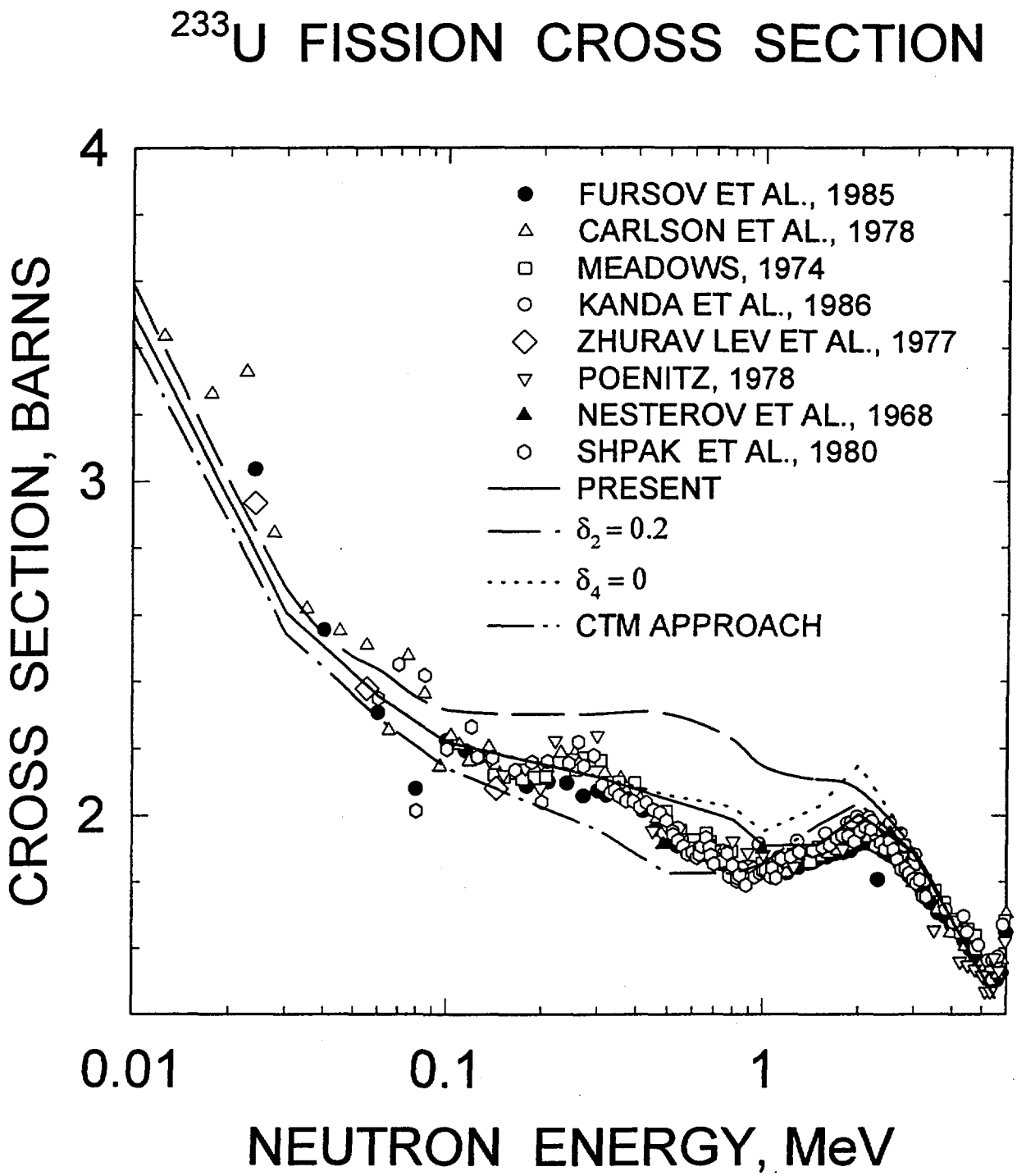
^{233}U FISSION CROSS SECTION
CROSS SECTION, BARNS
4
3
2
0.01
0.1
1
NEUTRON ENERGY, MeV
FURSOV ET AL., 1985
CARLSON ET AL., 1978
MEADOWS, 1974
KANDA ET AL., 1986
ZHURAV LEV ET AL., 1977
POENITZ, 1978
NESTEROV ET AL., 1968
SHPAK ET AL., 1980
PRESENT
$\delta_2 = 0.2$
$\delta_4 = 0$
CTM APPROACH

FIG. 15

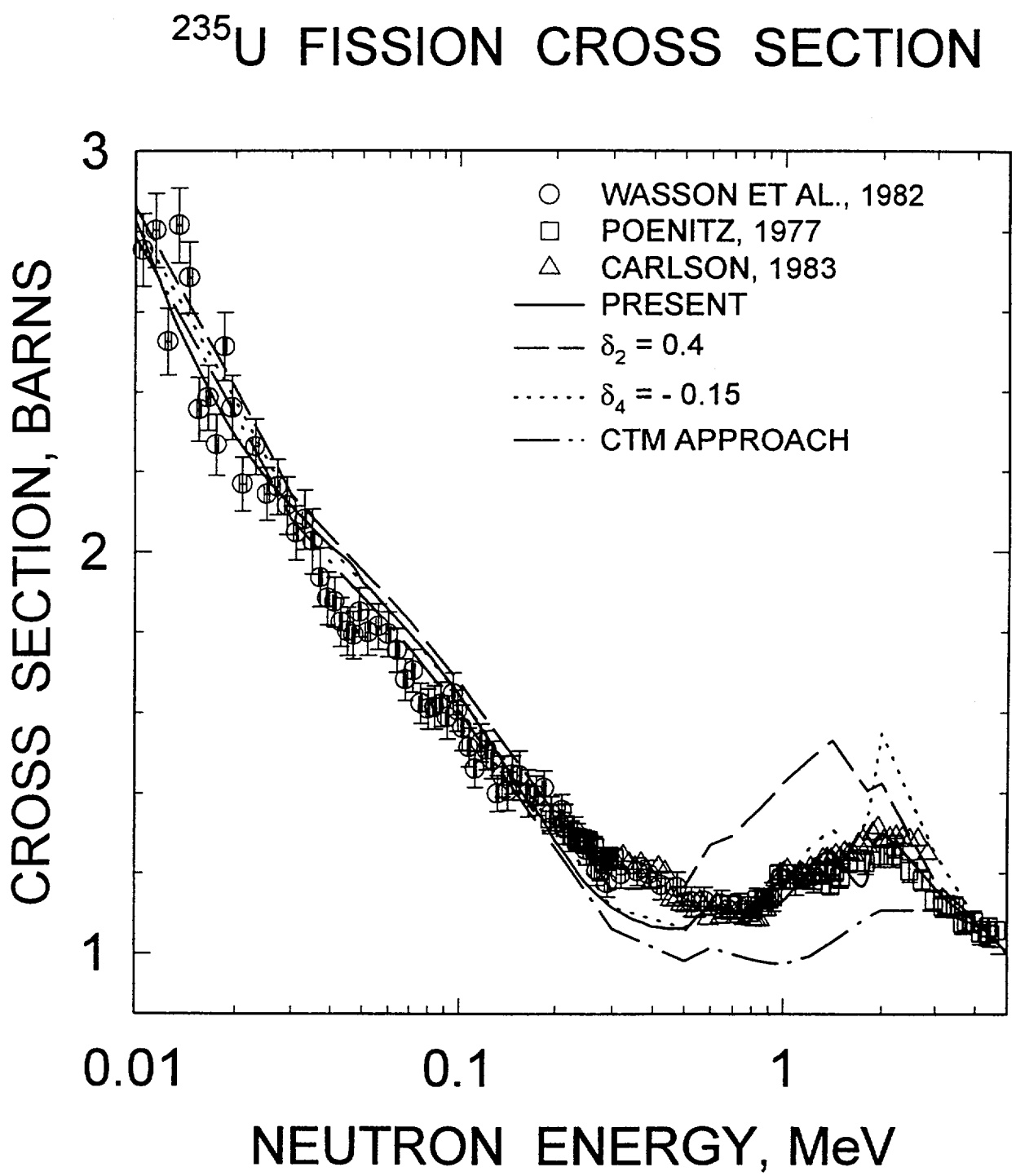
^{235}U FISSION CROSS SECTION
CROSS SECTION, BARNS
3
2
1
0.01
0.1
1
NEUTRON ENERGY, MeV
WASSON ET AL., 1982
POENITZ, 1977
CARLSON, 1983
PRESENT
δ_2 = 0.4
δ_4 = - 0.15
CTM APPROACH

FIG. 16

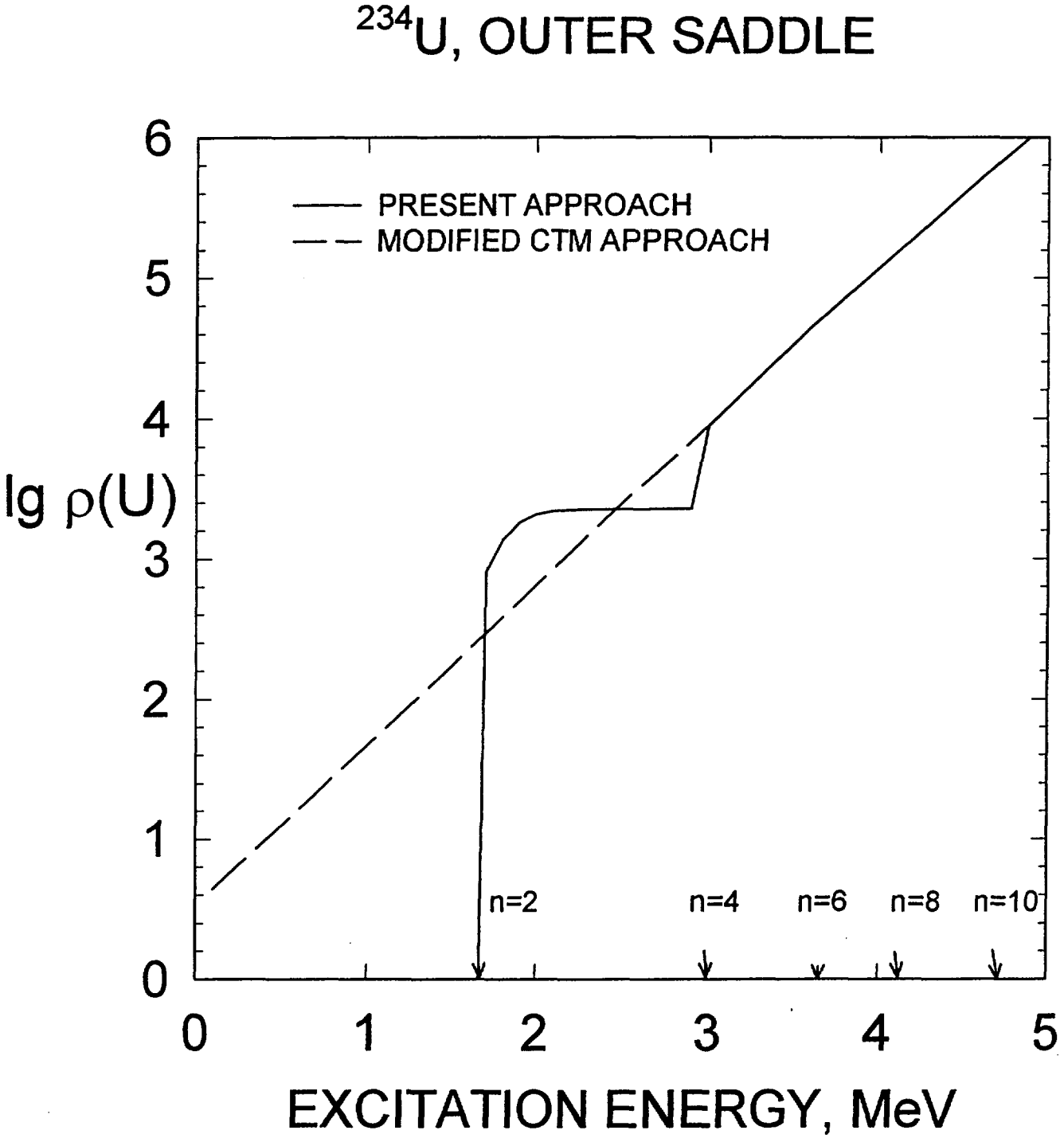
^{234}U, OUTER SADDLE
PRESENT APPROACH
MODIFIED CTM APPROACH
lg ρ(U)
n=2
n=4
n=6
n=8
n=10
0
1
2
3
4
5
6
EXCITATION ENERGY, MeV

FIG. 17

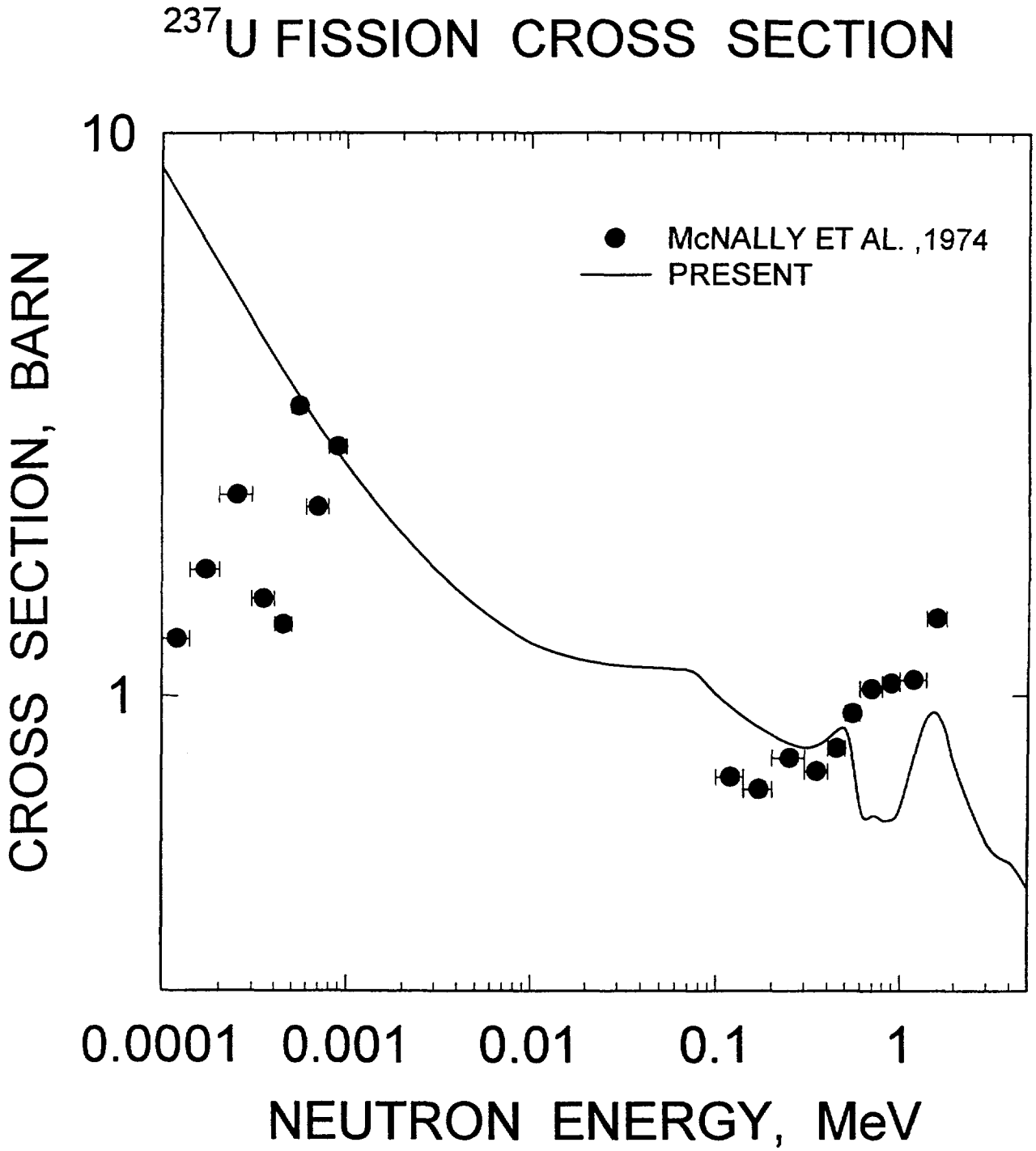
^{237}U FISSION CROSS SECTION
10
1
CROSS SECTION, BARN
McNALLY ET AL. ,1974
PRESENT
0.0001
0.001
0.01
0.1
1
NEUTRON ENERGY, MeV

FIG. 18

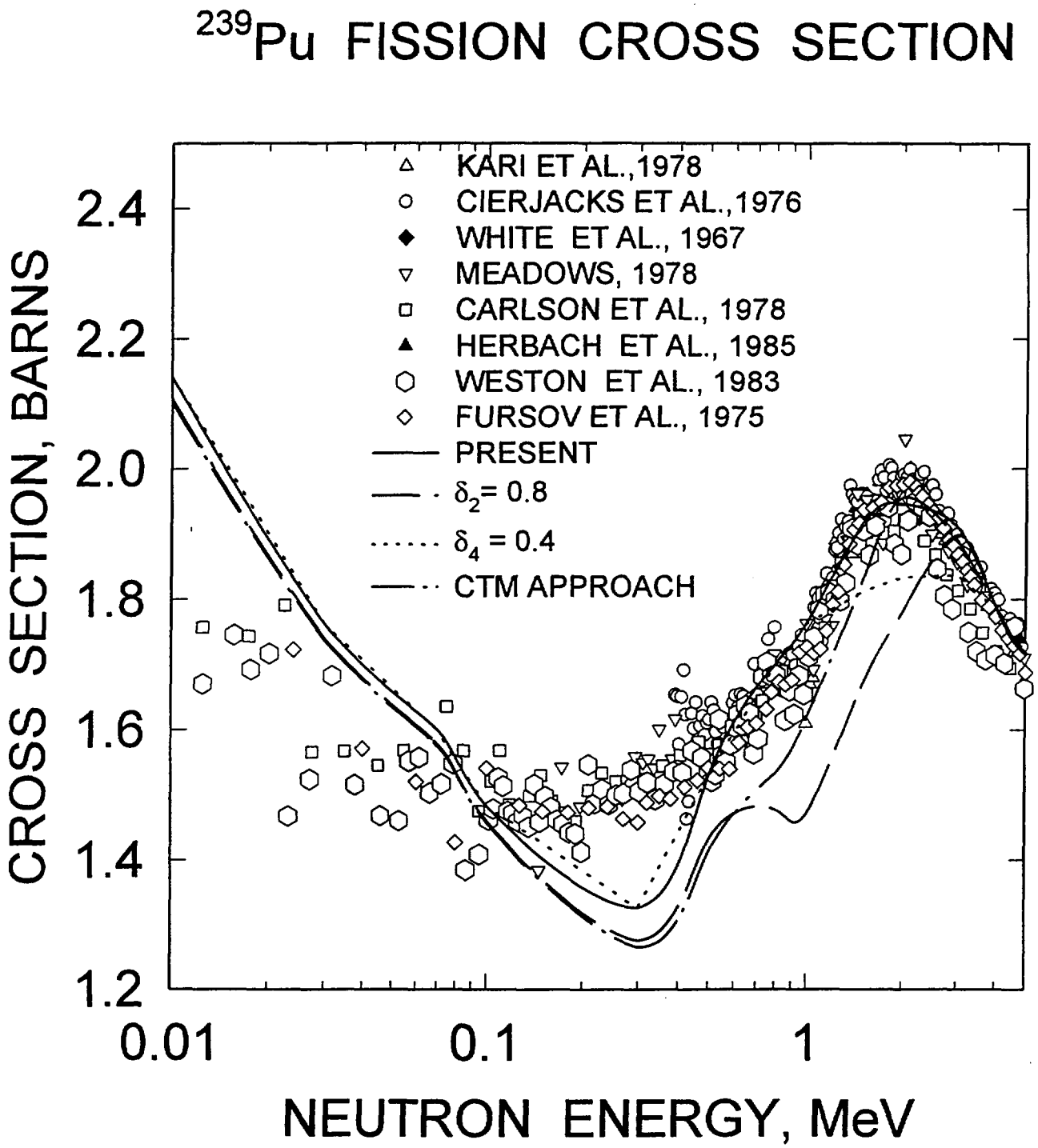
^{239}Pu FISSION CROSS SECTION
KARI ET AL.,1978
CIERJACKS ET AL.,1976
WHITE ET AL., 1967
MEADOWS, 1978
CARLSON ET AL., 1978
HERBACH ET AL., 1985
WESTON ET AL., 1983
FURSOV ET AL., 1975
PRESENT
δ_2= 0.8
δ_4 = 0.4
CTM APPROACH
CROSS SECTION, BARNS
2.4
2.2
2.0
1.8
1.6
1.4
1.2
0.01
0.1
1
NEUTRON ENERGY, MeV

FIG.19

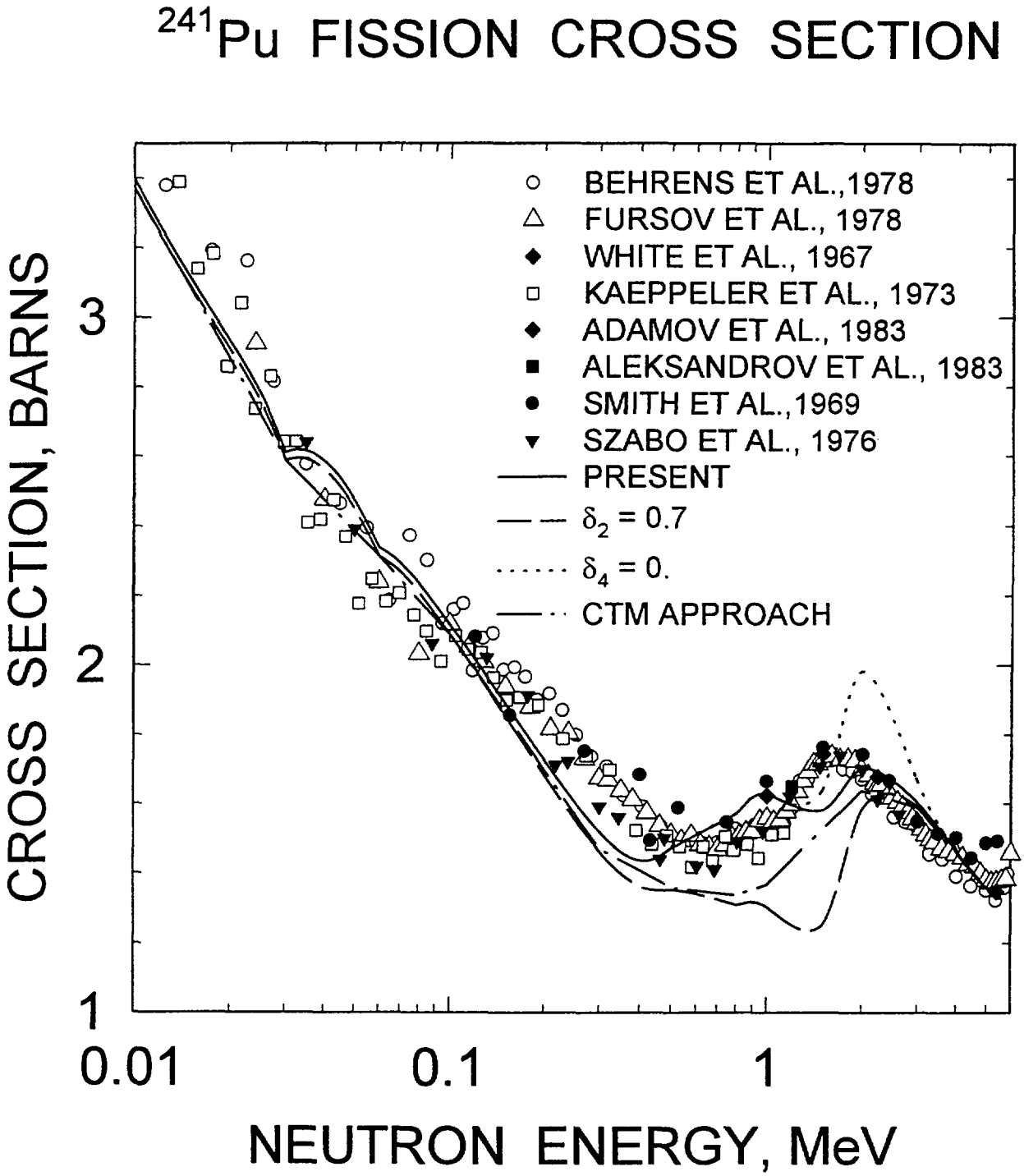
^{241}Pu FISSION CROSS SECTION
CROSS SECTION, BARNS
3
2
1
0.01
0.1
1
NEUTRON ENERGY, MeV
BEHRENS ET AL.,1978
FURSOV ET AL., 1978
WHITE ET AL., 1967
KAEPPELER ET AL., 1973
ADAMOV ET AL., 1983
ALEKSANDROV ET AL., 1983
SMITH ET AL.,1969
SZABO ET AL., 1976
PRESENT
δ_2 = 0.7
δ_4 = 0.
CTM APPROACH

FIG.20

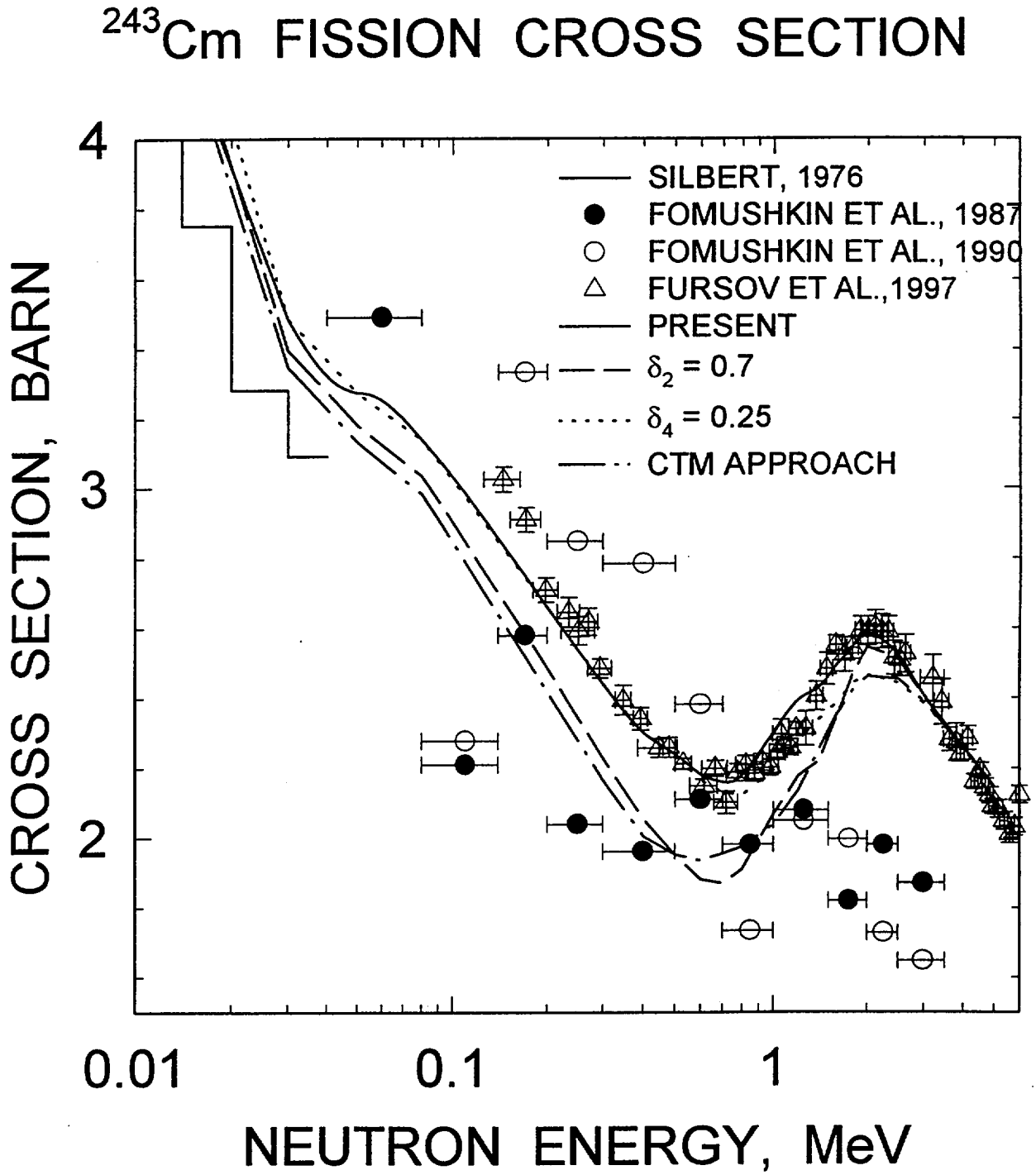
^{243}Cm FISSION CROSS SECTION
CROSS SECTION, BARN
4
3
2
0.01
0.1
1
NEUTRON ENERGY, MeV
SILBERT, 1976
FOMUSHKIN ET AL., 1987
FOMUSHKIN ET AL., 1990
FURSOV ET AL.,1997
PRESENT
δ_2 = 0.7
δ_4 = 0.25
CTM APPROACH

FIG. 21

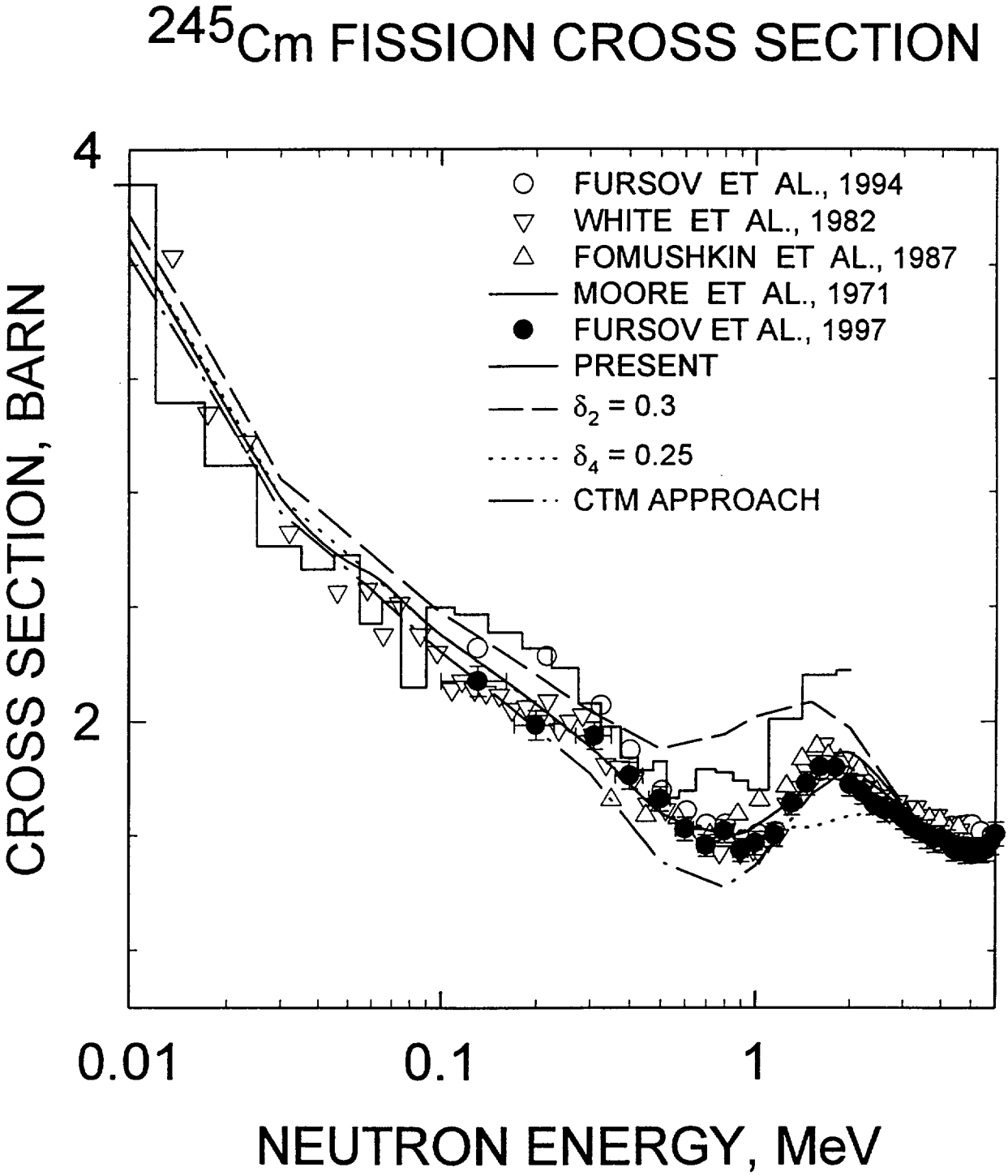
^{245}Cm FISSION CROSS SECTION
CROSS SECTION, BARN
4
2
0.01
0.1
1
NEUTRON ENERGY, MeV
FURSOV ET AL., 1994
WHITE ET AL., 1982
FOMUSHKIN ET AL., 1987
MOORE ET AL., 1971
FURSOV ET AL., 1997
PRESENT
δ_2 = 0.3
δ_4 = 0.25
CTM APPROACH

FIG. 22

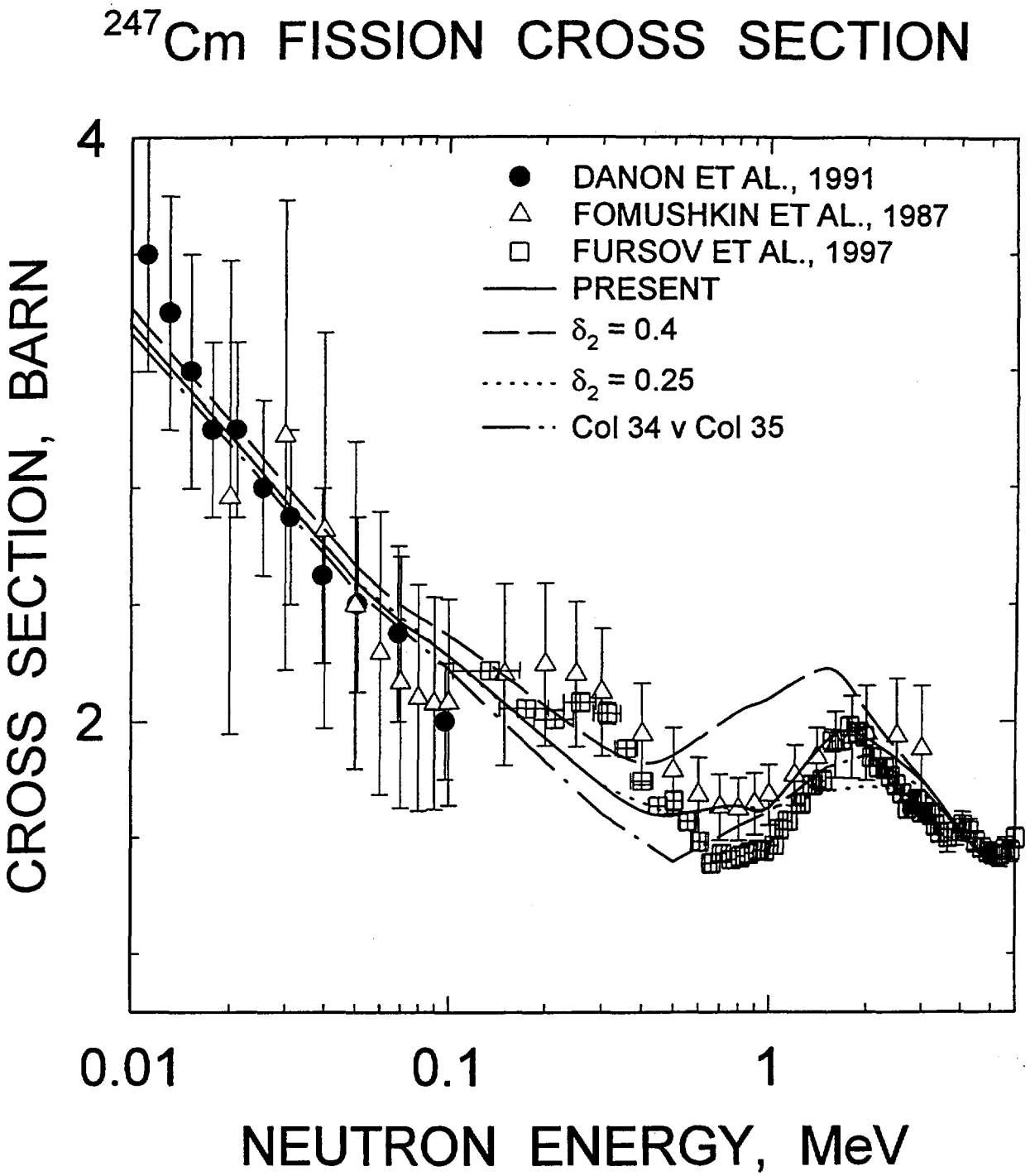
^{247}Cm FISSION CROSS SECTION
CROSS SECTION, BARN
4
2
0.01
0.1
1
NEUTRON ENERGY, MeV
DANON ET AL., 1991
FOMUSHKIN ET AL., 1987
FURSOV ET AL., 1997
PRESENT
δ_2 = 0.4
δ_2 = 0.25
Col 34 v Col 35

FIG. 23

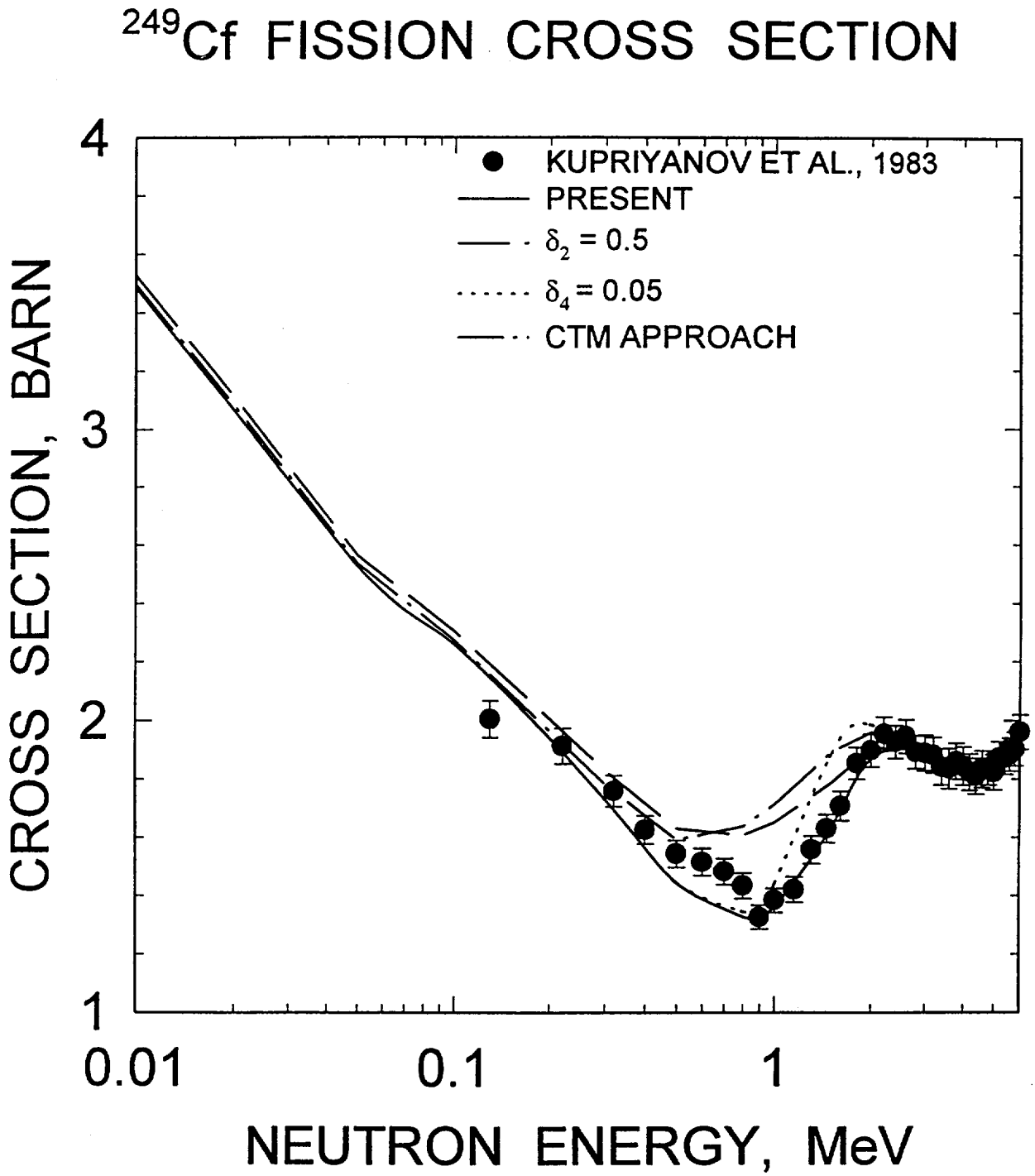
^{249}Cf FISSION CROSS SECTION
KUPRIYANOV ET AL., 1983
PRESENT
δ_2 = 0.5
δ_4 = 0.05
CTM APPROACH
CROSS SECTION, BARN
4
3
2
1
0.01
0.1
1
NEUTRON ENERGY, MeV

FIG. 24

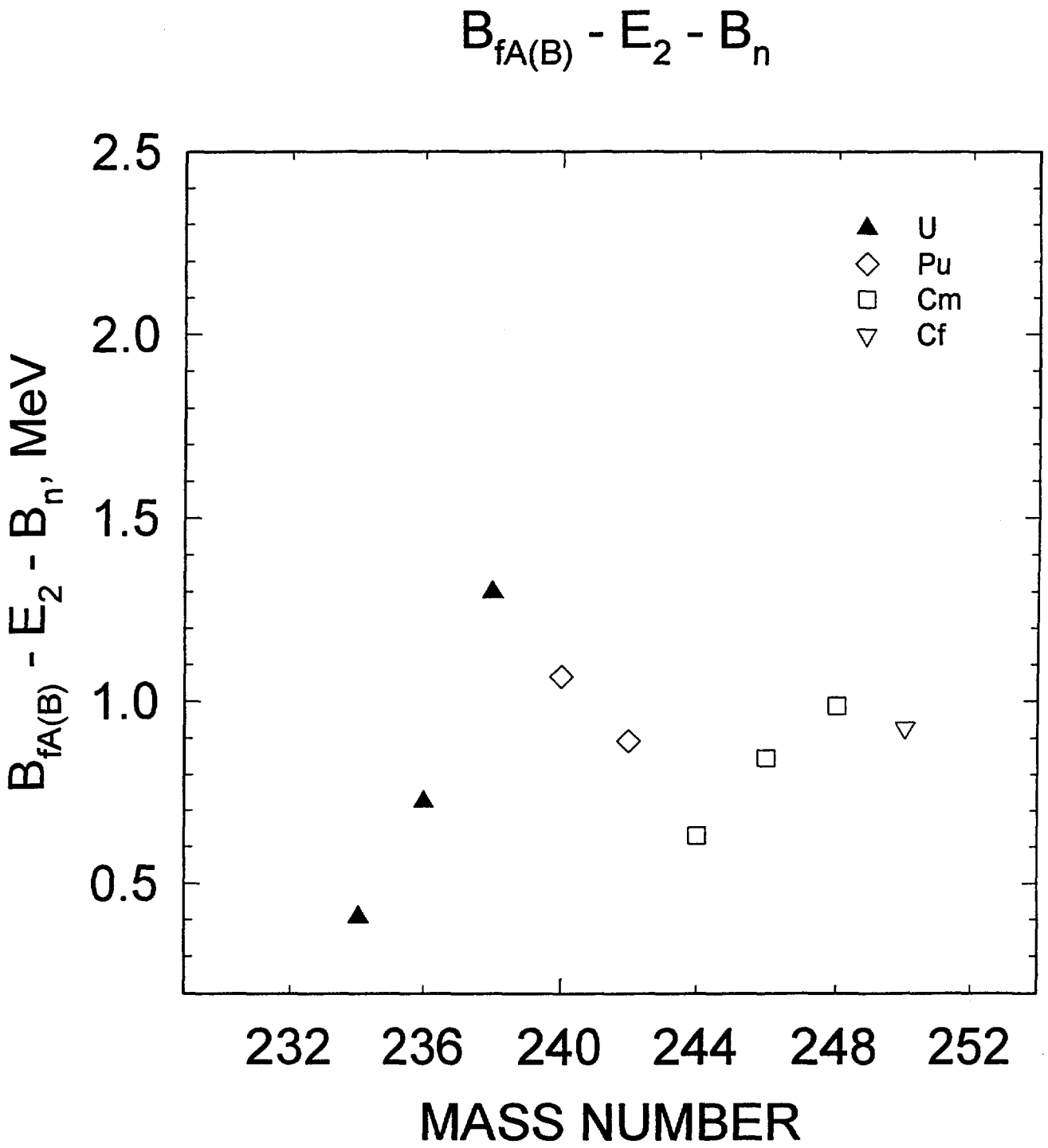
$B_{fA(B)} - E_2 - B_n$
2.5
2.0
1.5
1.0
0.5
$B_{fA(B)} - E_2 - B_n$, MeV
U
Pu
Cm
Cf
232
236
240
244
248
252
MASS NUMBER

FIG. 25

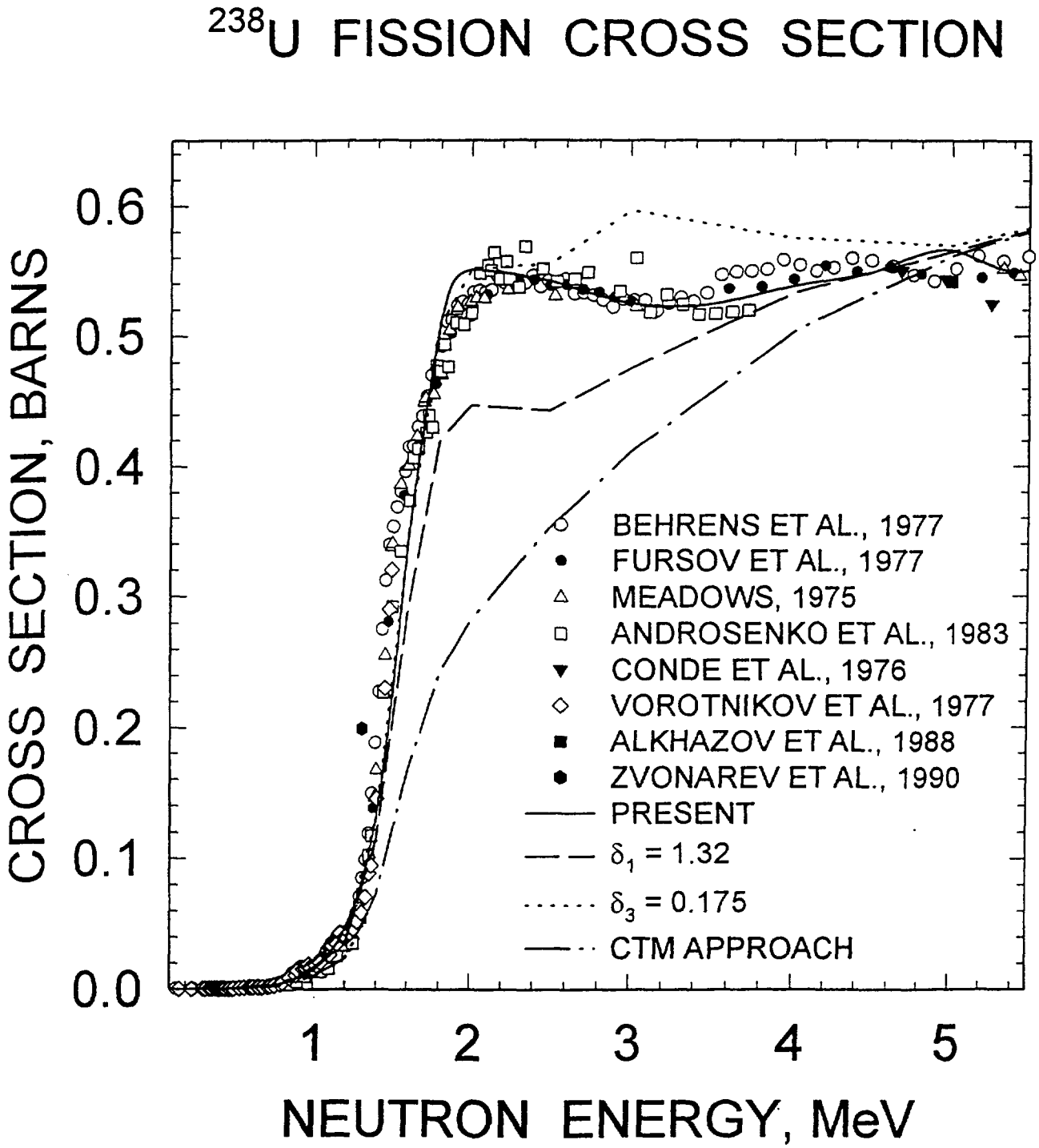
^{238}U FISSION CROSS SECTION
CROSS SECTION, BARNS
0.0
0.1
0.2
0.3
0.4
0.5
0.6
1
2
3
4
5
NEUTRON ENERGY, MeV
BEHRENS ET AL., 1977
FURSOV ET AL., 1977
MEADOWS, 1975
ANDROSENKO ET AL., 1983
CONDE ET AL., 1976
VOROTNIKOV ET AL., 1977
ALKHAZOV ET AL., 1988
ZVONAREV ET AL., 1990
PRESENT
δ_1 = 1.32
δ_3 = 0.175
CTM APPROACH

FIG. 26

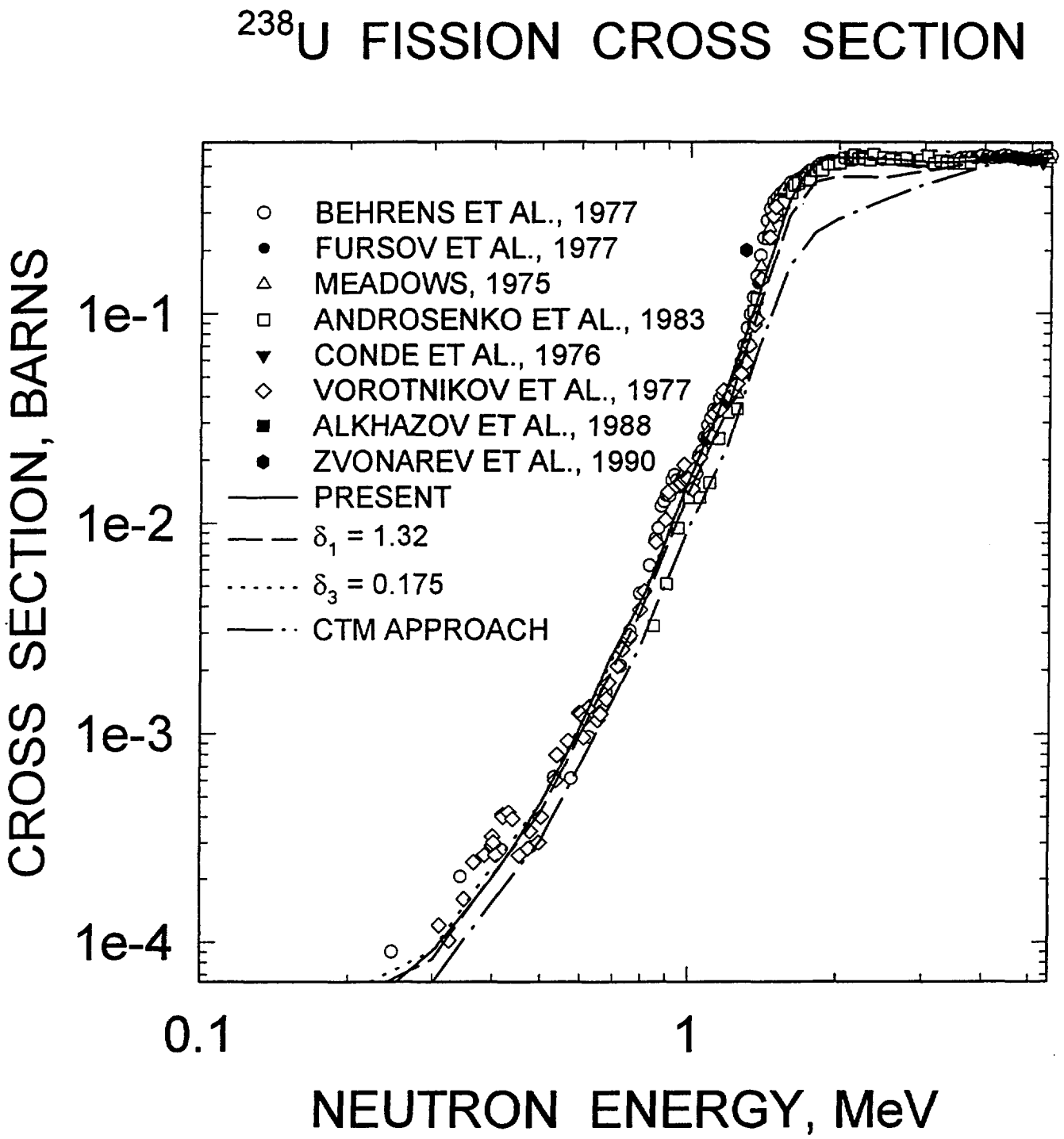
^{238}U FISSION CROSS SECTION
BEHRENS ET AL., 1977
FURSOV ET AL., 1977
MEADOWS, 1975
ANDROSENKO ET AL., 1983
CONDE ET AL., 1976
VOROTNIKOV ET AL., 1977
ALKHAZOV ET AL., 1988
ZVONAREV ET AL., 1990
PRESENT
δ_1 = 1.32
δ_3 = 0.175
CTM APPROACH
CROSS SECTION, BARNS
1e-1
1e-2
1e-3
1e-4
0.1
1
NEUTRON ENERGY, MeV

FIG. 26a

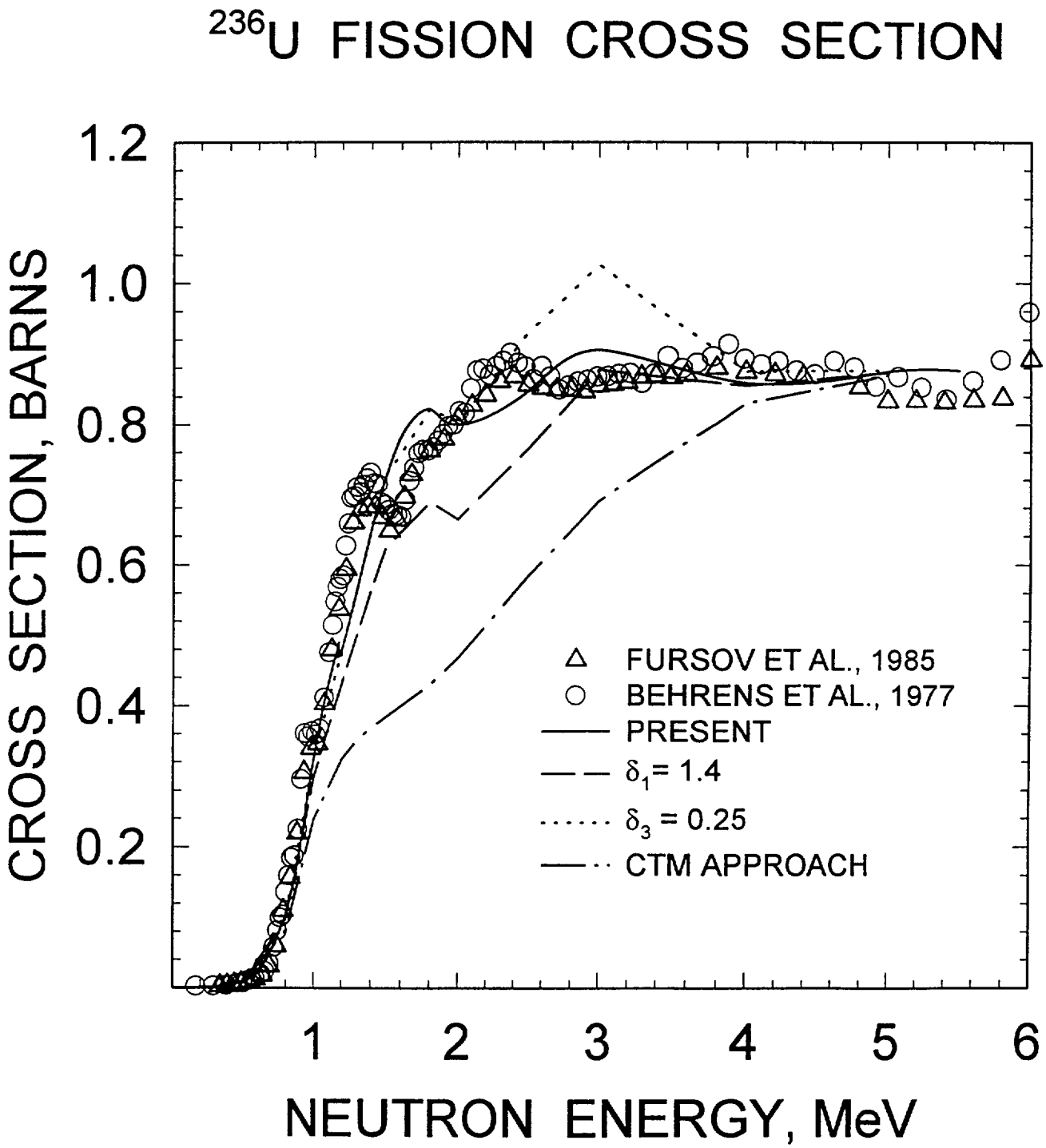
^{236}U FISSION CROSS SECTION
CROSS SECTION, BARNS
1.2
1.0
0.8
0.6
0.4
0.2
1
2
3
4
5
6
NEUTRON ENERGY, MeV
FURSOV ET AL., 1985
BEHRENS ET AL., 1977
PRESENT
δ_1= 1.4
δ_3 = 0.25
CTM APPROACH

FIG. 27

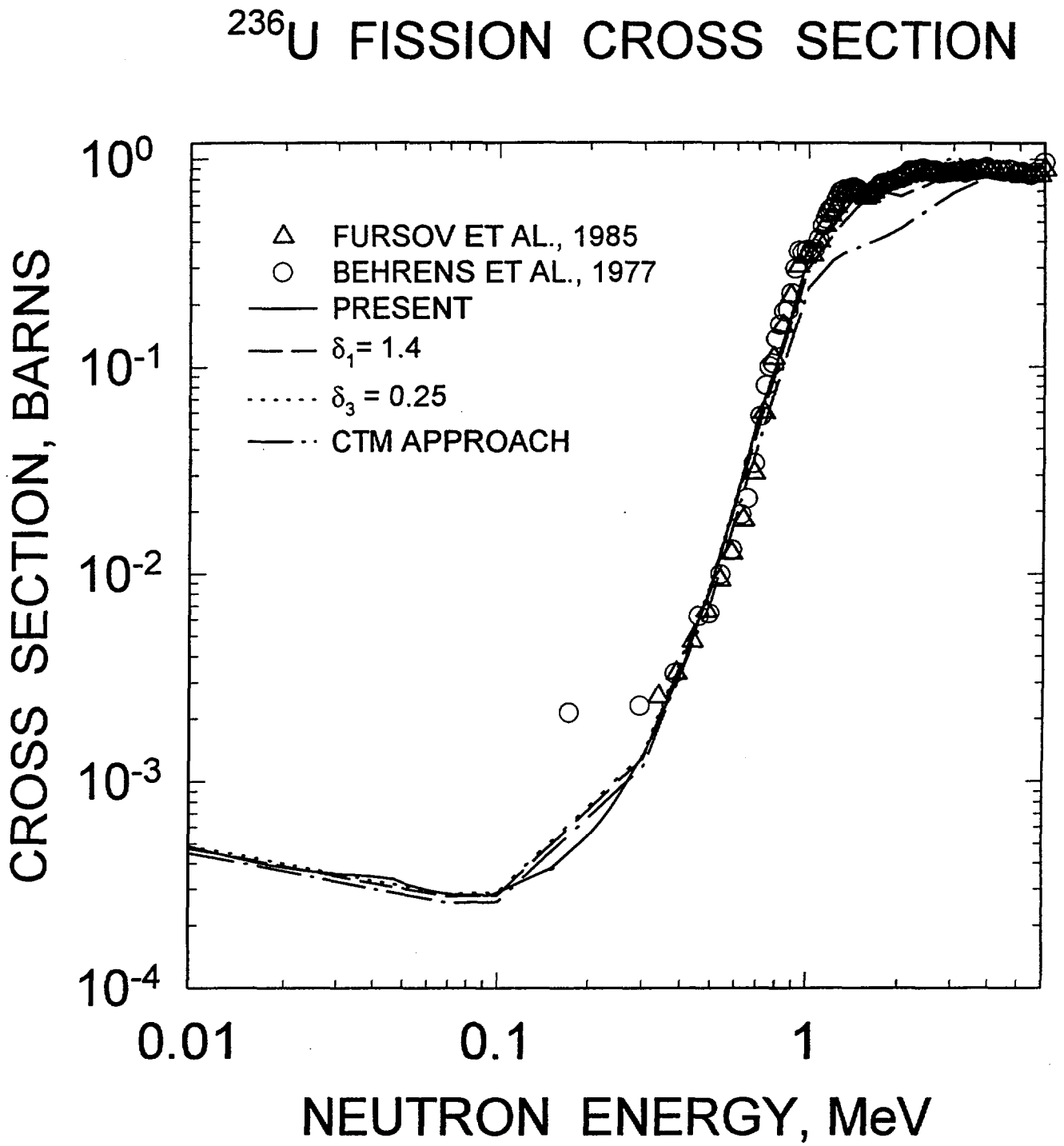
^{236}U FISSION CROSS SECTION
CROSS SECTION, BARNS
10^{0}
10^{-1}
10^{-2}
10^{-3}
10^{-4}
0.01
0.1
1
NEUTRON ENERGY, MeV
FURSOV ET AL., 1985
BEHRENS ET AL., 1977
PRESENT
δ_1= 1.4
δ_3 = 0.25
CTM APPROACH

FIG. 27a

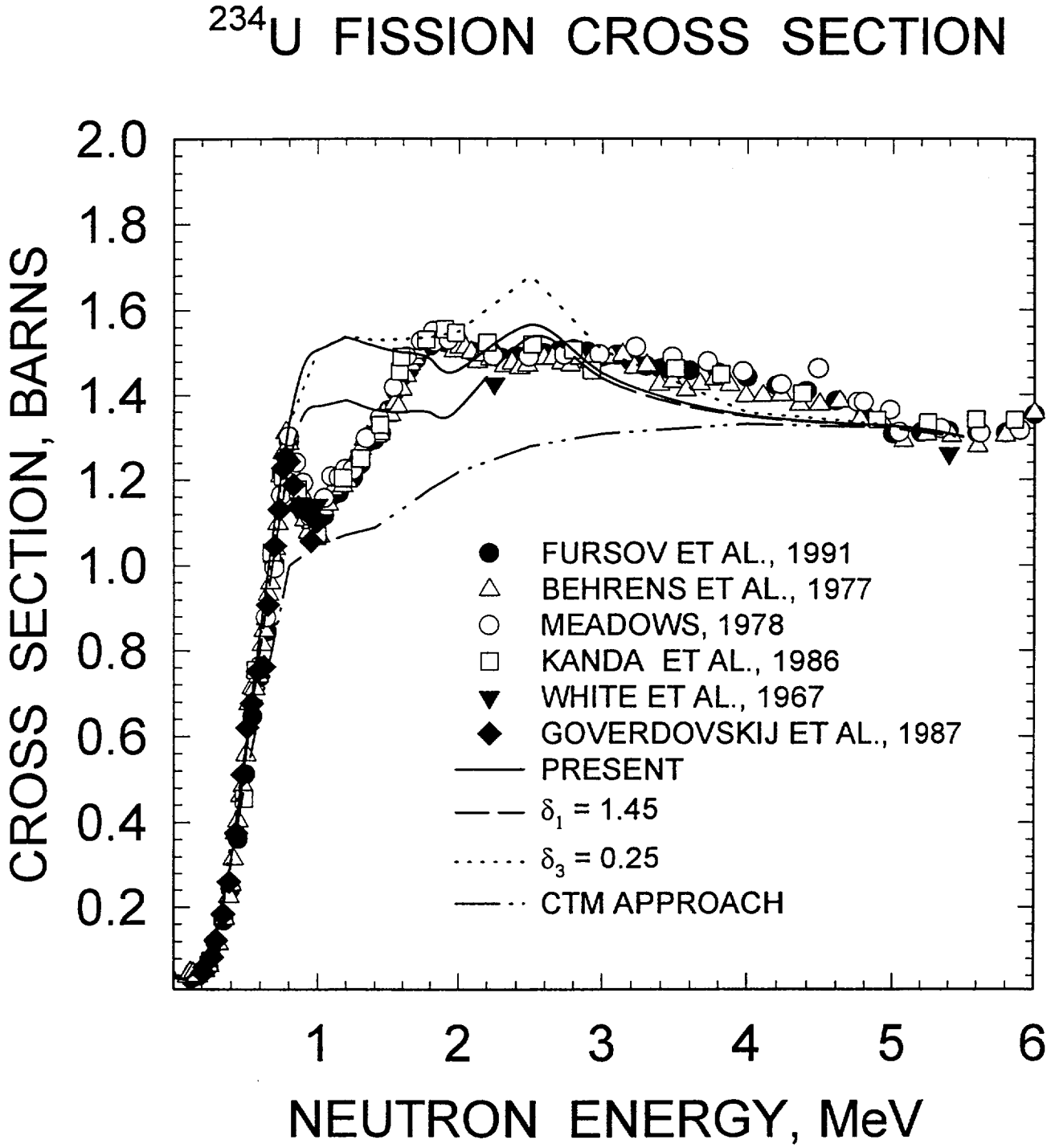
^{234}U FISSION CROSS SECTION
CROSS SECTION, BARNS
2.0
1.8
1.6
1.4
1.2
1.0
0.8
0.6
0.4
0.2
1
2
3
4
5
6
NEUTRON ENERGY, MeV
FURSOV ET AL., 1991
BEHRENS ET AL., 1977
MEADOWS, 1978
KANDA ET AL., 1986
WHITE ET AL., 1967
GOVERDOVSKIJ ET AL., 1987
PRESENT
δ_1 = 1.45
δ_3 = 0.25
CTM APPROACH

FIG.28

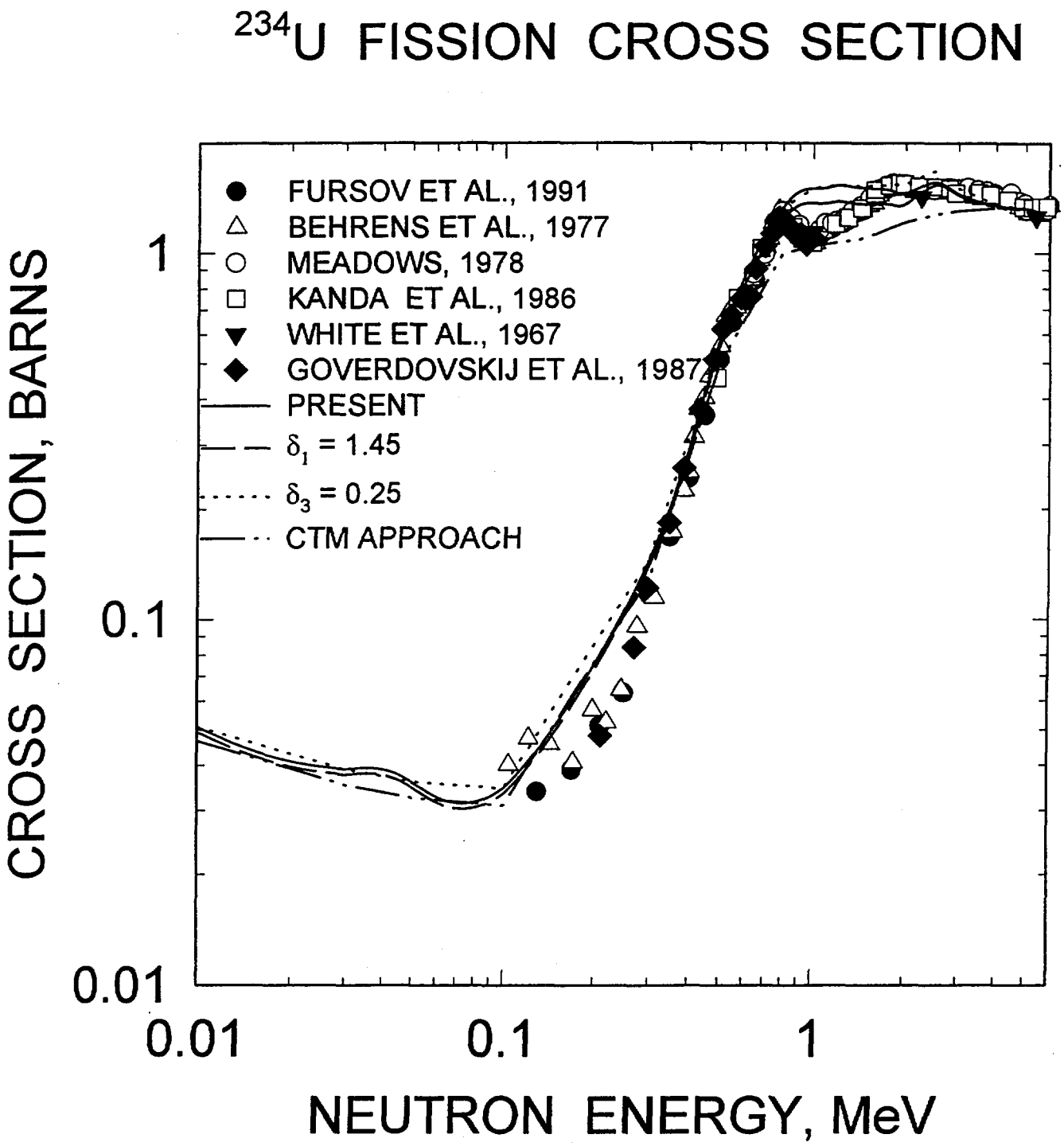
^{234}U FISSION CROSS SECTION
FURSOV ET AL., 1991
BEHRENS ET AL., 1977
MEADOWS, 1978
KANDA ET AL., 1986
WHITE ET AL., 1967
GOVERDOVSKIJ ET AL., 1987
PRESENT
δ_1 = 1.45
δ_3 = 0.25
CTM APPROACH
CROSS SECTION, BARNS
1
0.1
0.01
0.01
0.1
1
NEUTRON ENERGY, MeV

FIG.28a

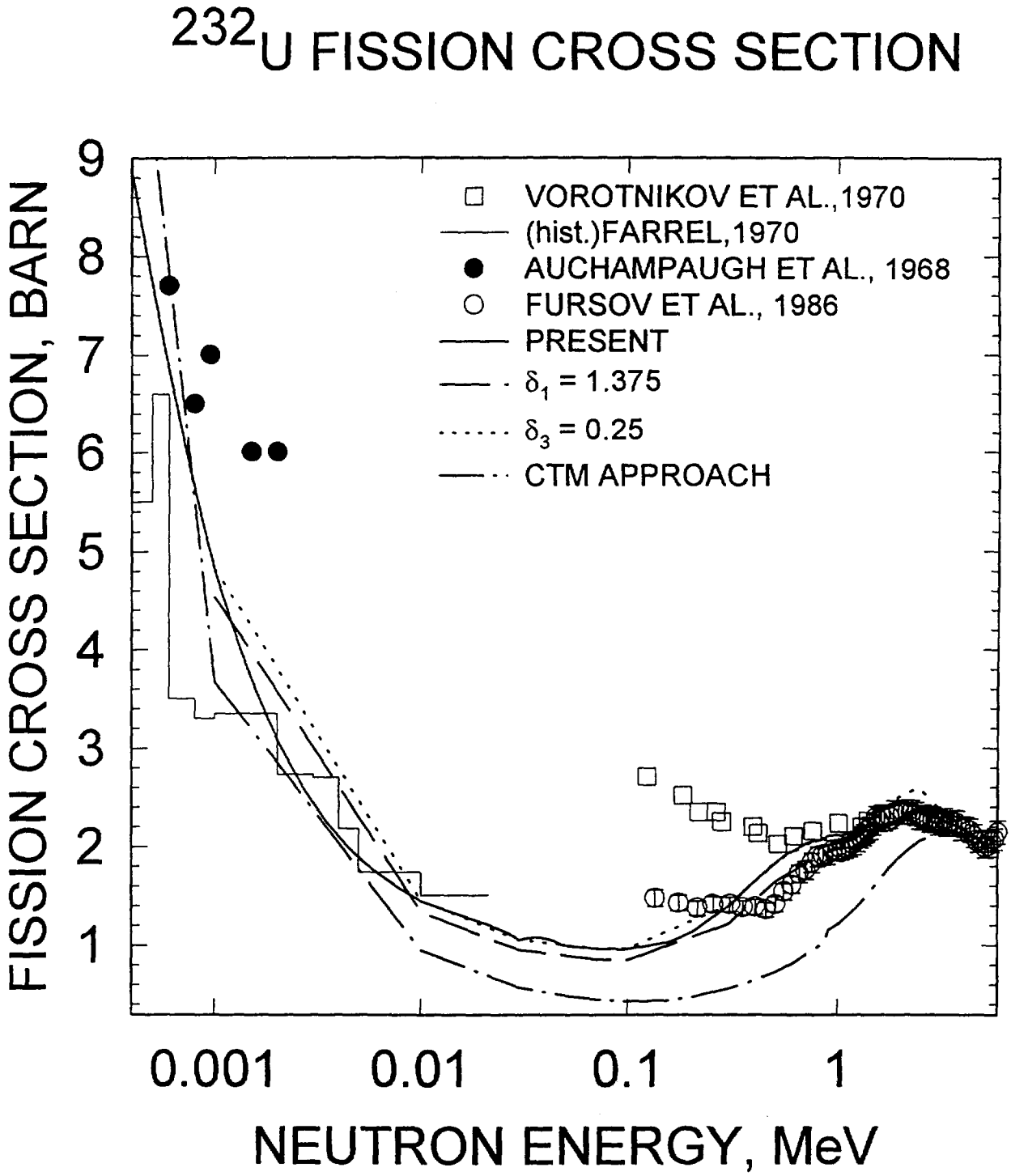
^{232}U FISSION CROSS SECTION
FISSION CROSS SECTION, BARN
9
8
7
6
5
4
3
2
1
VOROTNIKOV ET AL.,1970
(hist.)FARREL,1970
AUCHAMPAUGH ET AL., 1968
FURSOV ET AL., 1986
PRESENT
δ_1 = 1.375
δ_3 = 0.25
CTM APPROACH
0.001
0.01
0.1
1
NEUTRON ENERGY, MeV

FIG. 29

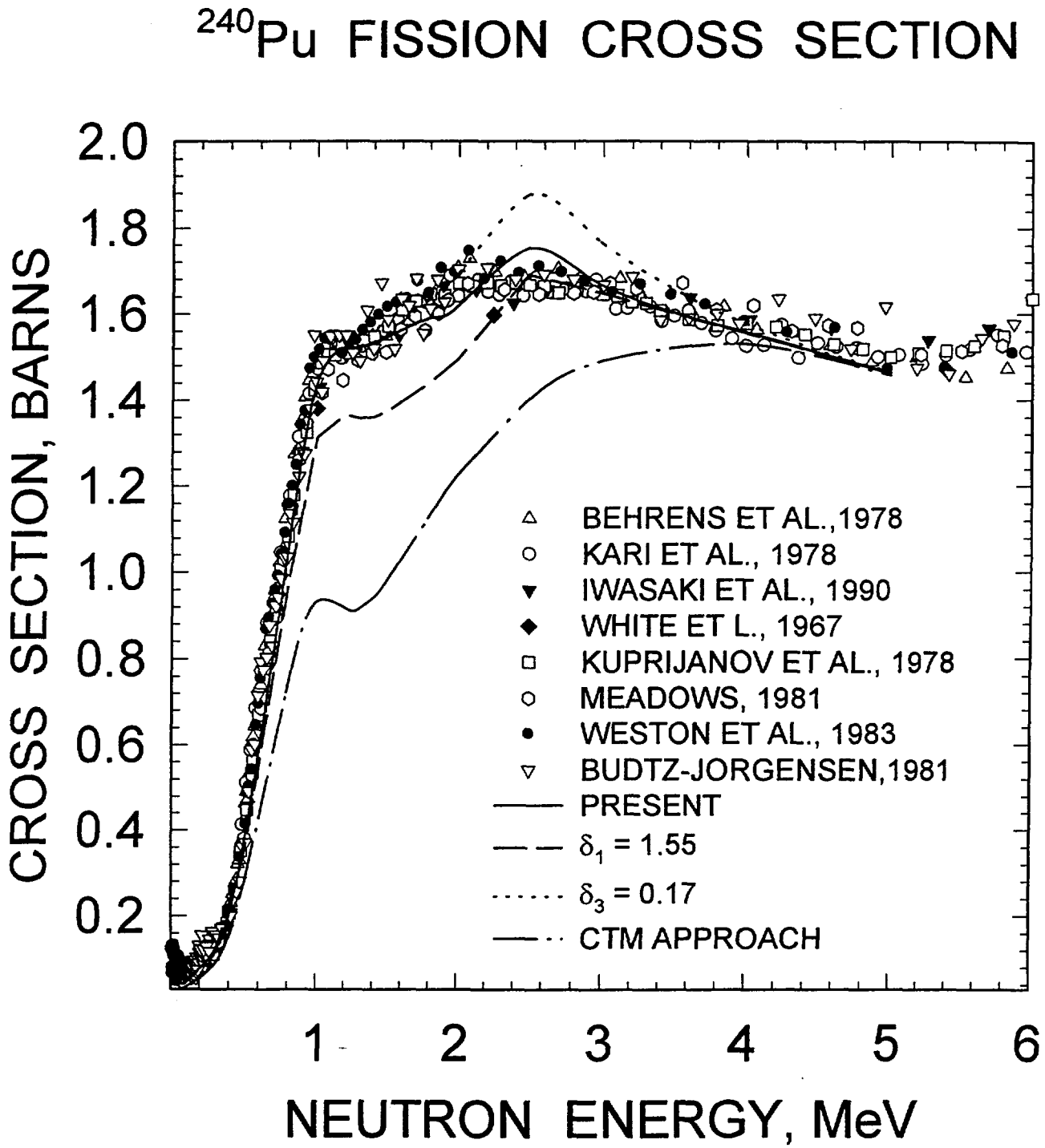
^{240}Pu FISSION CROSS SECTION
CROSS SECTION, BARNS
2.0
1.8
1.6
1.4
1.2
1.0
0.8
0.6
0.4
0.2
1
2
3
4
5
6
NEUTRON ENERGY, MeV
BEHRENS ET AL.,1978
KARI ET AL., 1978
IWASAKI ET AL., 1990
WHITE ET L., 1967
KUPRIJANOV ET AL., 1978
MEADOWS, 1981
WESTON ET AL., 1983
BUDTZ-JORGENSEN,1981
PRESENT
δ_1 = 1.55
δ_3 = 0.17
CTM APPROACH

FIG. 30

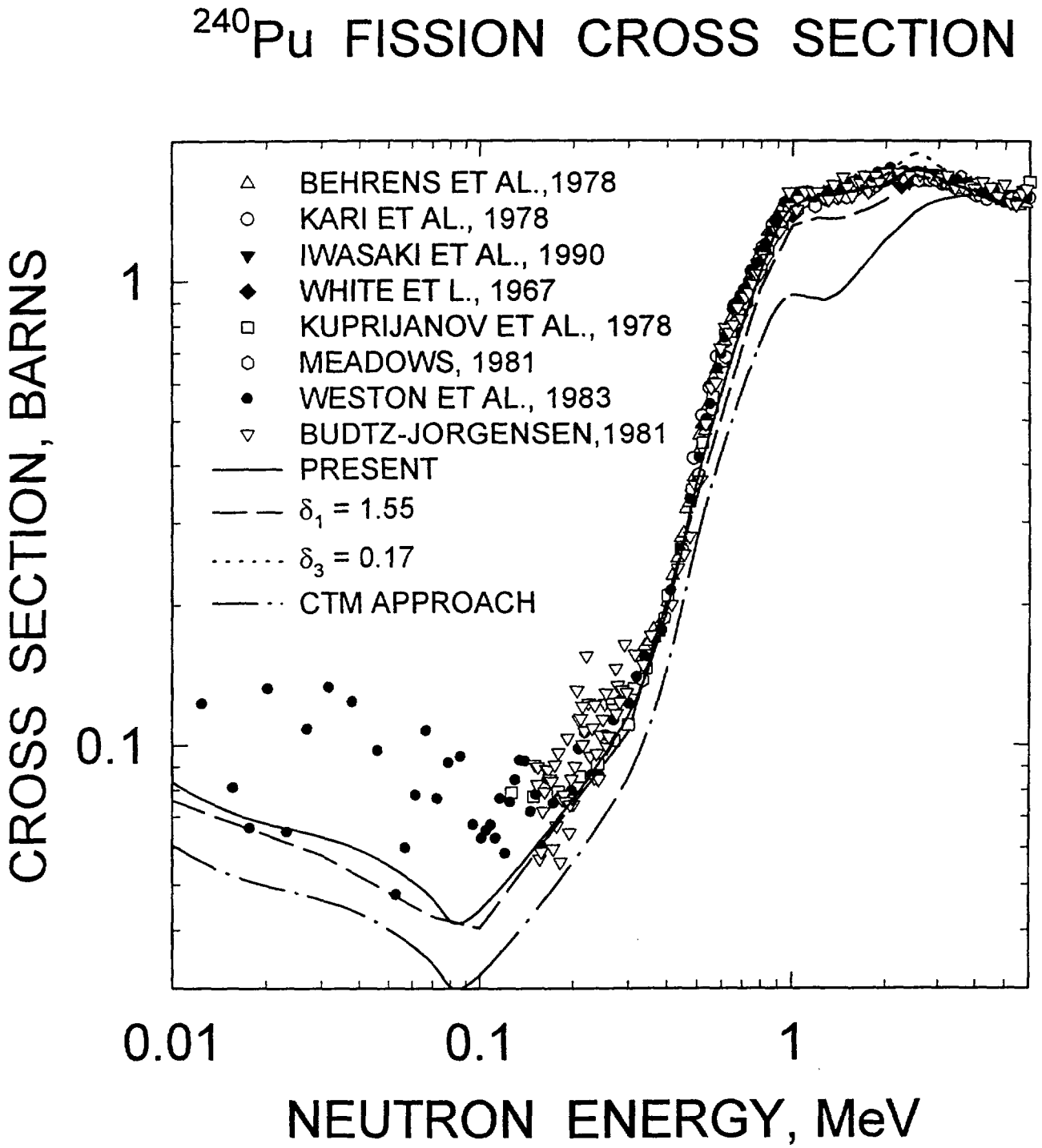
^{240}Pu FISSION CROSS SECTION
BEHRENS ET AL.,1978
KARI ET AL., 1978
IWASAKI ET AL., 1990
WHITE ET L., 1967
KUPRIJANOV ET AL., 1978
MEADOWS, 1981
WESTON ET AL., 1983
BUDTZ-JORGENSEN,1981
PRESENT
δ_1 = 1.55
δ_3 = 0.17
CTM APPROACH
CROSS SECTION, BARNS
1
0.1
0.01
0.1
1
NEUTRON ENERGY, MeV

FIG. 30a

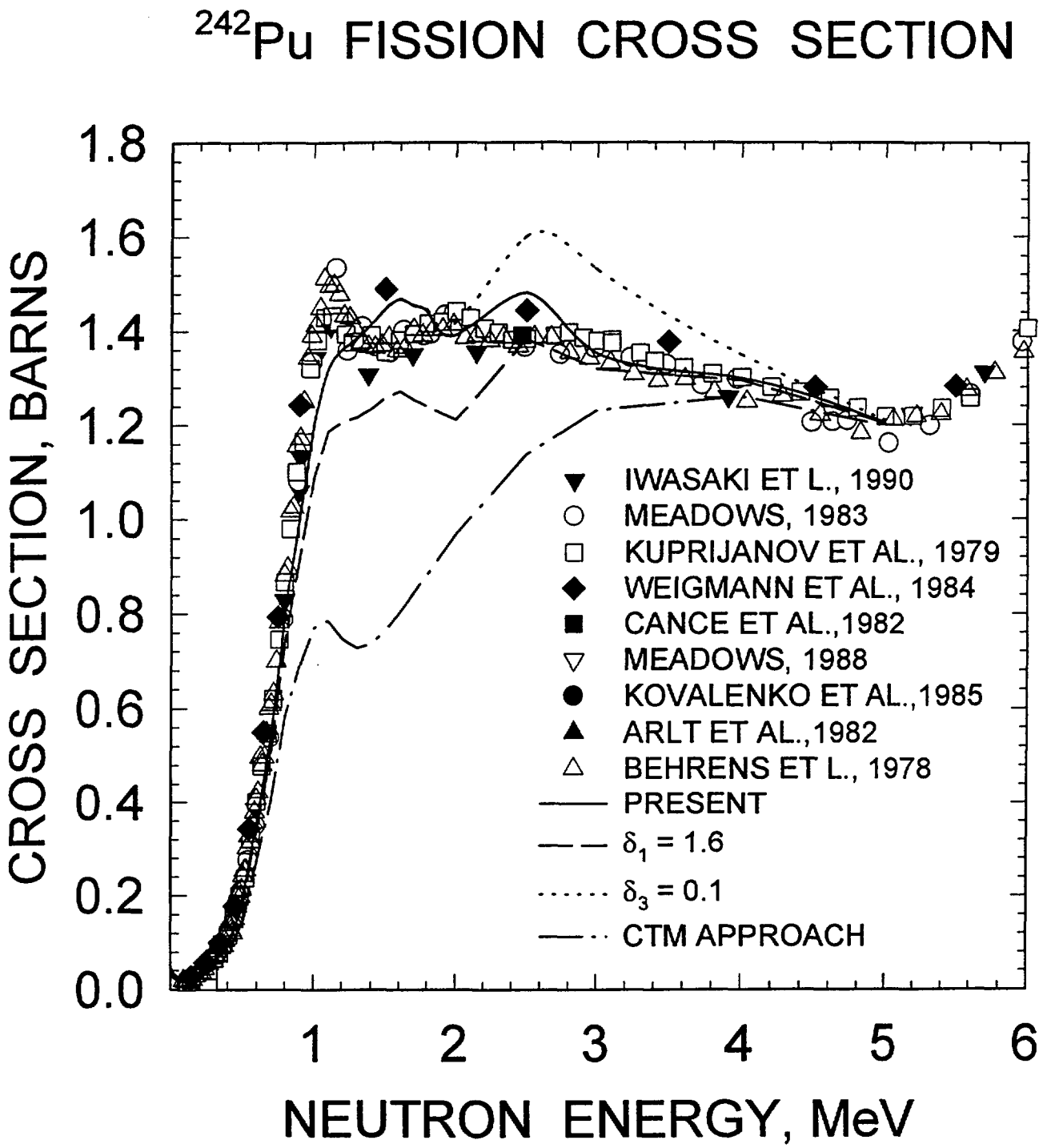
^{242}Pu FISSION CROSS SECTION
CROSS SECTION, BARNS
NEUTRON ENERGY, MeV
0.0
0.2
0.4
0.6
0.8
1.0
1.2
1.4
1.6
1.8
1
2
3
4
5
6
IWASAKI ET L., 1990
MEADOWS, 1983
KUPRIJANOV ET AL., 1979
WEIGMANN ET AL., 1984
CANCE ET AL.,1982
MEADOWS, 1988
KOVALENKO ET AL.,1985
ARLT ET AL.,1982
BEHRENS ET L., 1978
PRESENT
δ_1 = 1.6
δ_3 = 0.1
CTM APPROACH

FIG. 31

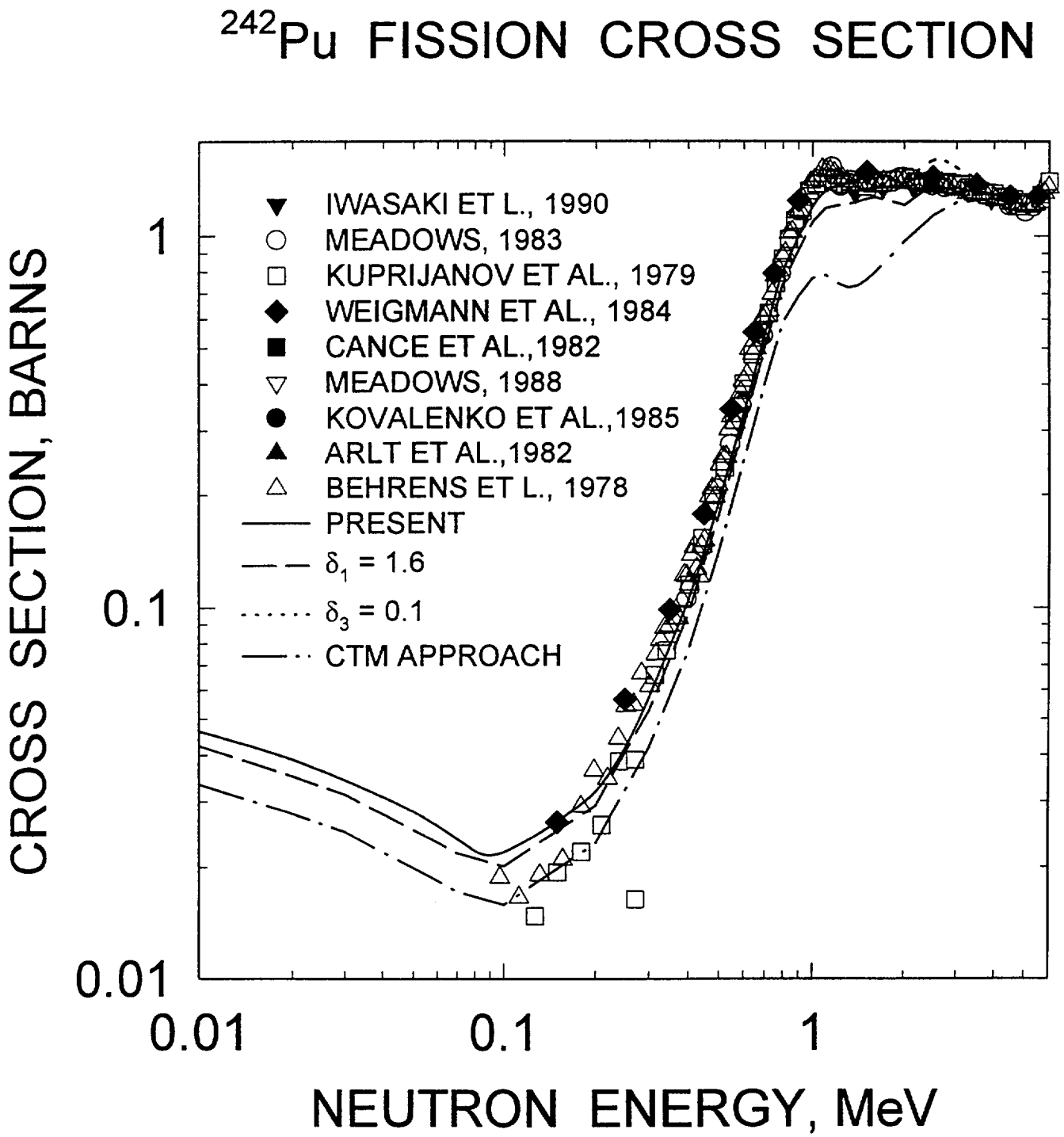
^{242}Pu FISSION CROSS SECTION
IWASAKI ET L., 1990
MEADOWS, 1983
KUPRIJANOV ET AL., 1979
WEIGMANN ET AL., 1984
CANCE ET AL.,1982
MEADOWS, 1988
KOVALENKO ET AL.,1985
ARLT ET AL.,1982
BEHRENS ET L., 1978
PRESENT
δ_1 = 1.6
δ_3 = 0.1
CTM APPROACH
CROSS SECTION, BARNS
1
0.1
0.01
0.01
0.1
1
NEUTRON ENERGY, MeV

FIG. 31a

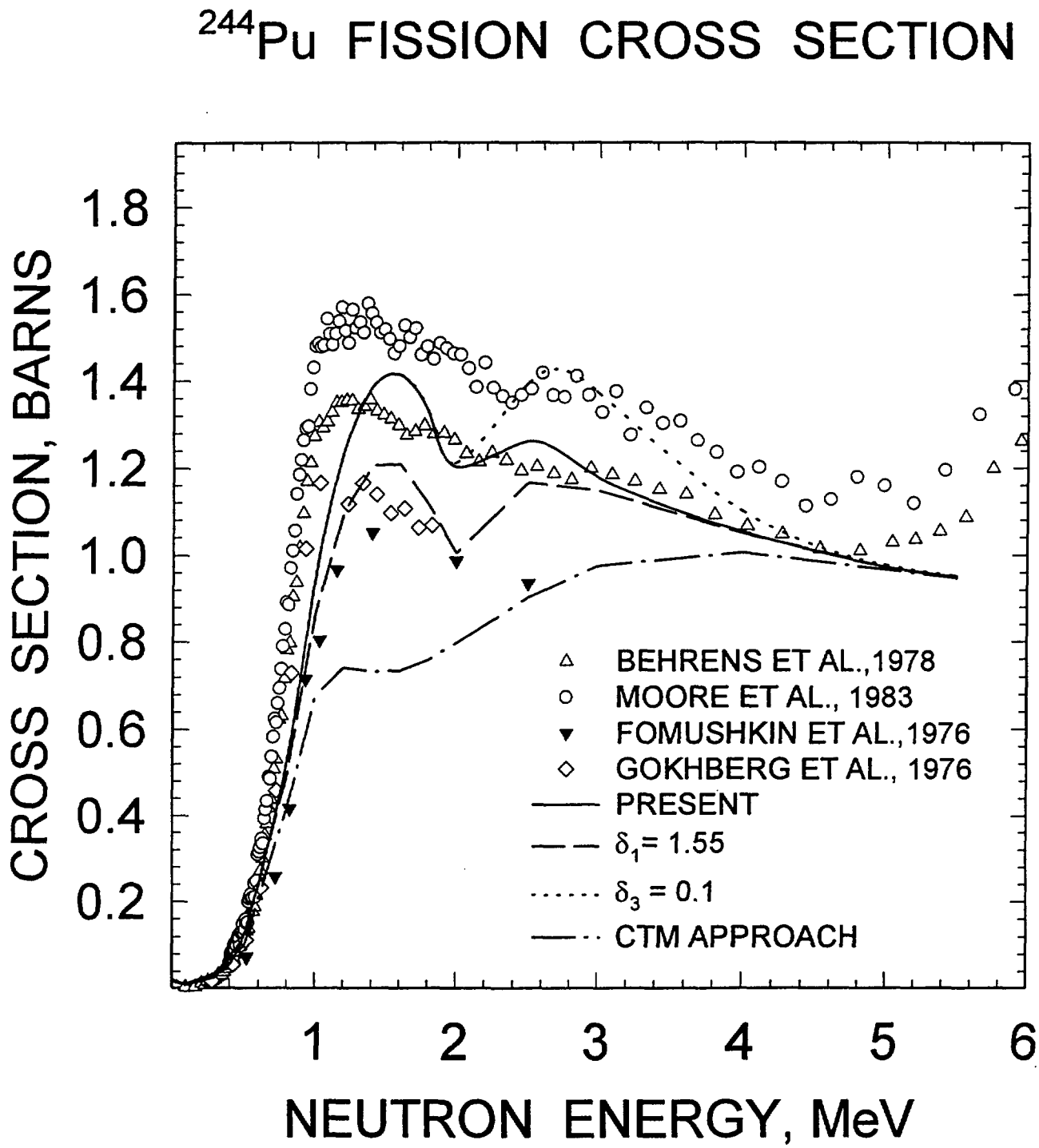
^{244}Pu FISSION CROSS SECTION
CROSS SECTION, BARNS
1.8
1.6
1.4
1.2
1.0
0.8
0.6
0.4
0.2
1
2
3
4
5
6
NEUTRON ENERGY, MeV
BEHRENS ET AL.,1978
MOORE ET AL., 1983
FOMUSHKIN ET AL.,1976
GOKHBERG ET AL., 1976
PRESENT
δ_1= 1.55
δ_3 = 0.1
CTM APPROACH

FIG. 32

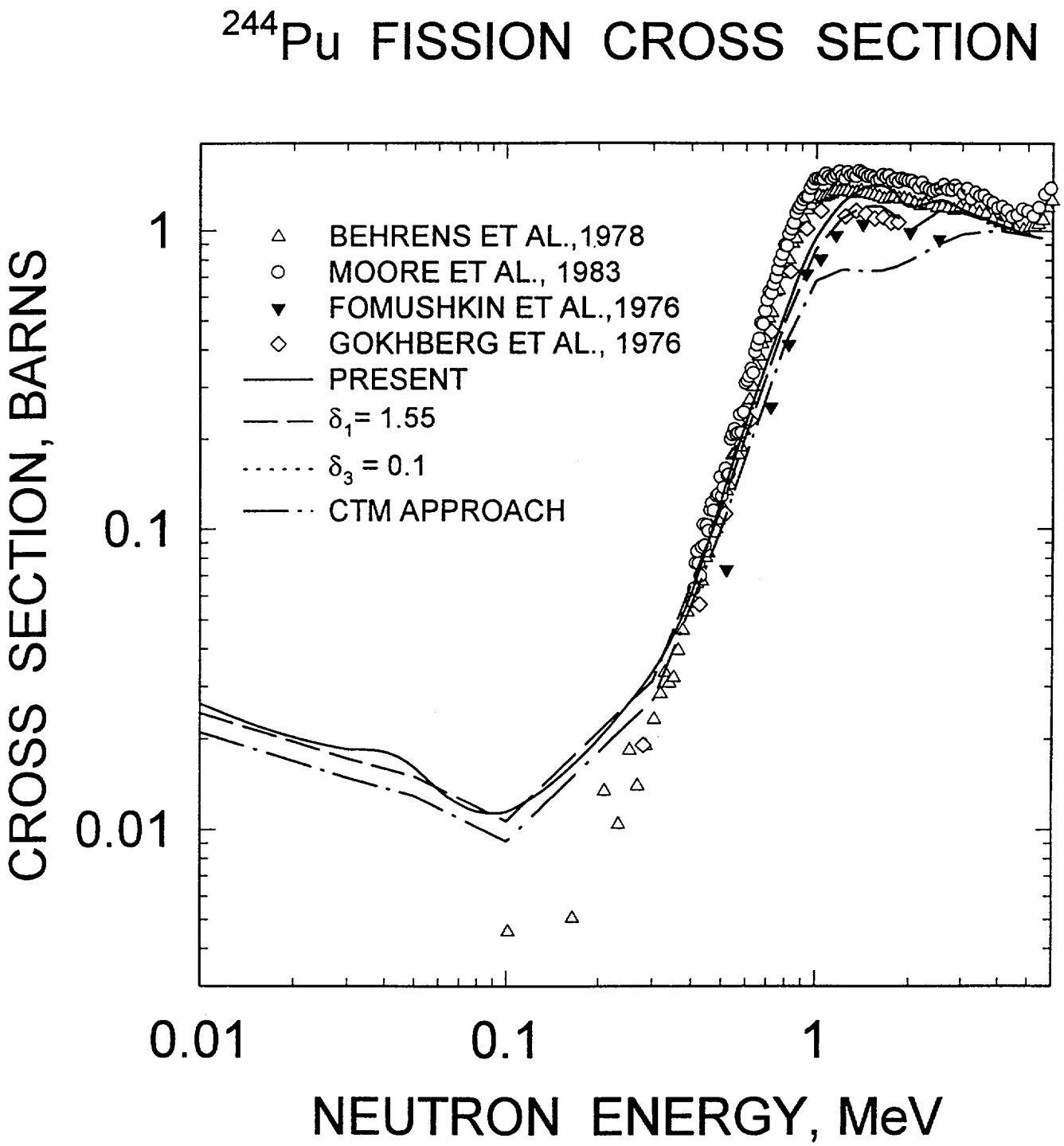
^{244}Pu FISSION CROSS SECTION
CROSS SECTION, BARNS
1
0.1
0.01
BEHRENS ET AL.,1978
MOORE ET AL., 1983
FOMUSHKIN ET AL.,1976
GOKHBERG ET AL., 1976
PRESENT
δ_1= 1.55
δ_3 = 0.1
CTM APPROACH
0.01
0.1
1
NEUTRON ENERGY, MeV

FIG. 32a

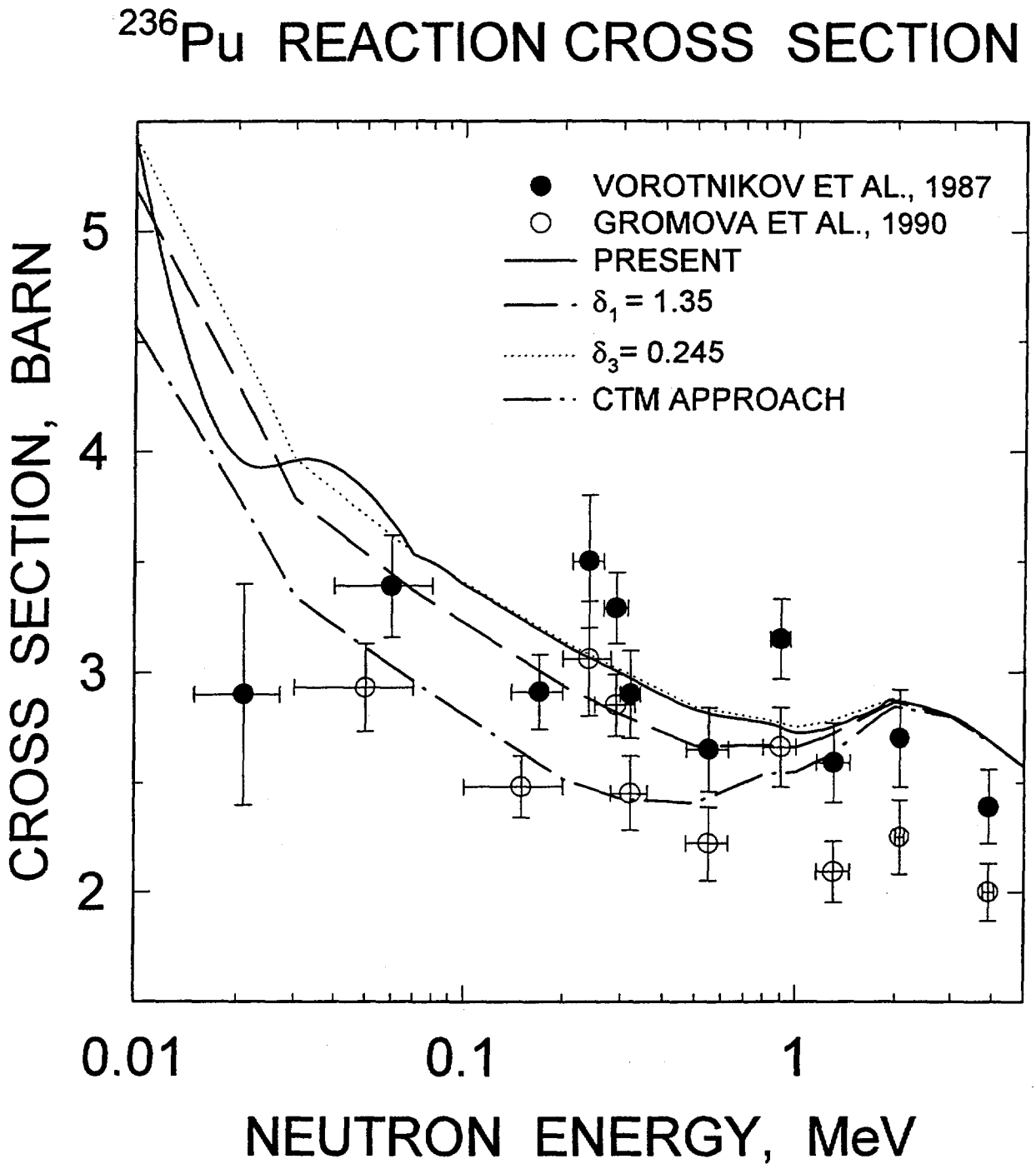
^{236}Pu REACTION CROSS SECTION
VOROTNIKOV ET AL., 1987
GROMOVA ET AL., 1990
PRESENT
δ_1 = 1.35
δ_3= 0.245
CTM APPROACH
CROSS SECTION, BARN
5
4
3
2
0.01
0.1
1
NEUTRON ENERGY, MeV

FIG. 33

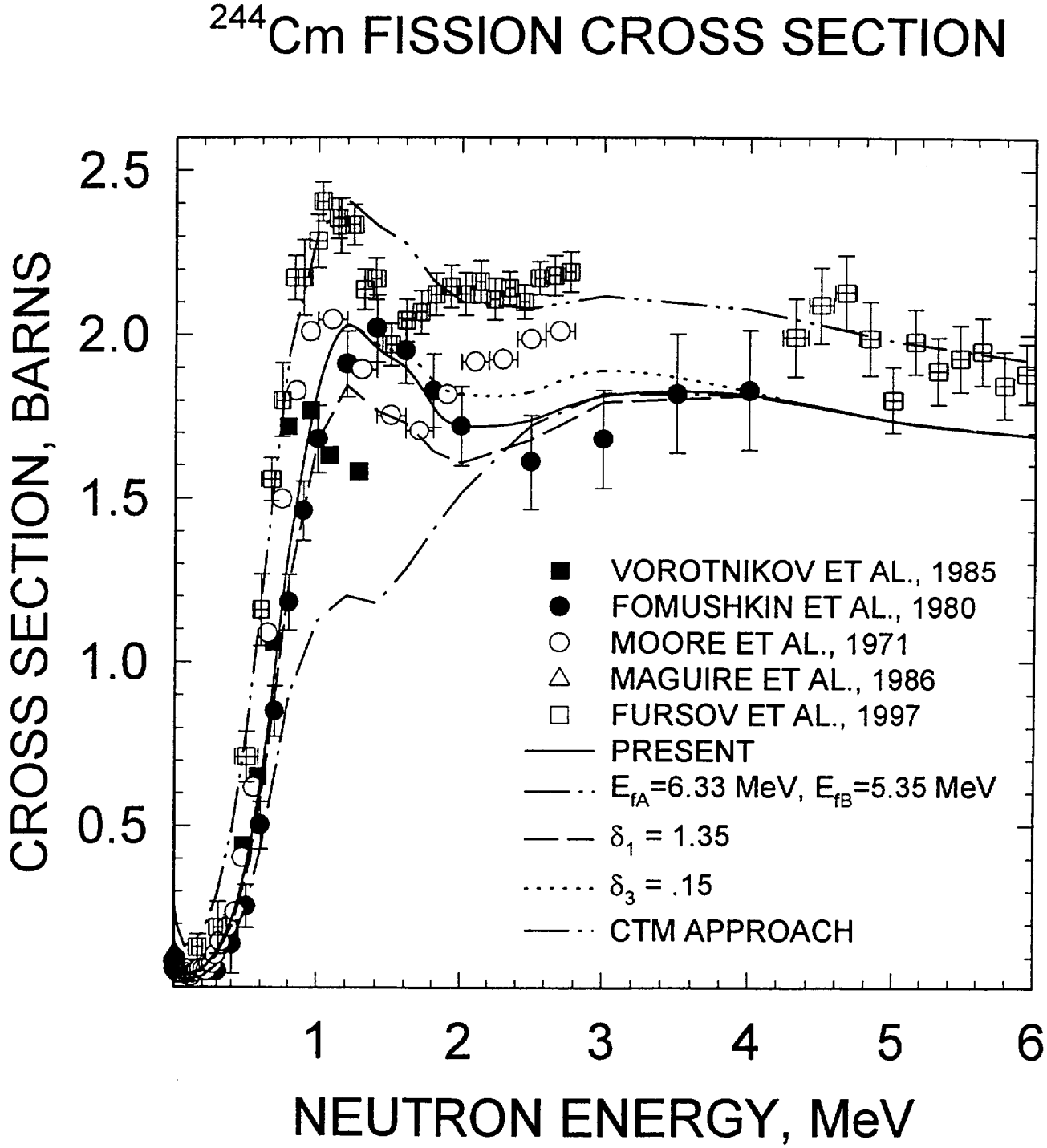
^{244}Cm FISSION CROSS SECTION
CROSS SECTION, BARNS
2.5
2.0
1.5
1.0
0.5
1
2
3
4
5
6
NEUTRON ENERGY, MeV
VOROTNIKOV ET AL., 1985
FOMUSHKIN ET AL., 1980
MOORE ET AL., 1971
MAGUIRE ET AL., 1986
FURSOV ET AL., 1997
PRESENT
E_{fA}=6.33 MeV, E_{fB}=5.35 MeV
δ_1 = 1.35
δ_3 = .15
CTM APPROACH

FIG. 34

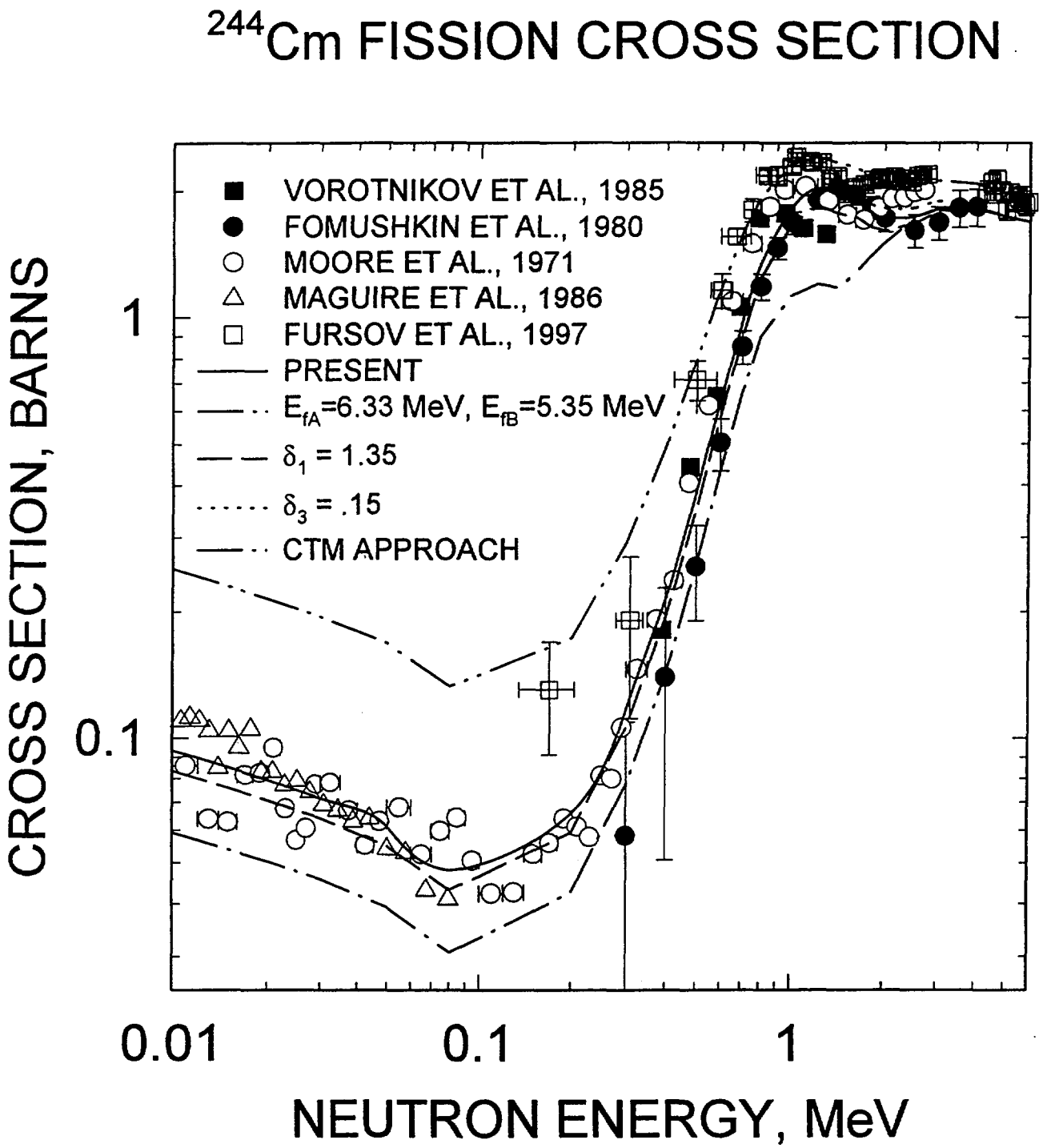
^{244}Cm FISSION CROSS SECTION
VOROTNIKOV ET AL., 1985
FOMUSHKIN ET AL., 1980
MOORE ET AL., 1971
MAGUIRE ET AL., 1986
FURSOV ET AL., 1997
PRESENT
E_{fA}=6.33 MeV, E_{fB}=5.35 MeV
δ_1 = 1.35
δ_3 = .15
CTM APPROACH
CROSS SECTION, BARNS
1
0.1
0.01
0.1
1
NEUTRON ENERGY, MeV

FIG. 34a

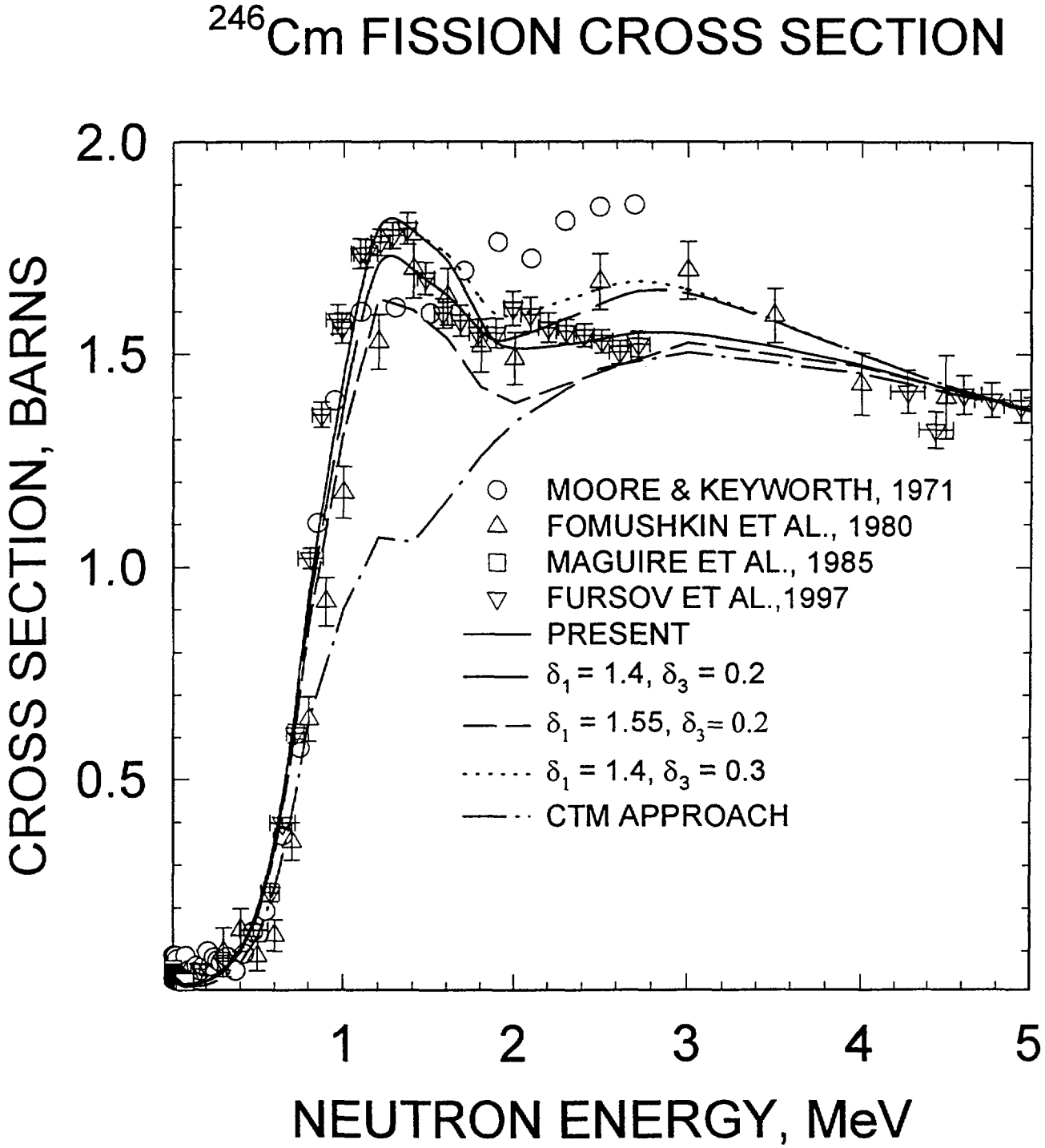
^{246}Cm FISSION CROSS SECTION
CROSS SECTION, BARNS
2.0
1.5
1.0
0.5
1
2
3
4
5
NEUTRON ENERGY, MeV
MOORE & KEYWORTH, 1971
FOMUSHKIN ET AL., 1980
MAGUIRE ET AL., 1985
FURSOV ET AL.,1997
PRESENT
δ_1 = 1.4, δ_3 = 0.2
δ_1 = 1.55, δ_3 = 0.2
δ_1 = 1.4, δ_3 = 0.3
CTM APPROACH

FIG. 35

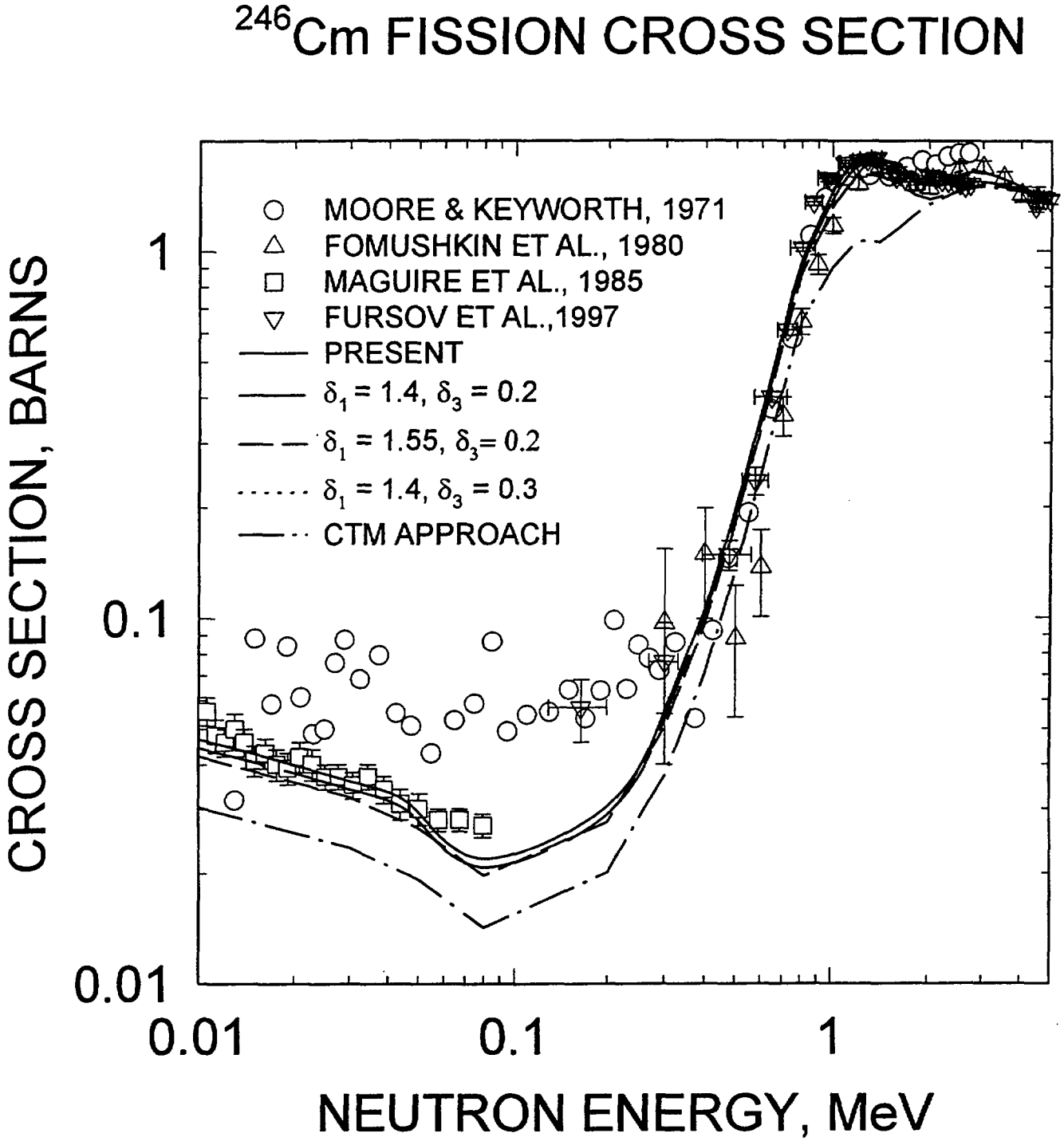
^{246}Cm FISSION CROSS SECTION
MOORE & KEYWORTH, 1971
FOMUSHKIN ET AL., 1980
MAGUIRE ET AL., 1985
FURSOV ET AL.,1997
PRESENT
δ_1 = 1.4, δ_3 = 0.2
δ_1 = 1.55, δ_3= 0.2
δ_1 = 1.4, δ_3 = 0.3
CTM APPROACH
CROSS SECTION, BARNS
1
0.1
0.01
0.01
0.1
1
NEUTRON ENERGY, MeV

FIG. 35a

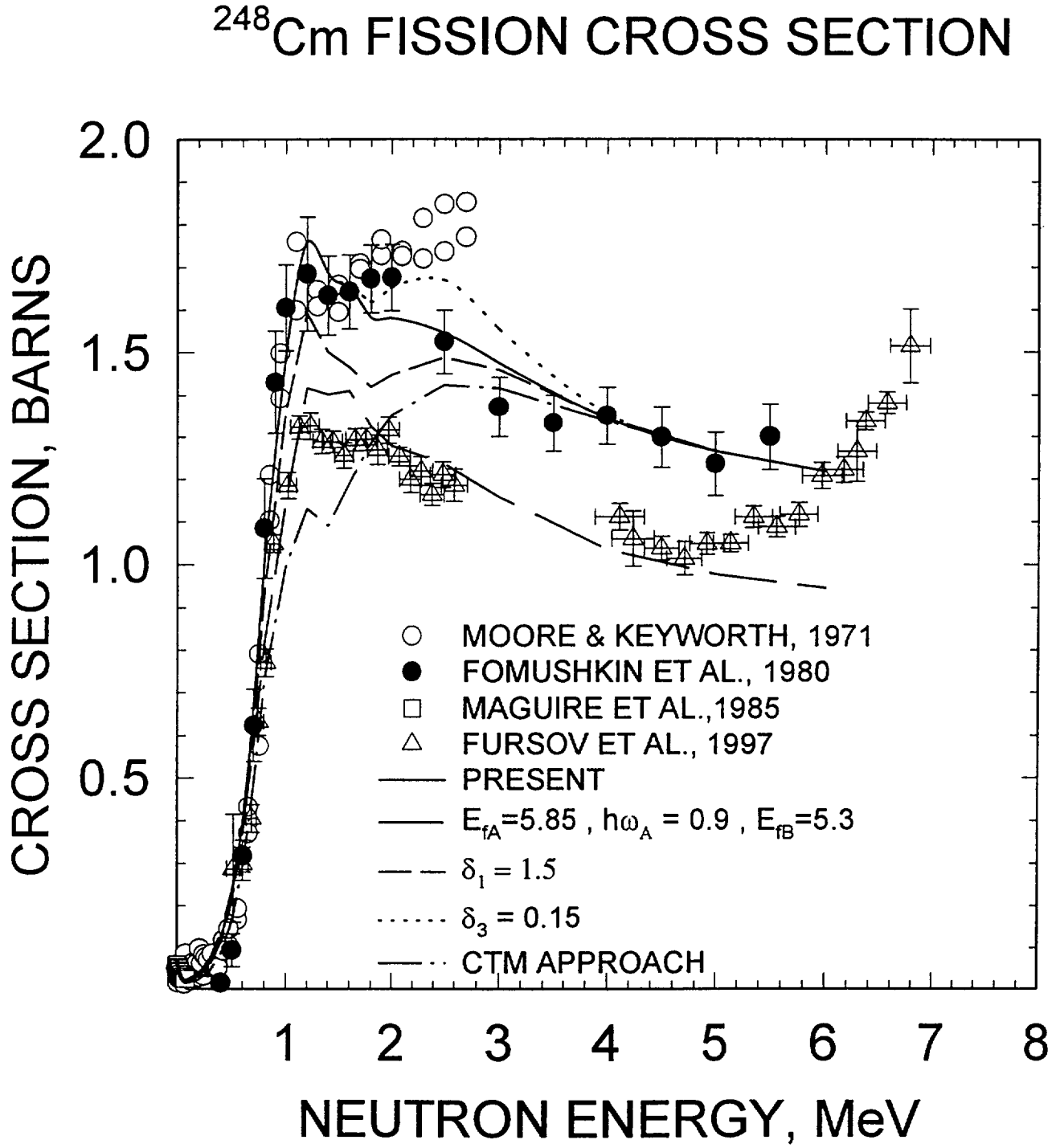
^{248}Cm FISSION CROSS SECTION
CROSS SECTION, BARNS
2.0
1.5
1.0
0.5
1
2
3
4
5
6
7
8
NEUTRON ENERGY, MeV
MOORE & KEYWORTH, 1971
FOMUSHKIN ET AL., 1980
MAGUIRE ET AL.,1985
FURSOV ET AL., 1997
PRESENT
E_{fA}=5.85 , $h\omega_A$ = 0.9 , E_{fB}=5.3
δ_1 = 1.5
δ_3 = 0.15
CTM APPROACH

FIG. 36

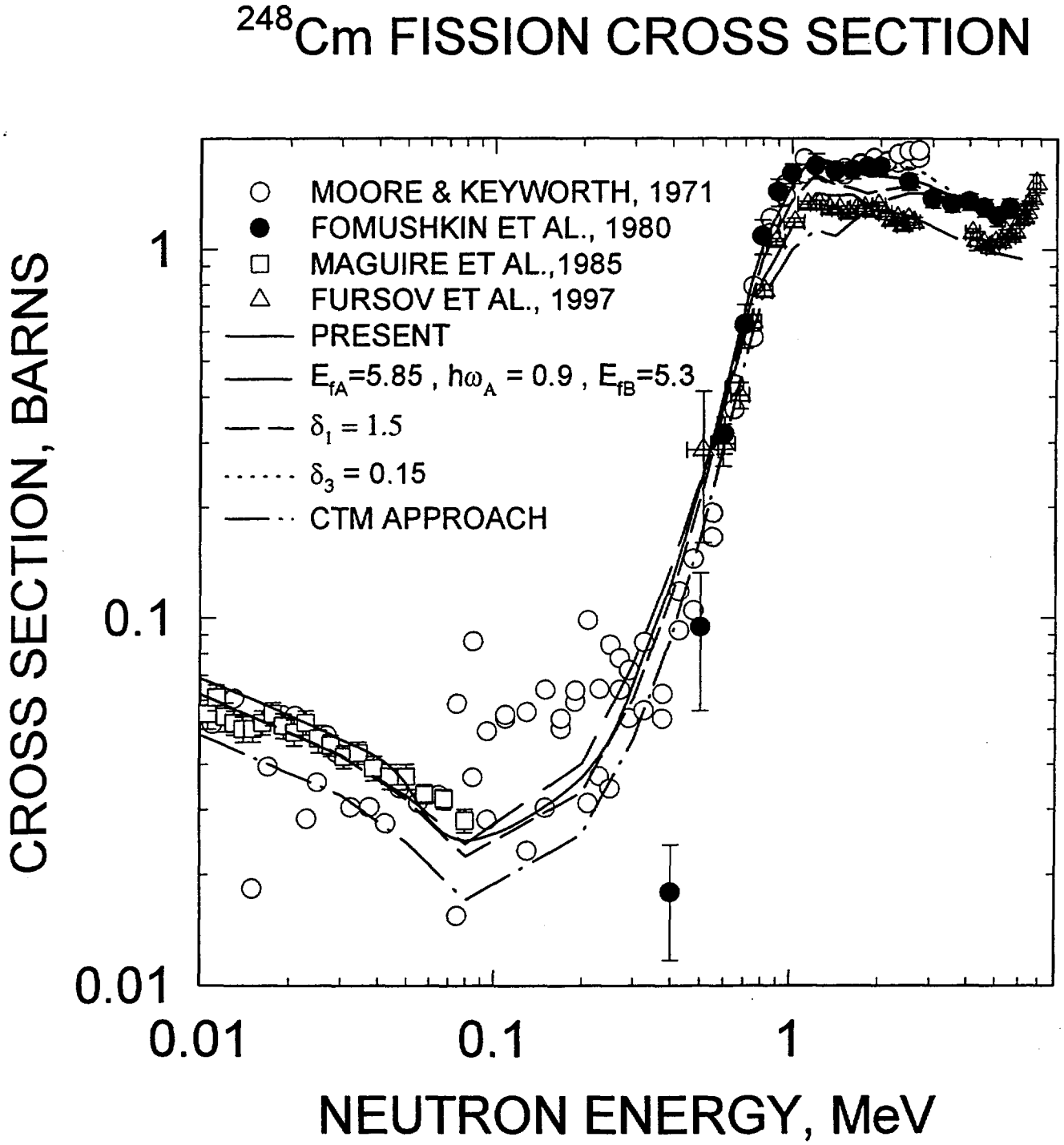
^{248}Cm FISSION CROSS SECTION
MOORE & KEYWORTH, 1971
FOMUSHKIN ET AL., 1980
MAGUIRE ET AL.,1985
FURSOV ET AL., 1997
PRESENT
E_{fA}=5.85 , $h\omega_A$ = 0.9 , E_{fB}=5.3
δ_1 = 1.5
δ_3 = 0.15
CTM APPROACH
CROSS SECTION, BARNS
1
0.1
0.01
0.01
0.1
1
NEUTRON ENERGY, MeV

FIG. 36a

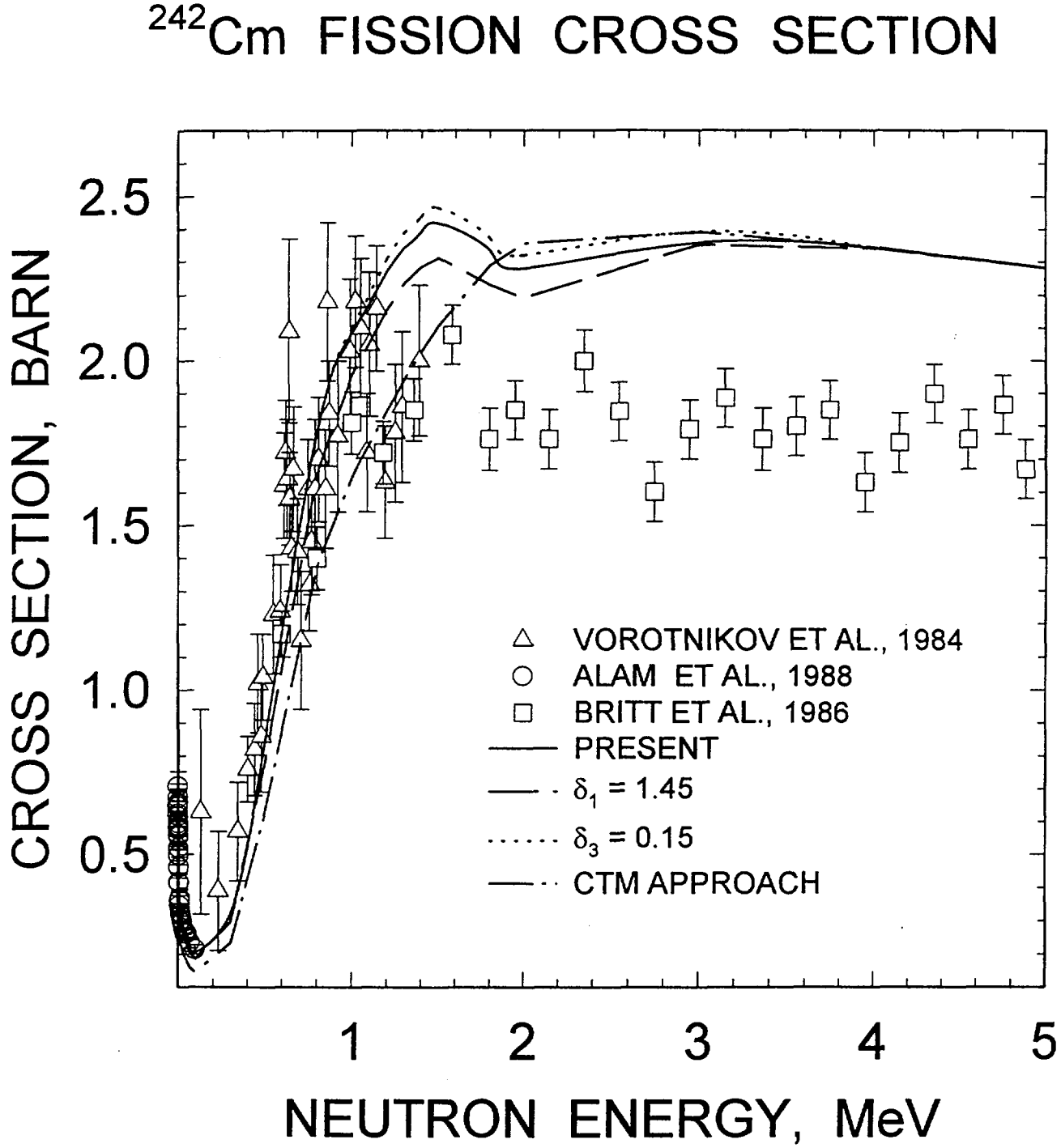
^{242}Cm FISSION CROSS SECTION
CROSS SECTION, BARN
2.5
2.0
1.5
1.0
0.5
1
2
3
4
5
NEUTRON ENERGY, MeV
VOROTNIKOV ET AL., 1984
ALAM ET AL., 1988
BRITT ET AL., 1986
PRESENT
δ_1 = 1.45
δ_3 = 0.15
CTM APPROACH

FIG. 37

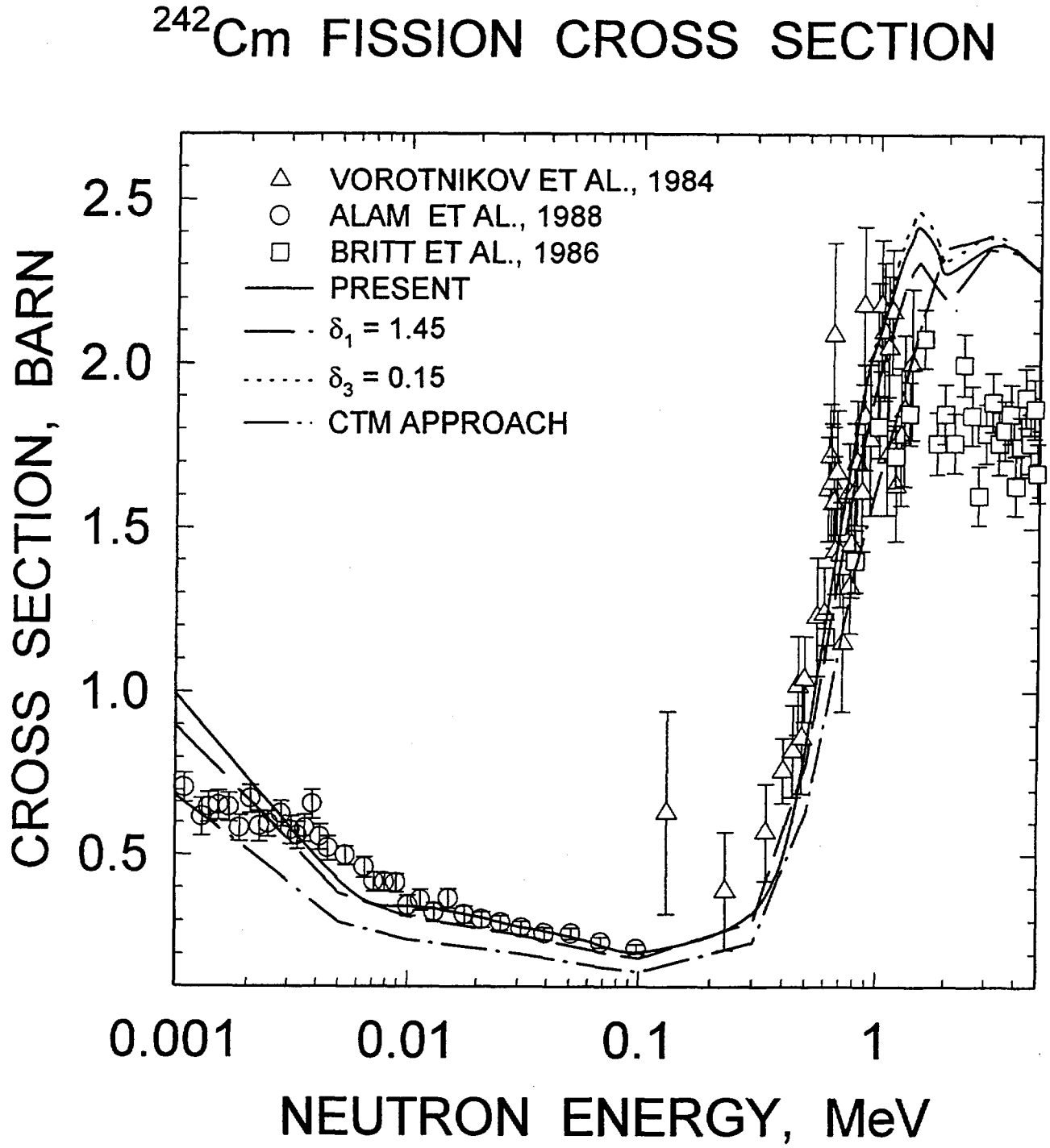
^{242}Cm FISSION CROSS SECTION
VOROTNIKOV ET AL., 1984
ALAM ET AL., 1988
BRITT ET AL., 1986
PRESENT
δ_1 = 1.45
δ_3 = 0.15
CTM APPROACH
CROSS SECTION, BARN
2.5
2.0
1.5
1.0
0.5
0.001
0.01
0.1
1
NEUTRON ENERGY, MeV

FIG. 37a

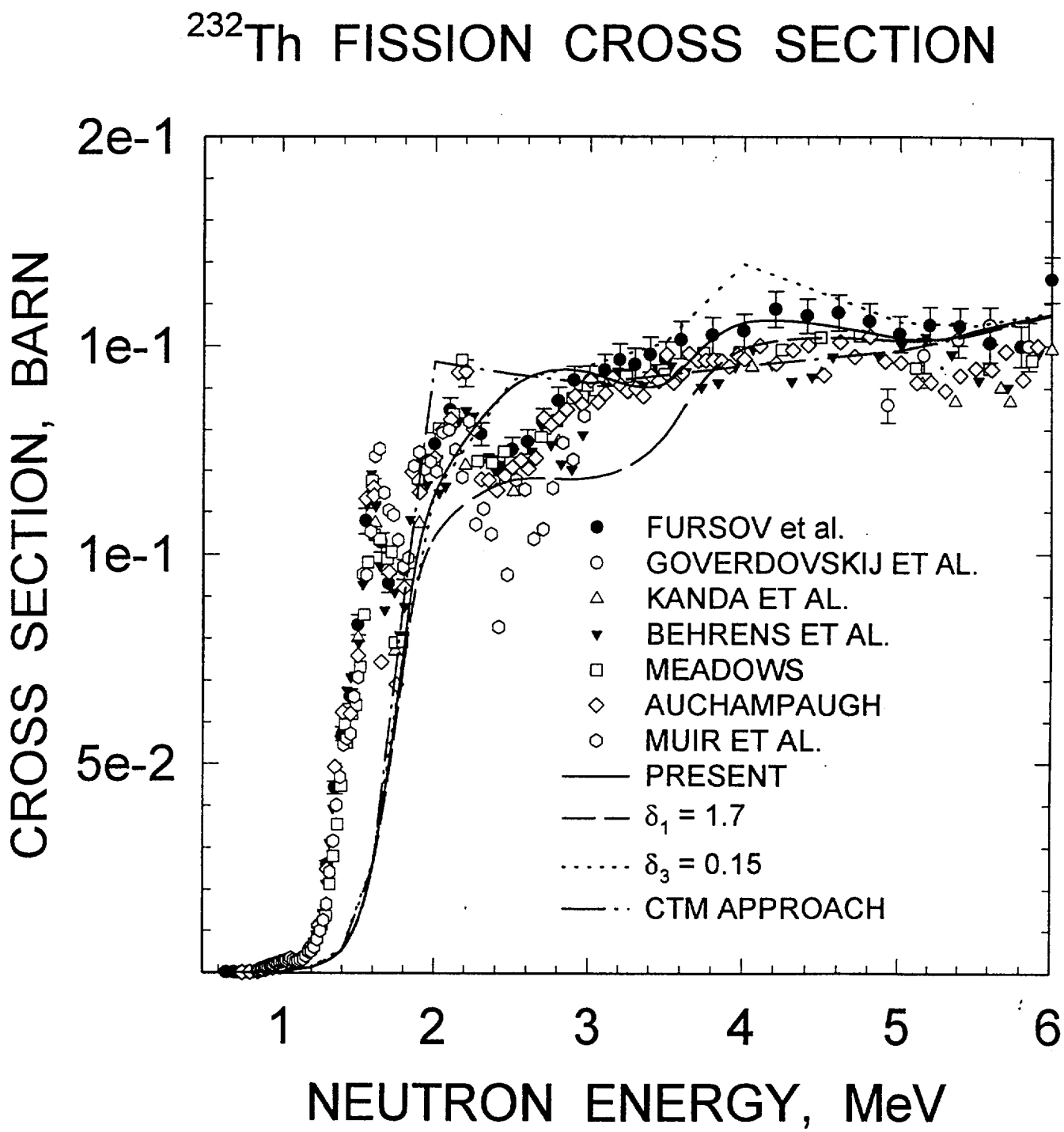
^{232}Th FISSION CROSS SECTION
CROSS SECTION, BARN
2e-1
1e-1
1e-1
5e-2
1
2
3
4
5
6
NEUTRON ENERGY, MeV
FURSOV et al.
GOVERDOVSKIJ ET AL.
KANDA ET AL.
BEHRENS ET AL.
MEADOWS
AUCHAMPAUGH
MUIR ET AL.
PRESENT
δ_1 = 1.7
δ_3 = 0.15
CTM APPROACH

FIG. 38

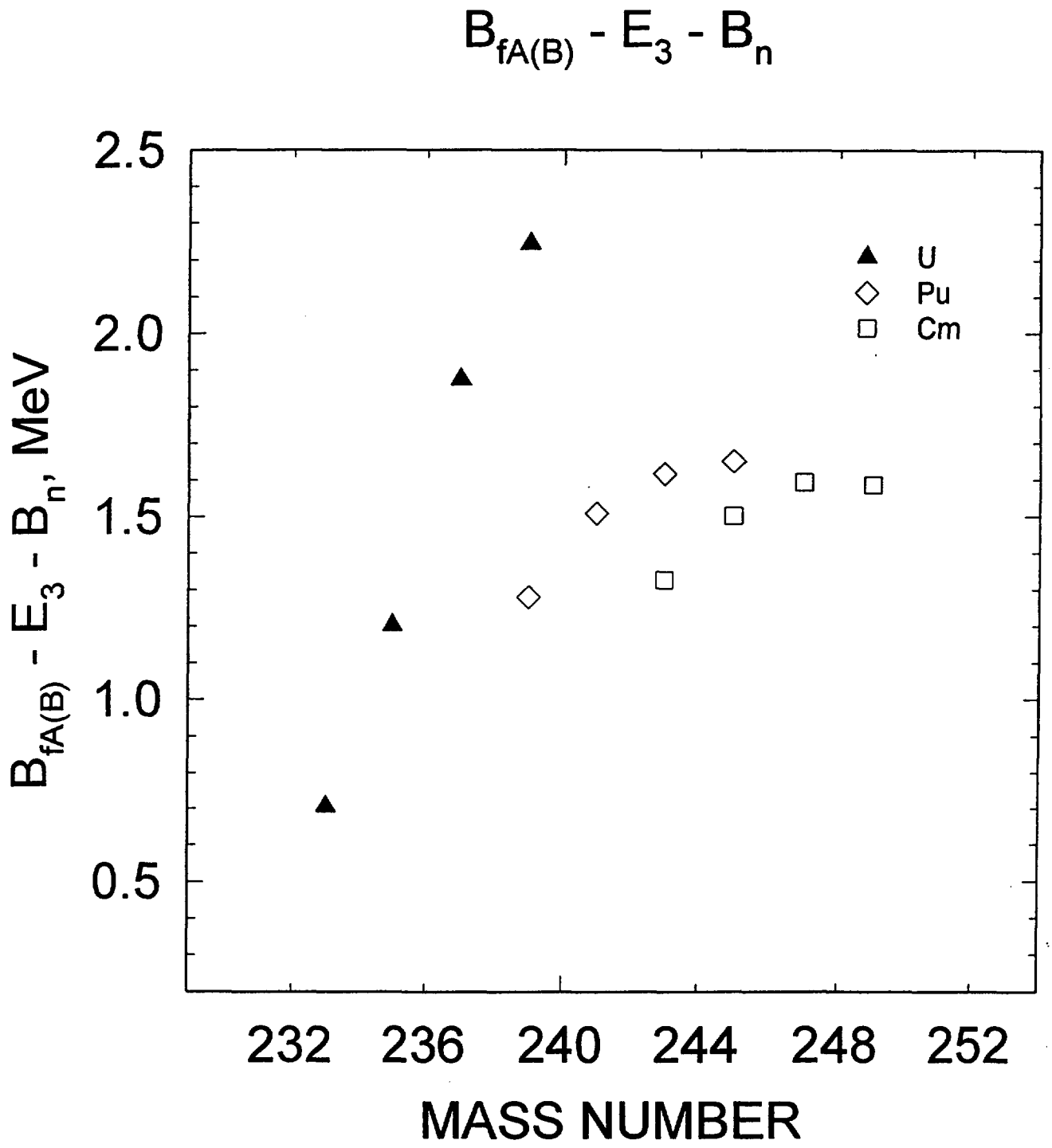
$B_{fA(B)} - E_3 - B_n$
$B_{fA(B)} - E_3 - B_n$, MeV
2.5
2.0
1.5
1.0
0.5
U
Pu
Cm
232
236
240
244
248
252
MASS NUMBER

FIG. 39

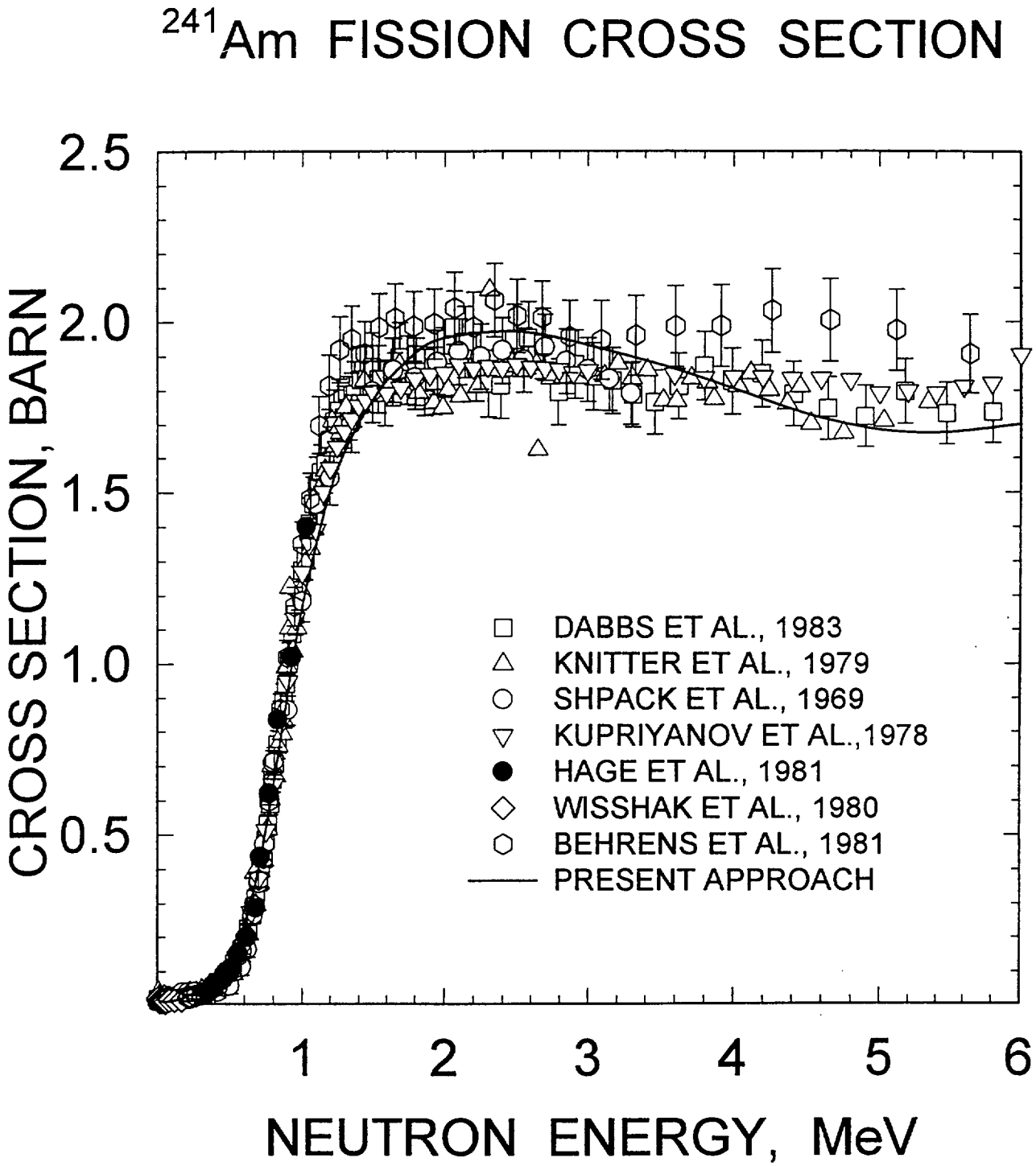
^{241}Am FISSION CROSS SECTION
CROSS SECTION, BARN
2.5
2.0
1.5
1.0
0.5
1
2
3
4
5
6
NEUTRON ENERGY, MeV
DABBS ET AL., 1983
KNITTER ET AL., 1979
SHPACK ET AL., 1969
KUPRIYANOV ET AL.,1978
HAGE ET AL., 1981
WISSHAK ET AL., 1980
BEHRENS ET AL., 1981
PRESENT APPROACH

FIG.40

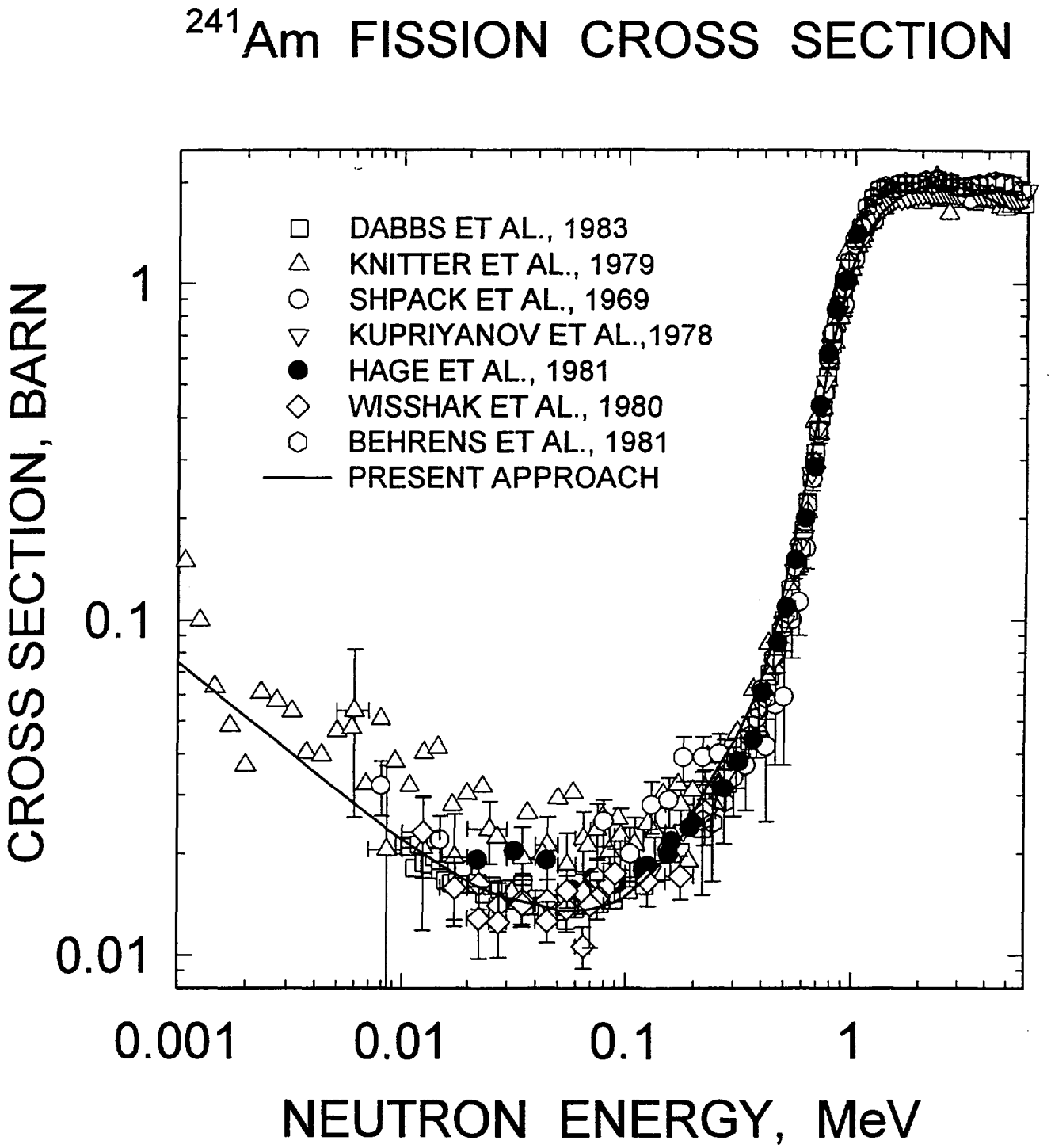
^{241}Am FISSION CROSS SECTION
DABBS ET AL., 1983
KNITTER ET AL., 1979
SHPACK ET AL., 1969
KUPRIYANOV ET AL.,1978
HAGE ET AL., 1981
WISSHAK ET AL., 1980
BEHRENS ET AL., 1981
PRESENT APPROACH
CROSS SECTION, BARN
1
0.1
0.01
0.001
0.01
0.1
1
NEUTRON ENERGY, MeV

FIG.40a

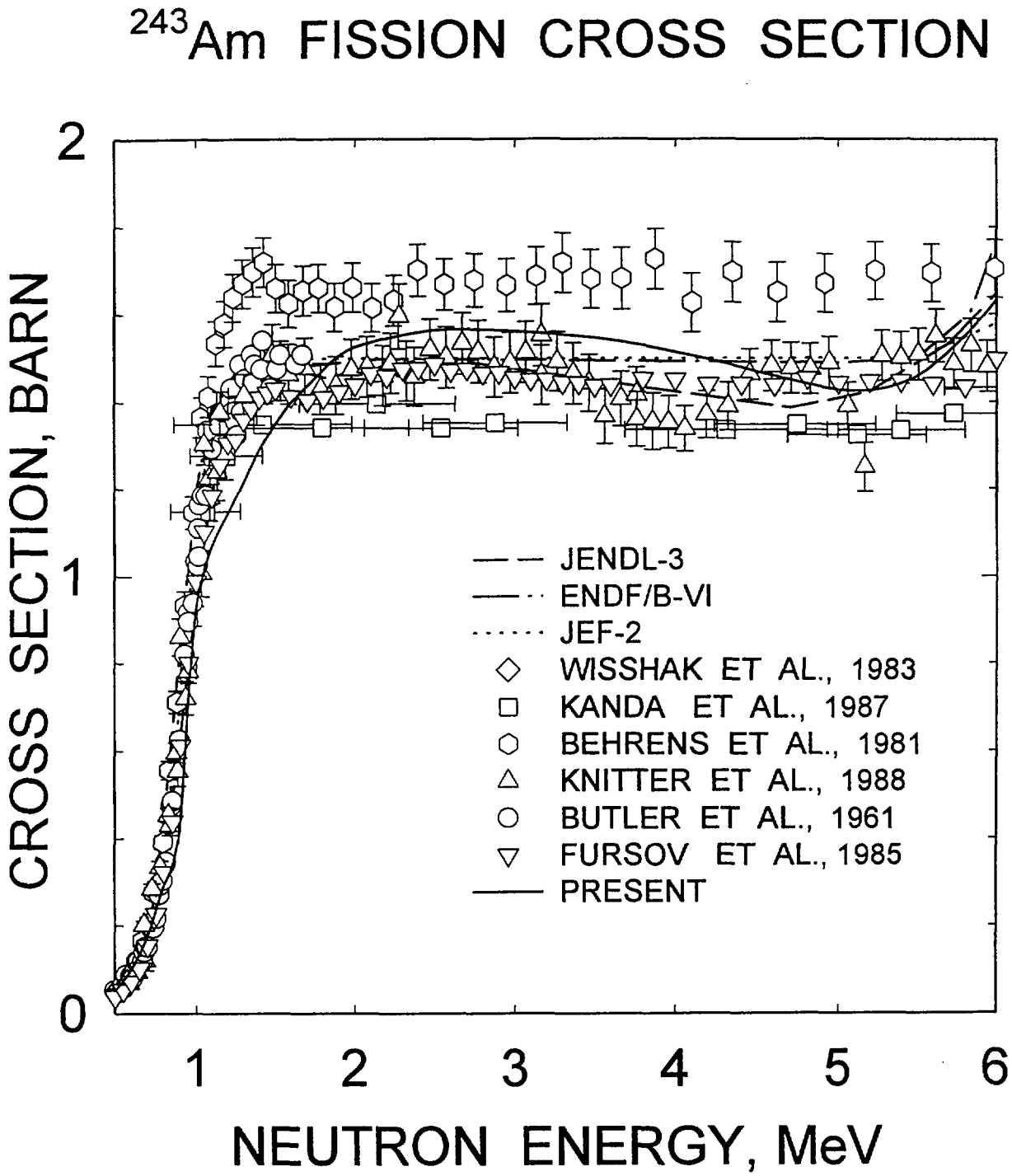
^{243}Am FISSION CROSS SECTION
CROSS SECTION, BARN
NEUTRON ENERGY, MeV
0
1
2
1
2
3
4
5
6
JENDL-3
ENDF/B-VI
JEF-2
WISSHAK ET AL., 1983
KANDA ET AL., 1987
BEHRENS ET AL., 1981
KNITTER ET AL., 1988
BUTLER ET AL., 1961
FURSOV ET AL., 1985
PRESENT

FIG.41

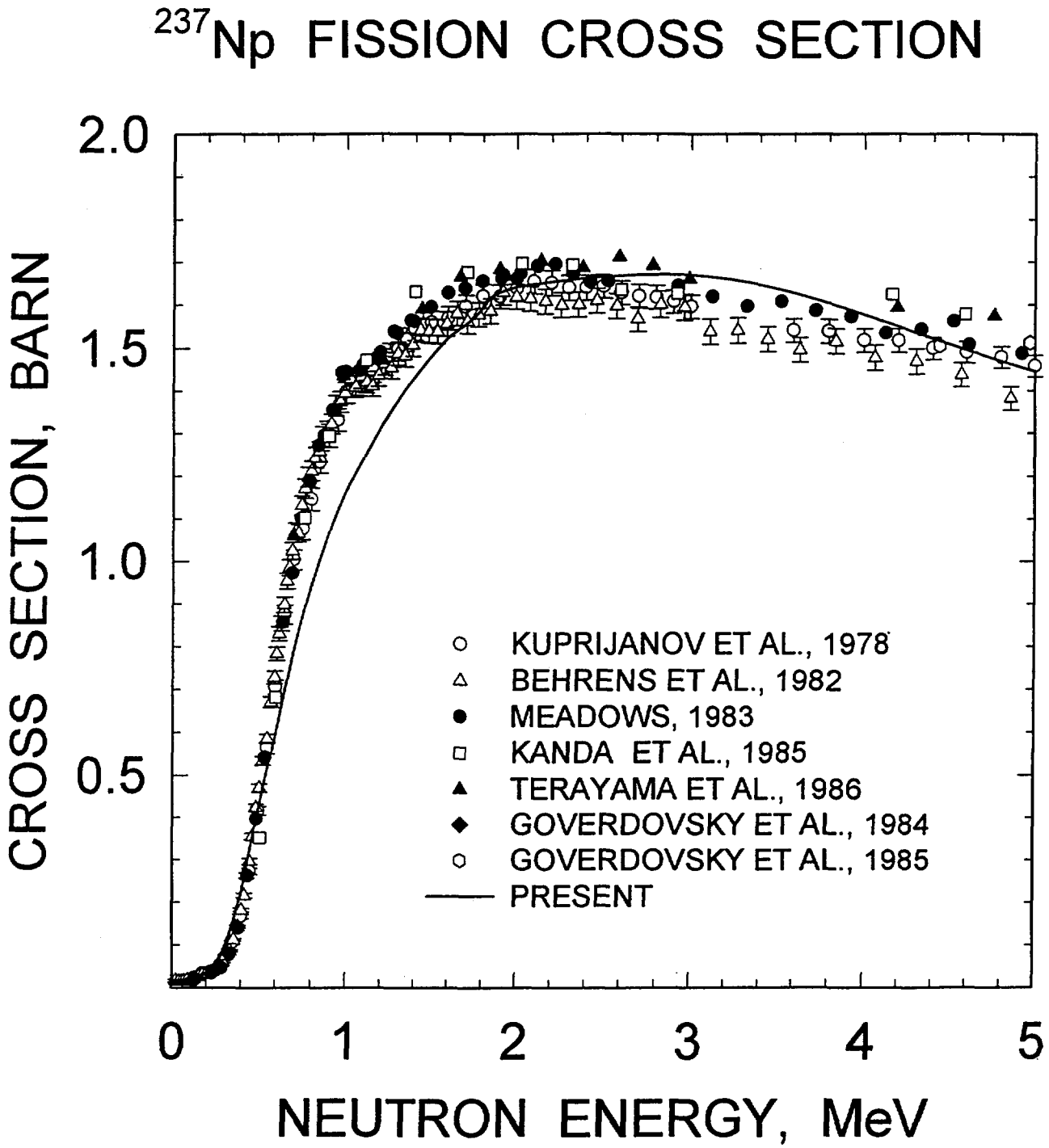
^{237}Np FISSION CROSS SECTION
CROSS SECTION, BARN
2.0
1.5
1.0
0.5
0
1
2
3
4
5
NEUTRON ENERGY, MeV
KUPRIJANOV ET AL., 1978
BEHRENS ET AL., 1982
MEADOWS, 1983
KANDA ET AL., 1985
TERAYAMA ET AL., 1986
GOVERDOVSKY ET AL., 1984
GOVERDOVSKY ET AL., 1985
PRESENT

FIG. 42

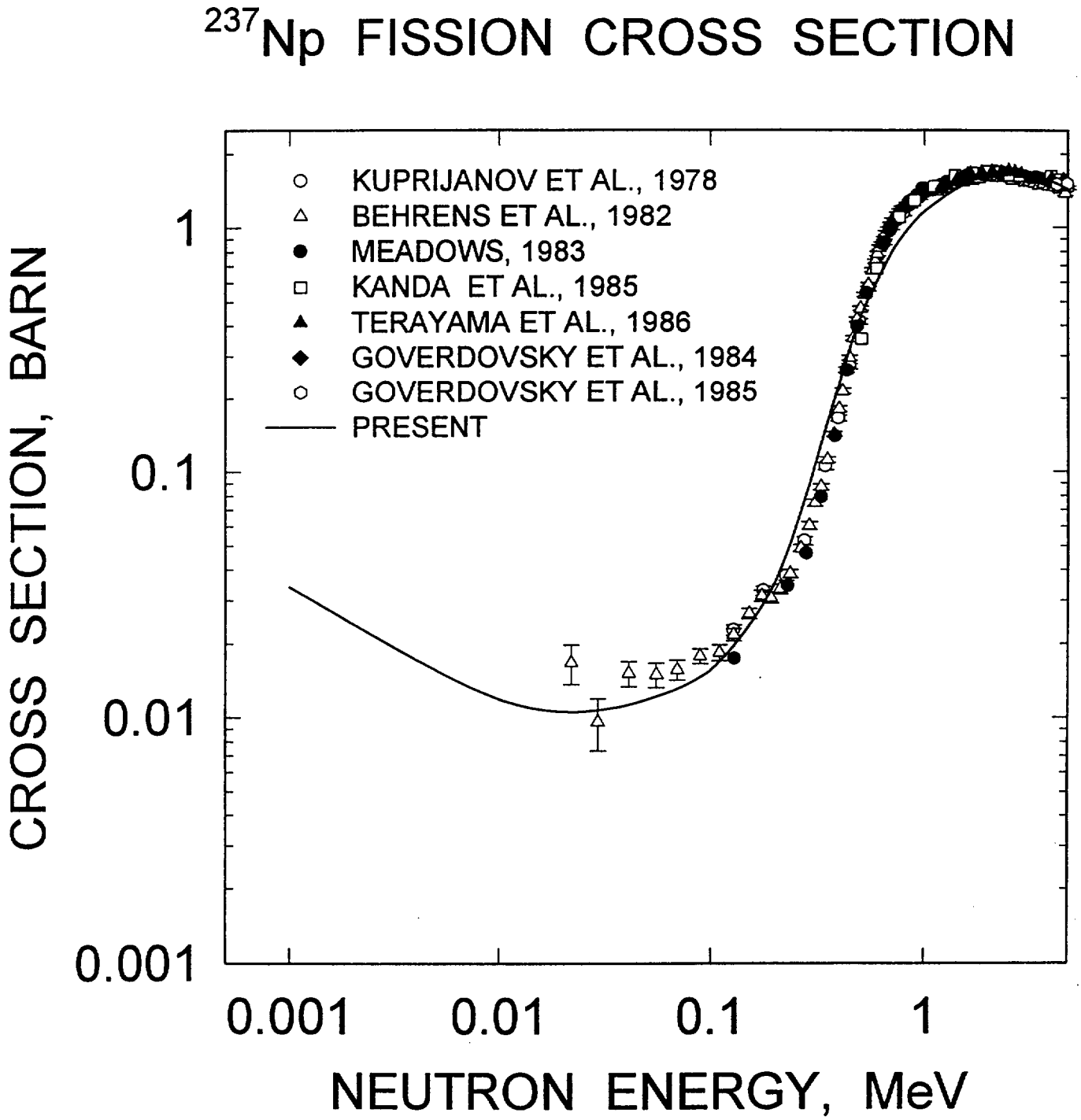
^{237}Np FISSION CROSS SECTION
KUPRIJANOV ET AL., 1978
BEHRENS ET AL., 1982
MEADOWS, 1983
KANDA ET AL., 1985
TERAYAMA ET AL., 1986
GOVERDOVSKY ET AL., 1984
GOVERDOVSKY ET AL., 1985
PRESENT
CROSS SECTION, BARN
1
0.1
0.01
0.001
0.001
0.01
0.1
1
NEUTRON ENERGY, MeV

FIG. 42a

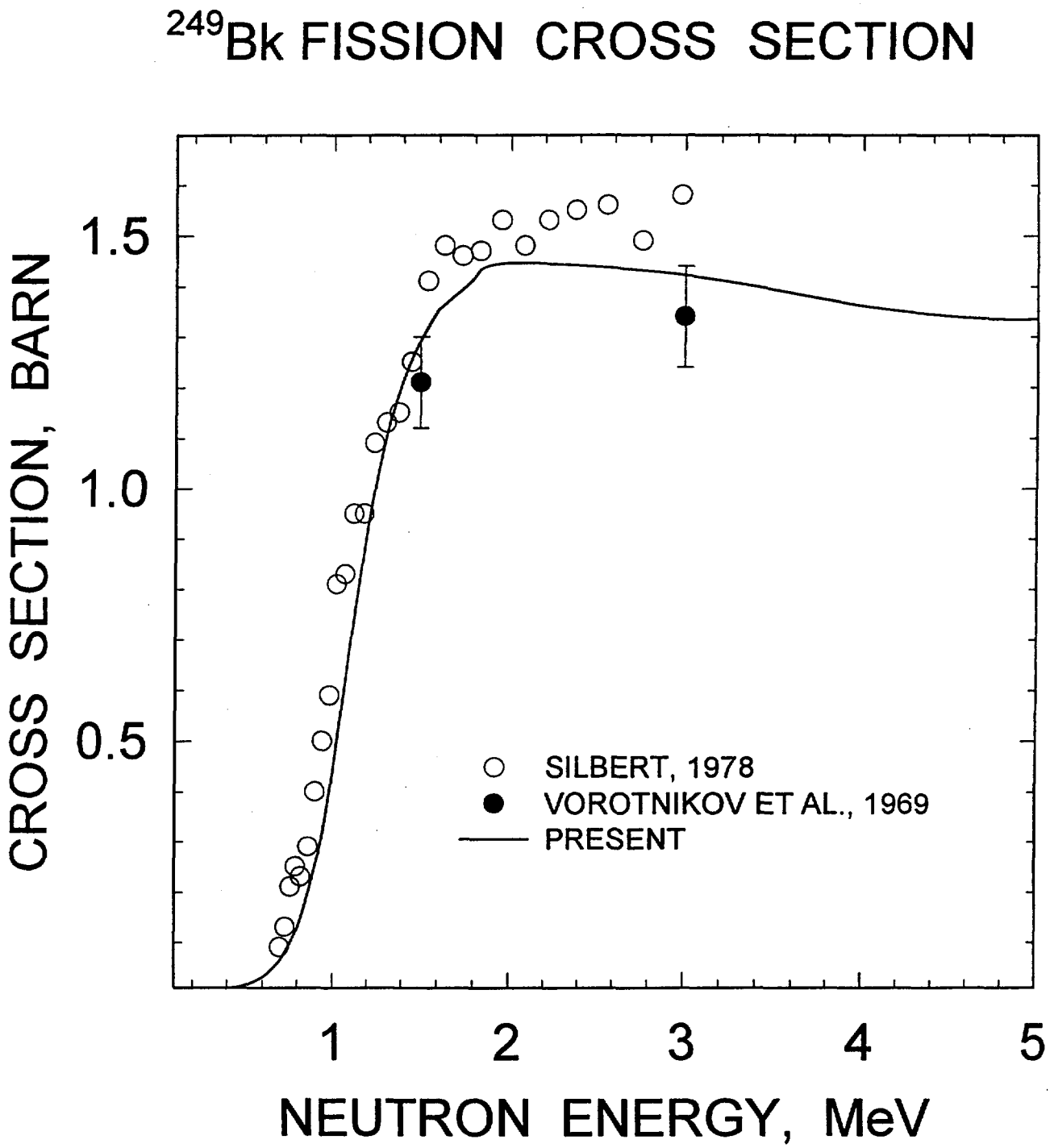
^{249}Bk FISSION CROSS SECTION
CROSS SECTION, BARN
1.5
1.0
0.5
1
2
3
4
5
NEUTRON ENERGY, MeV
SILBERT, 1978
VOROTNIKOV ET AL., 1969
PRESENT

FIG. 43

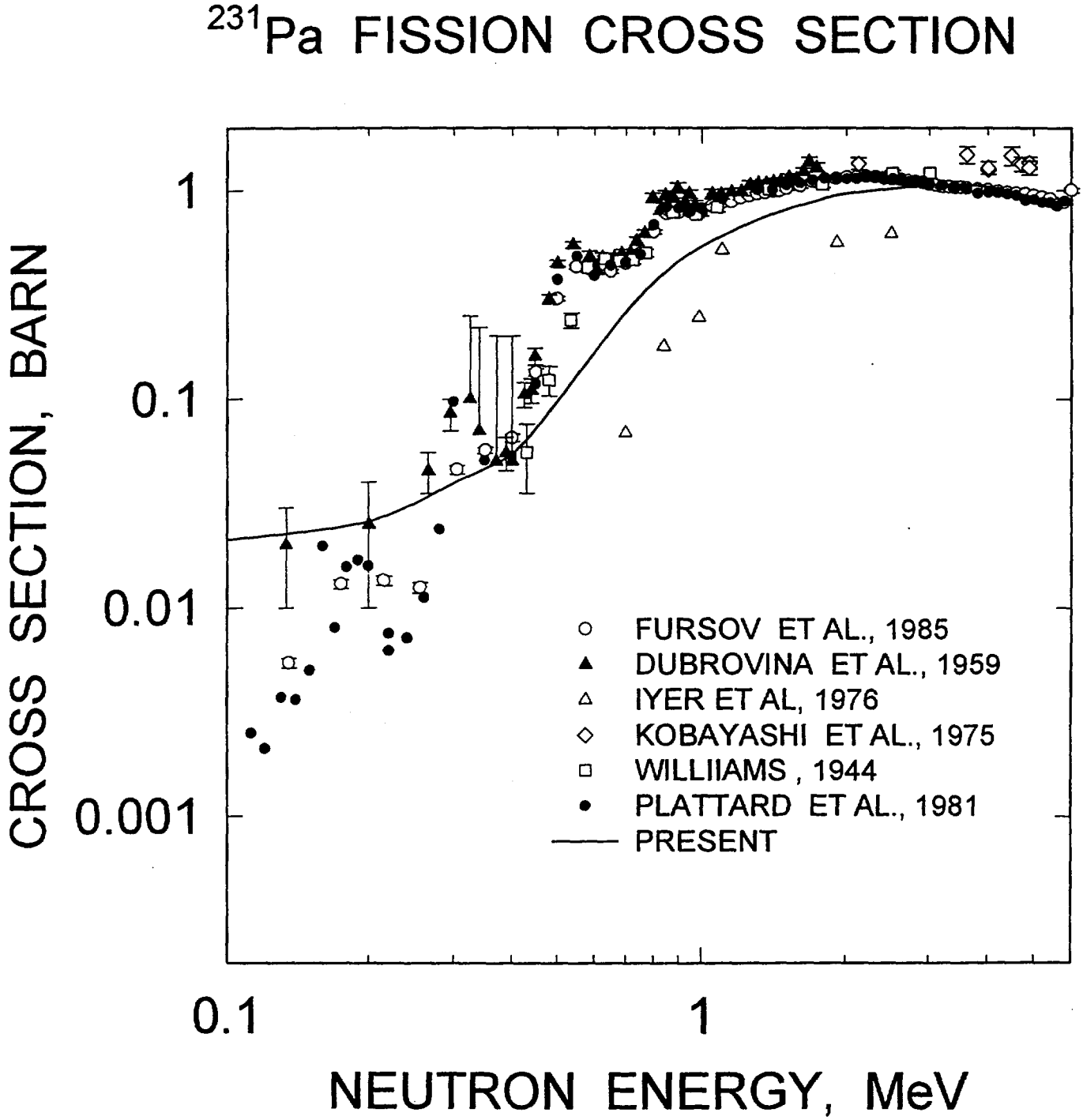
^{231}Pa FISSION CROSS SECTION
CROSS SECTION, BARN
1
0.1
0.01
0.001
0.1
1
NEUTRON ENERGY, MeV
FURSOV ET AL., 1985
DUBROVINA ET AL., 1959
IYER ET AL, 1976
KOBAYASHI ET AL., 1975
WILLIIAMS , 1944
PLATTARD ET AL., 1981
PRESENT

FIG. 44

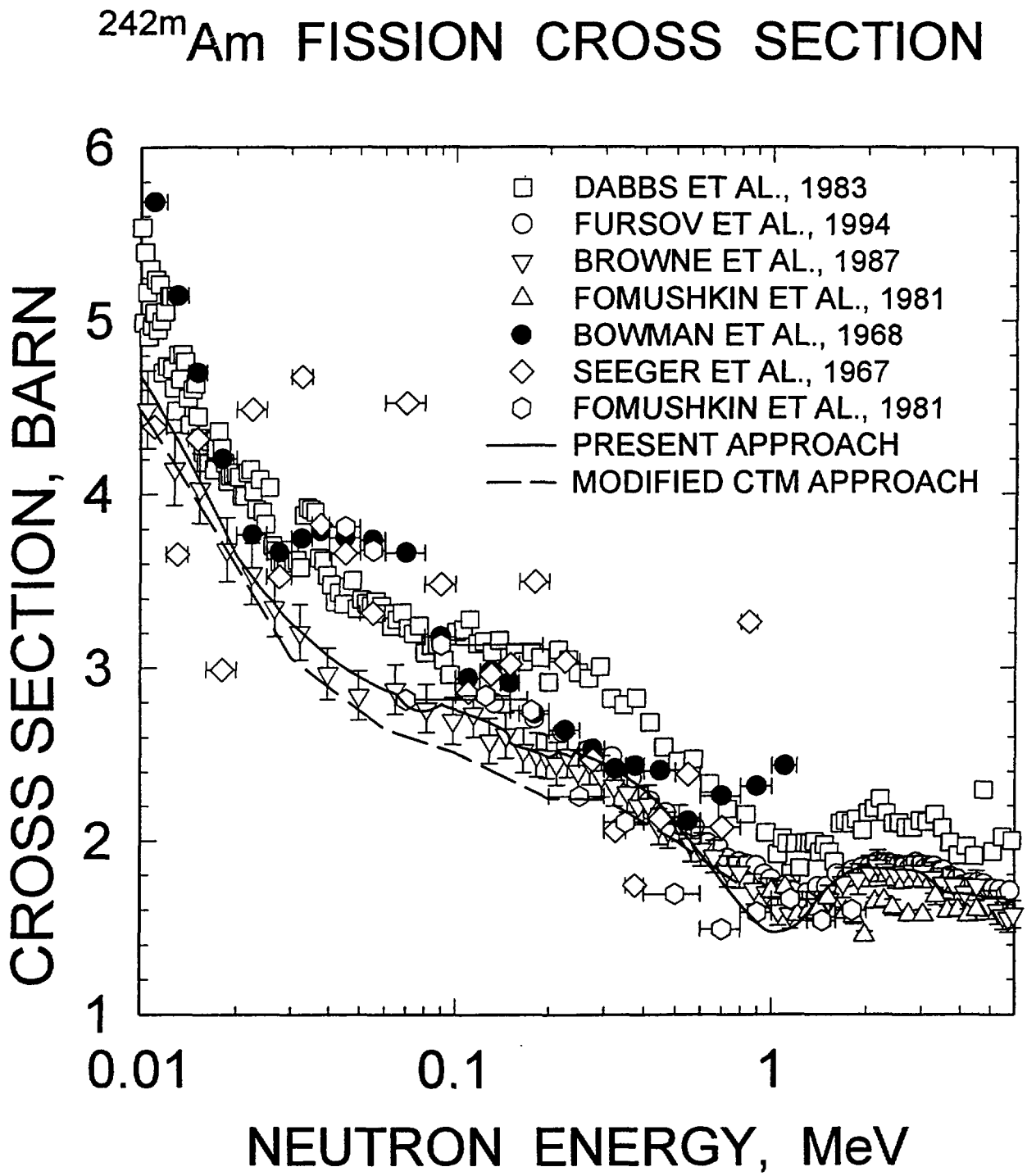
^{242m}Am FISSION CROSS SECTION
CROSS SECTION, BARN
6
5
4
3
2
1
0.01
0.1
1
NEUTRON ENERGY, MeV
DABBS ET AL., 1983
FURSOV ET AL., 1994
BROWNE ET AL., 1987
FOMUSHKIN ET AL., 1981
BOWMAN ET AL., 1968
SEEGER ET AL., 1967
FOMUSHKIN ET AL., 1981
PRESENT APPROACH
MODIFIED CTM APPROACH

FIG. 45

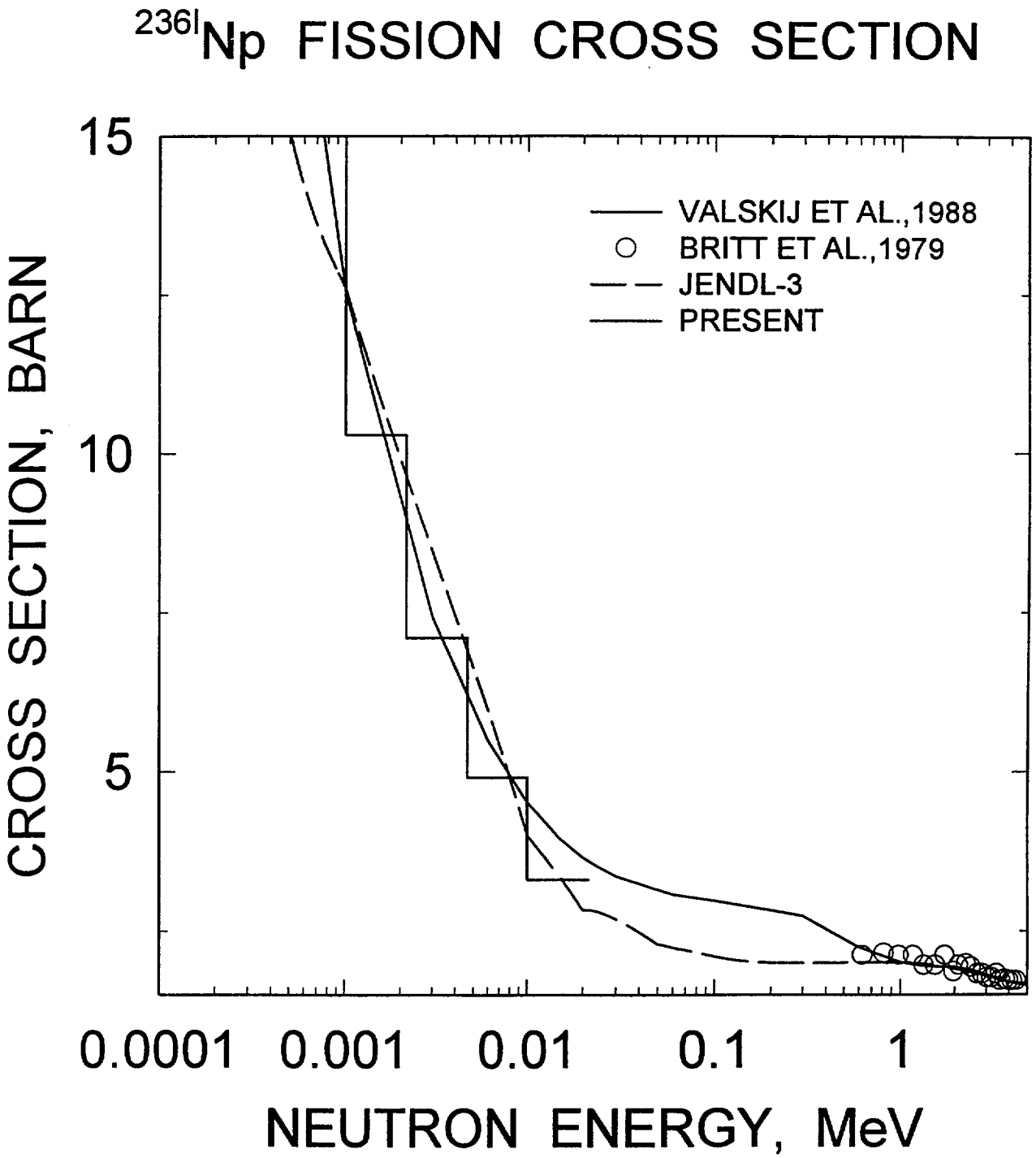
^{236}Np FISSION CROSS SECTION
15
10
5
CROSS SECTION, BARN
VALSKIJ ET AL.,1988
BRITT ET AL.,1979
JENDL-3
PRESENT
0.0001
0.001
0.01
0.1
1
NEUTRON ENERGY, MeV

FIG. 46

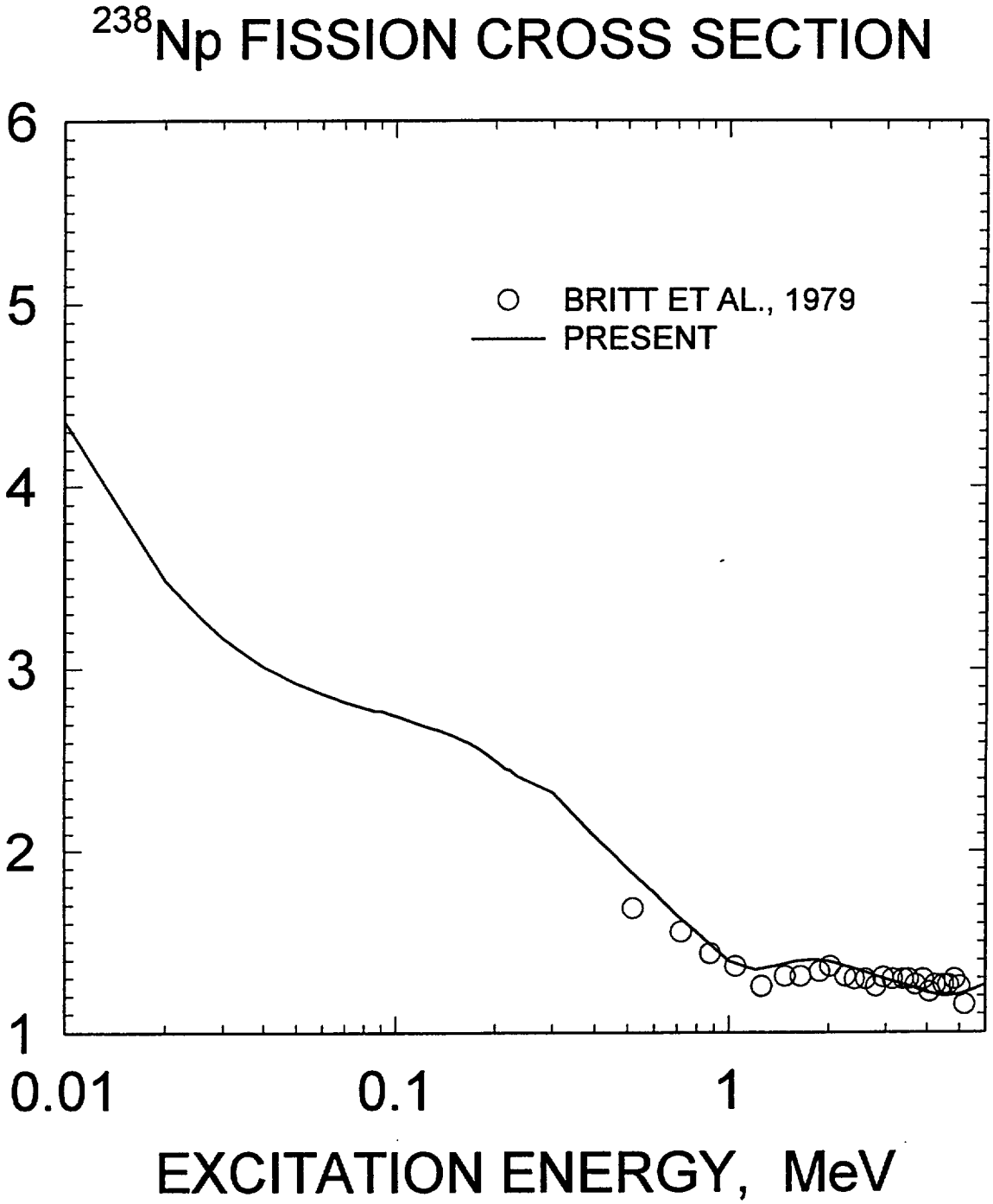
^{238}Np FISSION CROSS SECTION
6
5
4
3
2
1
0.01
0.1
1
BRITT ET AL., 1979
PRESENT
EXCITATION ENERGY, MeV

FIG. 47

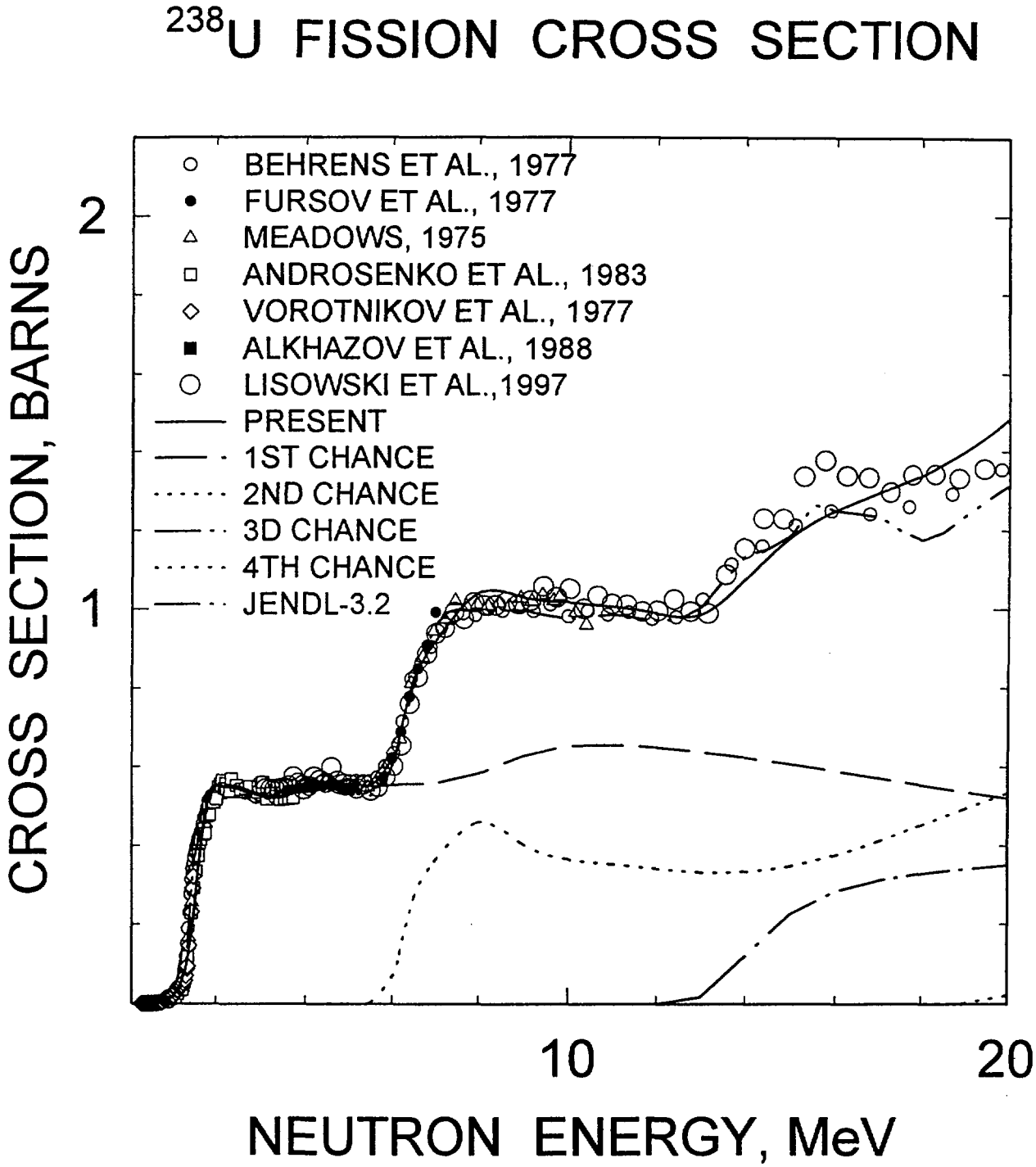
^{238}U FISSION CROSS SECTION
BEHRENS ET AL., 1977
FURSOV ET AL., 1977
MEADOWS, 1975
ANDROSENKO ET AL., 1983
VOROTNIKOV ET AL., 1977
ALKHAZOV ET AL., 1988
LISOWSKI ET AL.,1997
PRESENT
1ST CHANCE
2ND CHANCE
3D CHANCE
4TH CHANCE
JENDL-3.2
CROSS SECTION, BARNS
2
1
10
20
NEUTRON ENERGY, MeV

FIG. 48

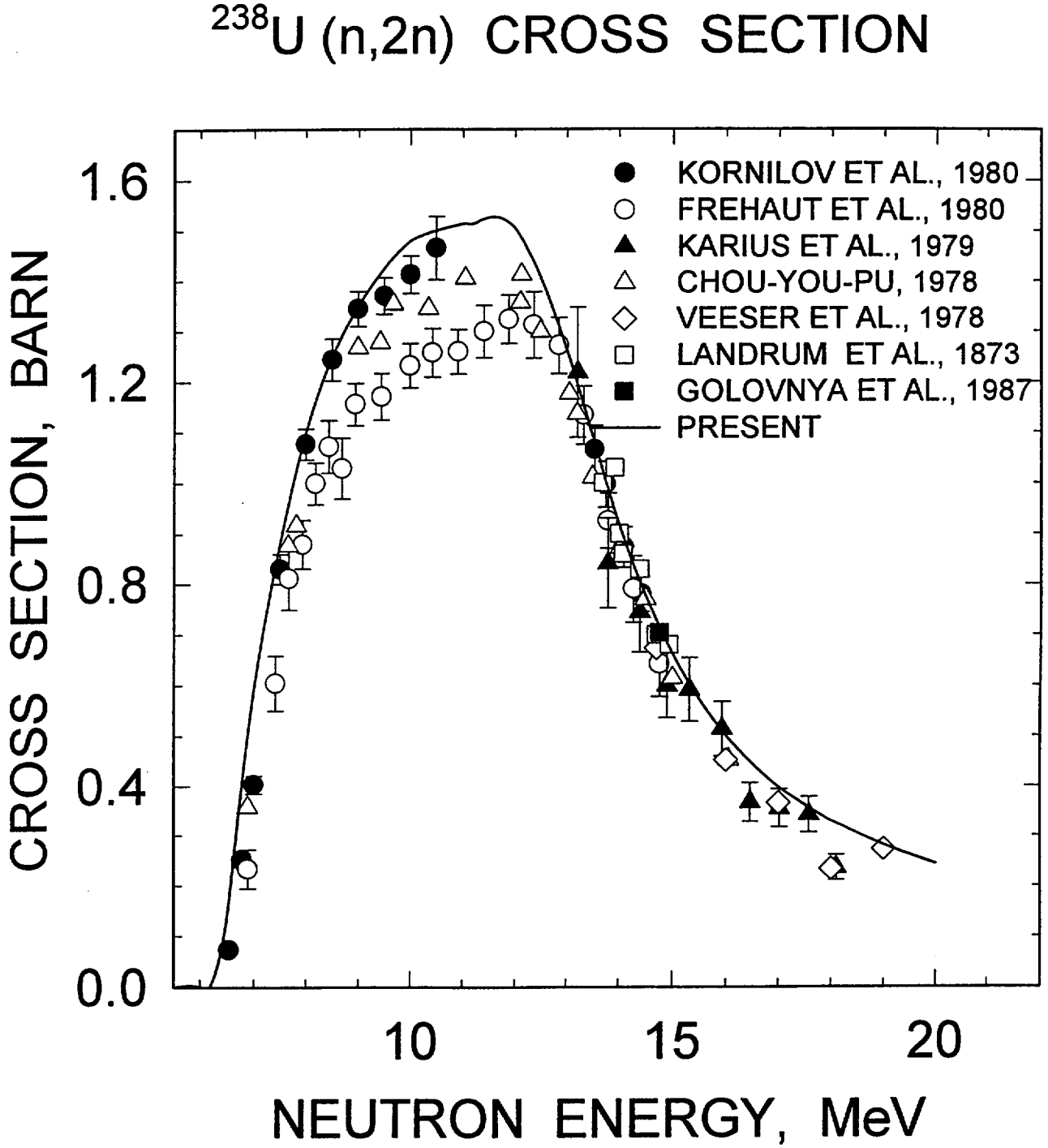
^{238}U (n,2n) CROSS SECTION
CROSS SECTION, BARN
1.6
1.2
0.8
0.4
0.0
10
15
20
NEUTRON ENERGY, MeV
KORNILOV ET AL., 1980
FREHAUT ET AL., 1980
KARIUS ET AL., 1979
CHOU-YOU-PU, 1978
VEESER ET AL., 1978
LANDRUM ET AL., 1873
GOLOVNYA ET AL., 1987
PRESENT

FIG. 49

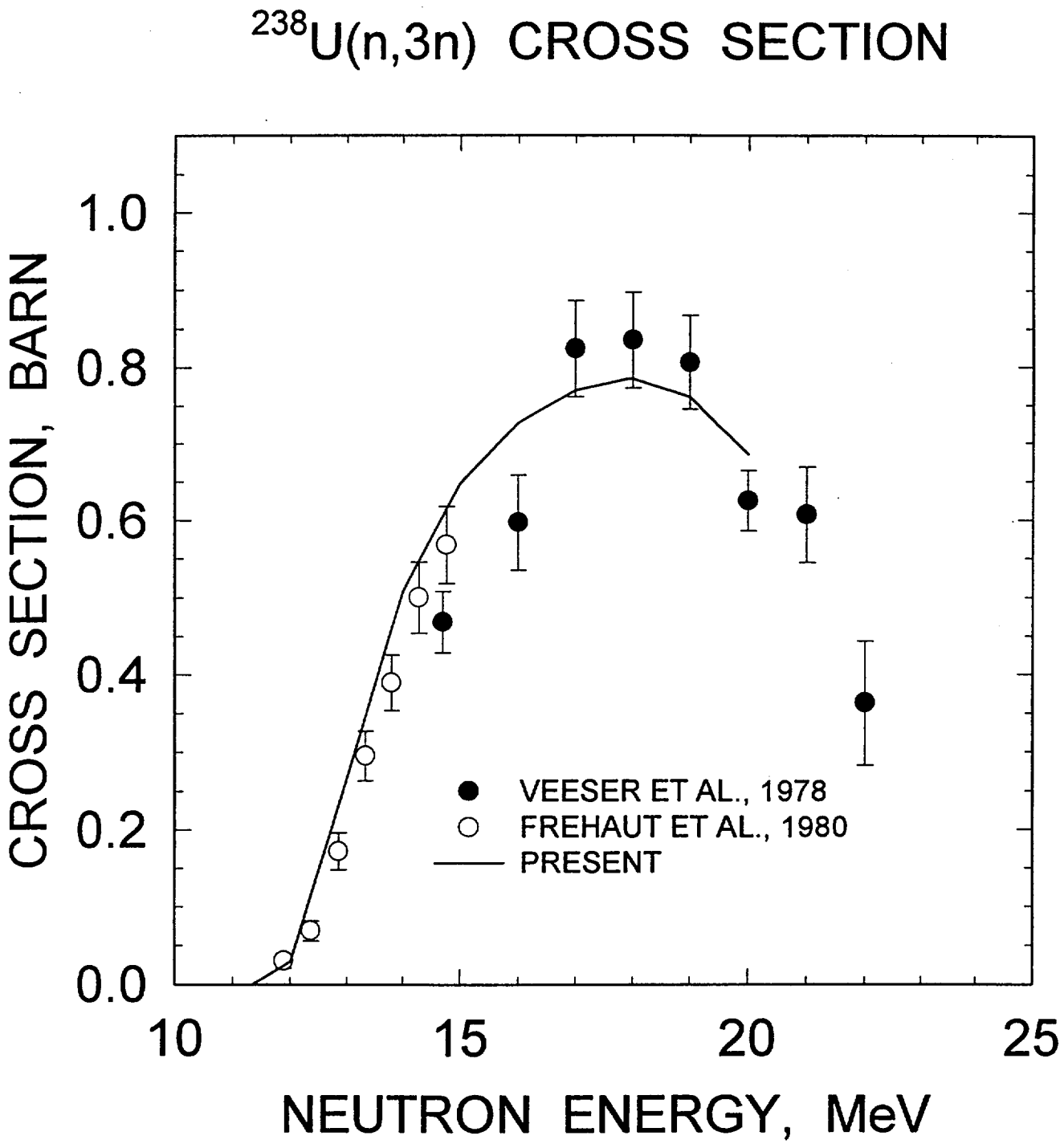
^{238}U(n,3n) CROSS SECTION
CROSS SECTION, BARN
1.0
0.8
0.6
0.4
0.2
0.0
10
15
20
25
NEUTRON ENERGY, MeV
VEESER ET AL., 1978
FREHAUT ET AL., 1980
PRESENT

FIG. 50

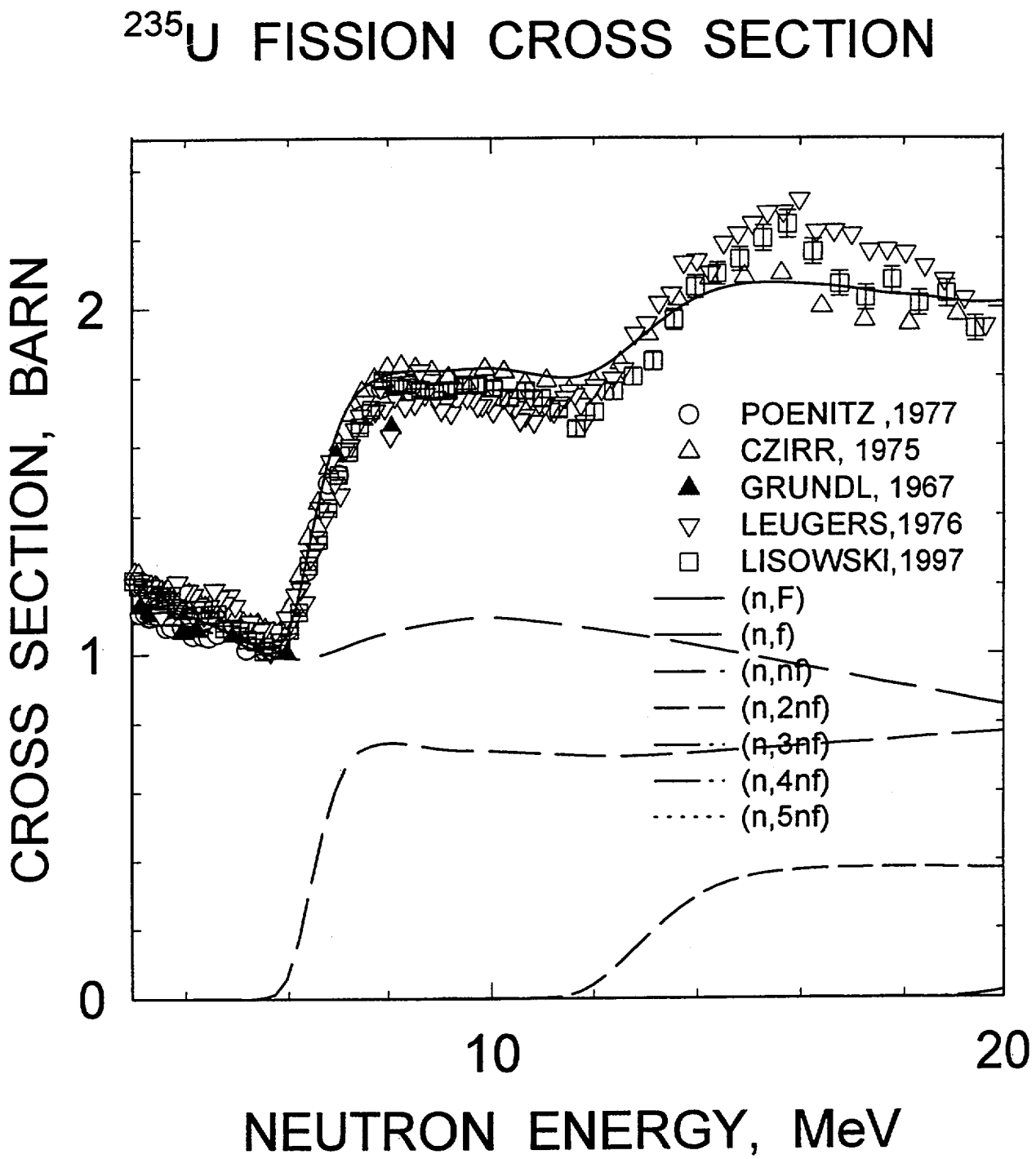
^{235}U FISSION CROSS SECTION
CROSS SECTION, BARN
0
1
2
10
20
NEUTRON ENERGY, MeV
POENITZ ,1977
CZIRR, 1975
GRUNDL, 1967
LEUGERS,1976
LISOWSKI,1997
(n,F)
(n,f)
(n,nf)
(n,2nf)
(n,3nf)
(n,4nf)
(n,5nf)

FIG. 51

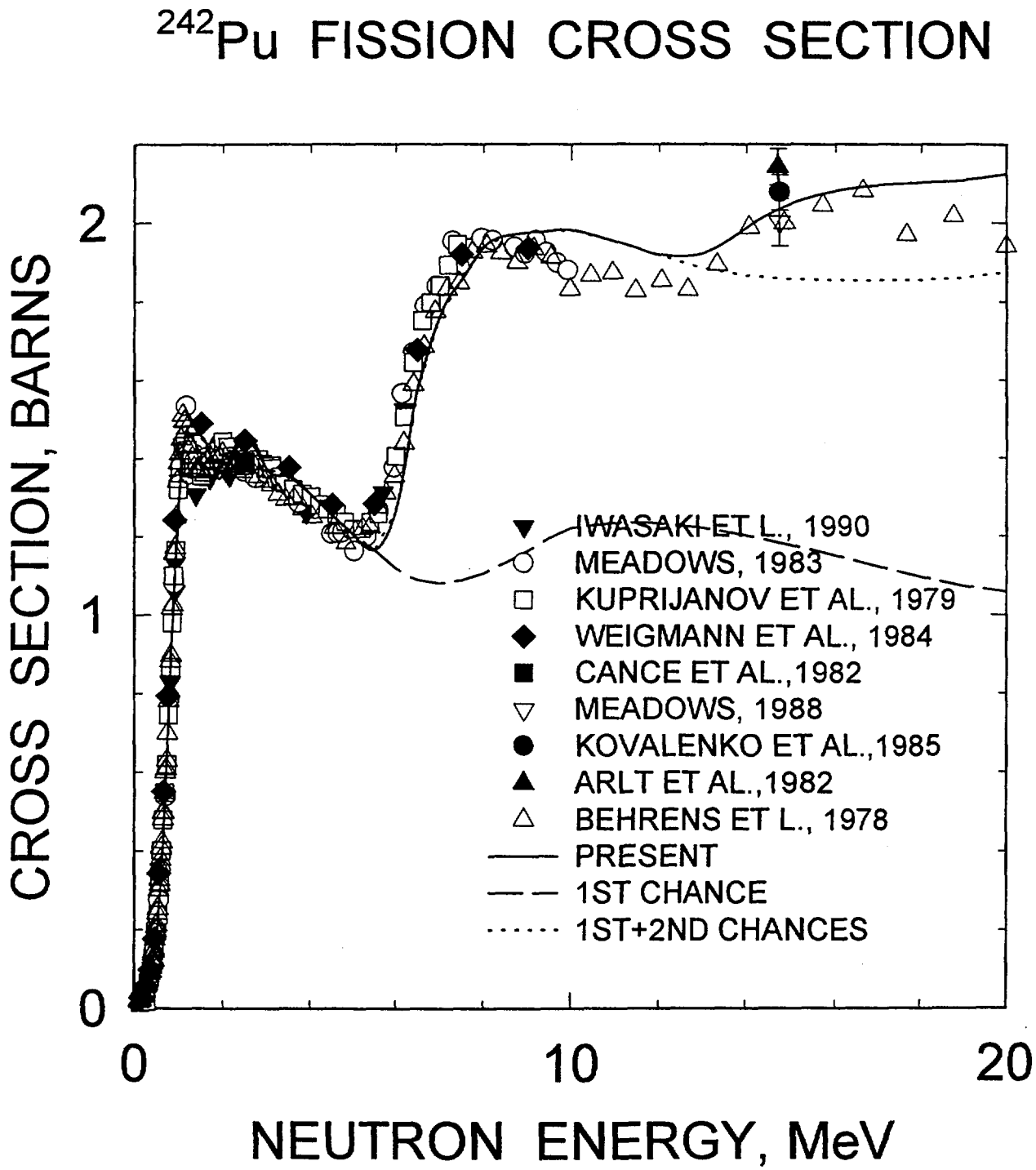
^{242}Pu FISSION CROSS SECTION
CROSS SECTION, BARNS
0
1
2
0
10
20
NEUTRON ENERGY, MeV
IWASAKI ET L., 1990
MEADOWS, 1983
KUPRIJANOV ET AL., 1979
WEIGMANN ET AL., 1984
CANCE ET AL.,1982
MEADOWS, 1988
KOVALENKO ET AL.,1985
ARLT ET AL.,1982
BEHRENS ET L., 1978
PRESENT
1ST CHANCE
1ST+2ND CHANCES

FIG. 52

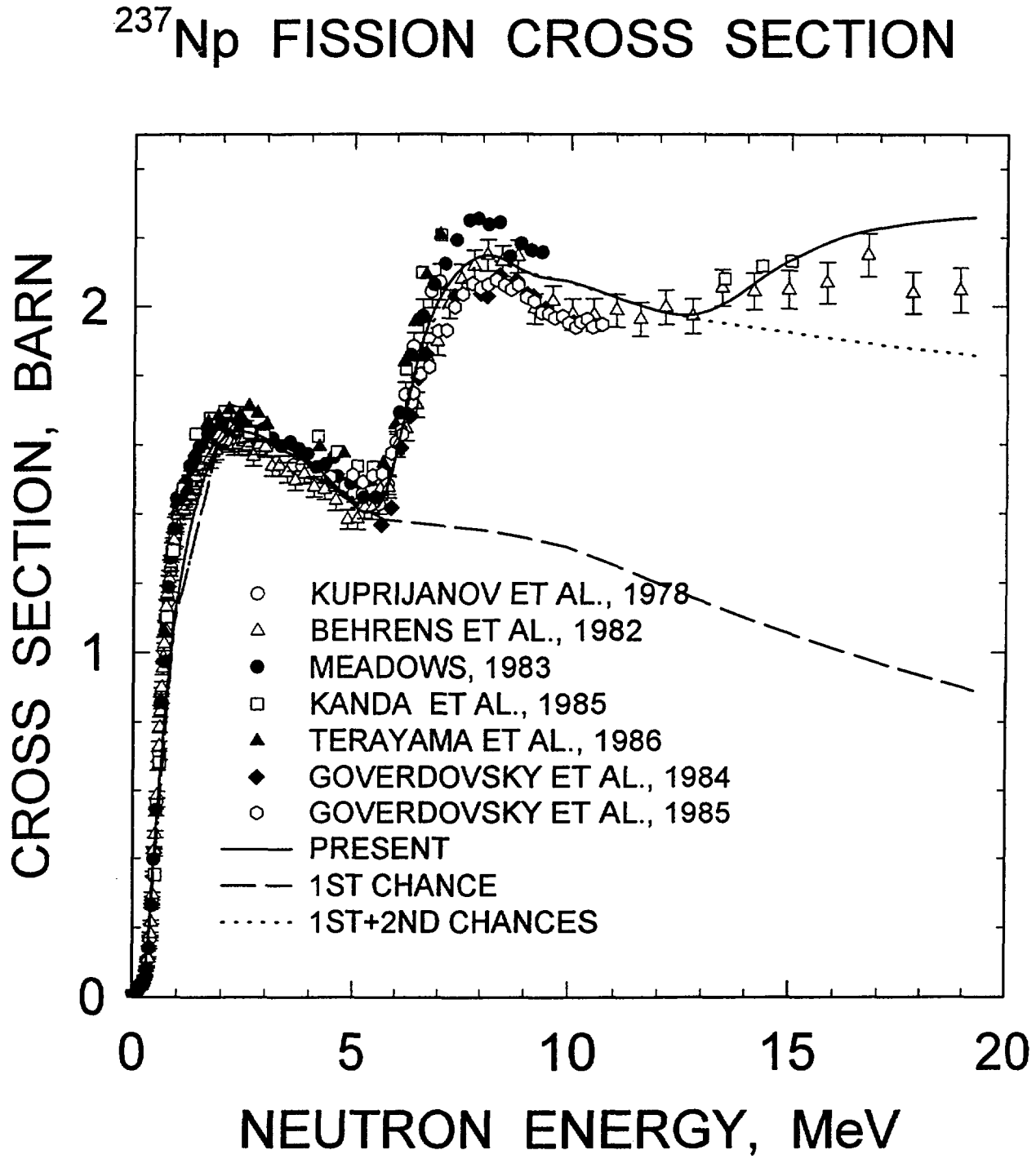
^{237}Np FISSION CROSS SECTION
CROSS SECTION, BARN
0
1
2
0
5
10
15
20
NEUTRON ENERGY, MeV
KUPRIJANOV ET AL., 1978
BEHRENS ET AL., 1982
MEADOWS, 1983
KANDA ET AL., 1985
TERAYAMA ET AL., 1986
GOVERDOVSKY ET AL., 1984
GOVERDOVSKY ET AL., 1985
PRESENT
1ST CHANCE
1ST+2ND CHANCES

FIG. 53

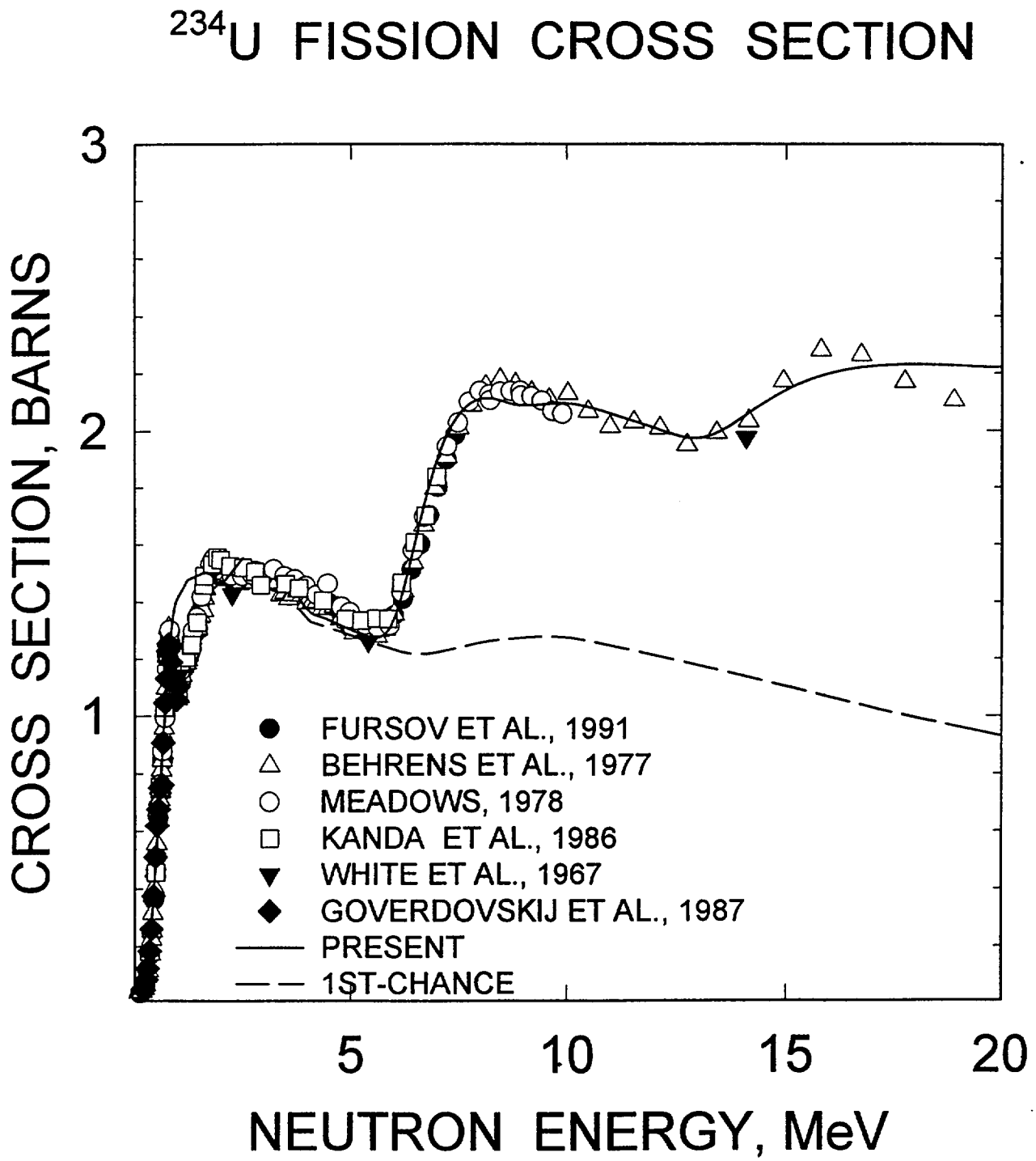
^{234}U FISSION CROSS SECTION
CROSS SECTION, BARNS
3
2
1
5
10
15
20
NEUTRON ENERGY, MeV
FURSOV ET AL., 1991
BEHRENS ET AL., 1977
MEADOWS, 1978
KANDA ET AL., 1986
WHITE ET AL., 1967
GOVERDOVSKIJ ET AL., 1987
PRESENT
1ST-CHANCE

FIG.54

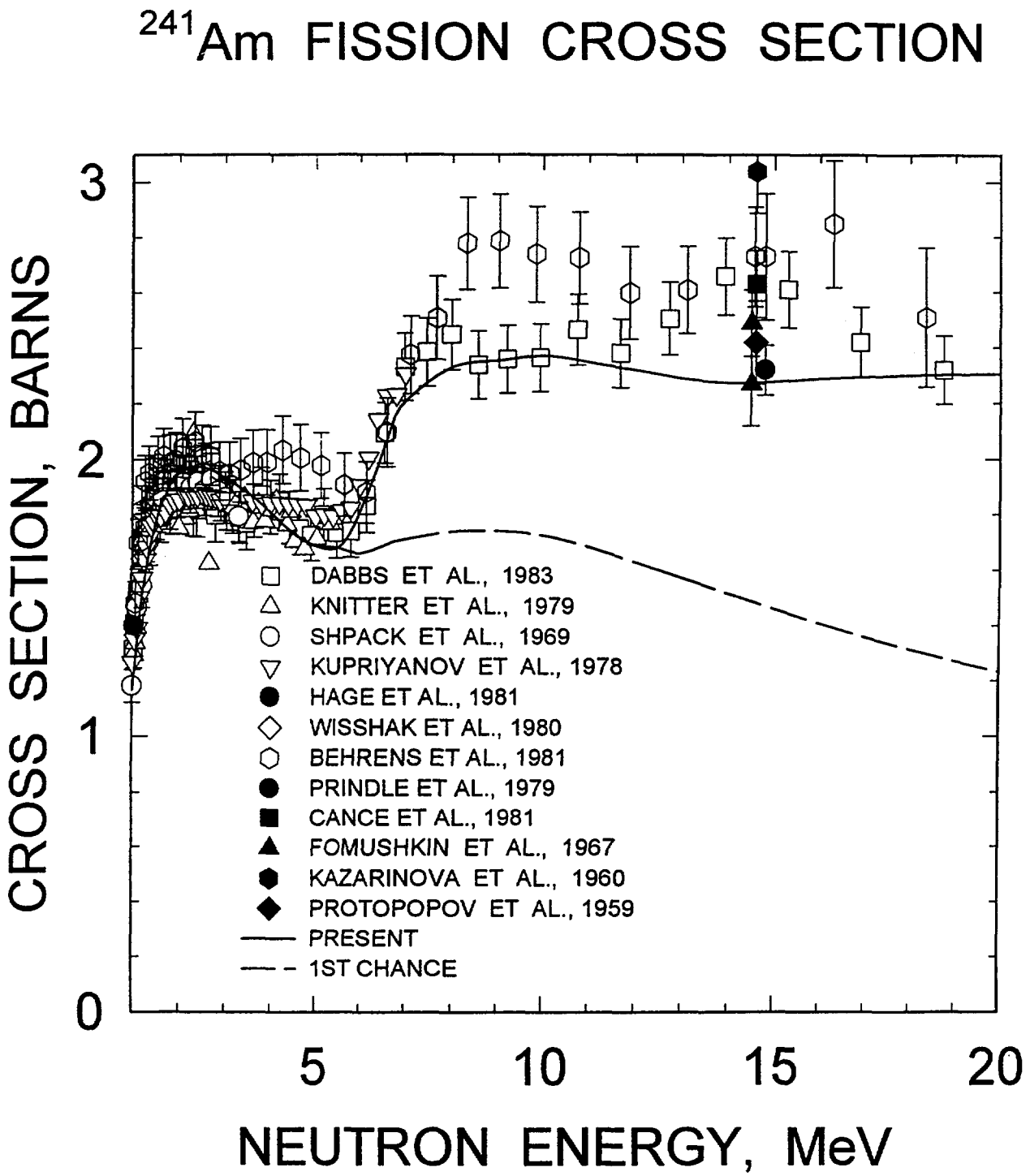
^{241}Am FISSION CROSS SECTION
CROSS SECTION, BARNS
NEUTRON ENERGY, MeV
0
1
2
3
5
10
15
20
DABBS ET AL., 1983
KNITTER ET AL., 1979
SHPACK ET AL., 1969
KUPRIYANOV ET AL., 1978
HAGE ET AL., 1981
WISSHAK ET AL., 1980
BEHRENS ET AL., 1981
PRINDLE ET AL., 1979
CANCE ET AL., 1981
FOMUSHKIN ET AL., 1967
KAZARINOVA ET AL., 1960
PROTOPOPOV ET AL., 1959
PRESENT
1ST CHANCE

FIG. 55

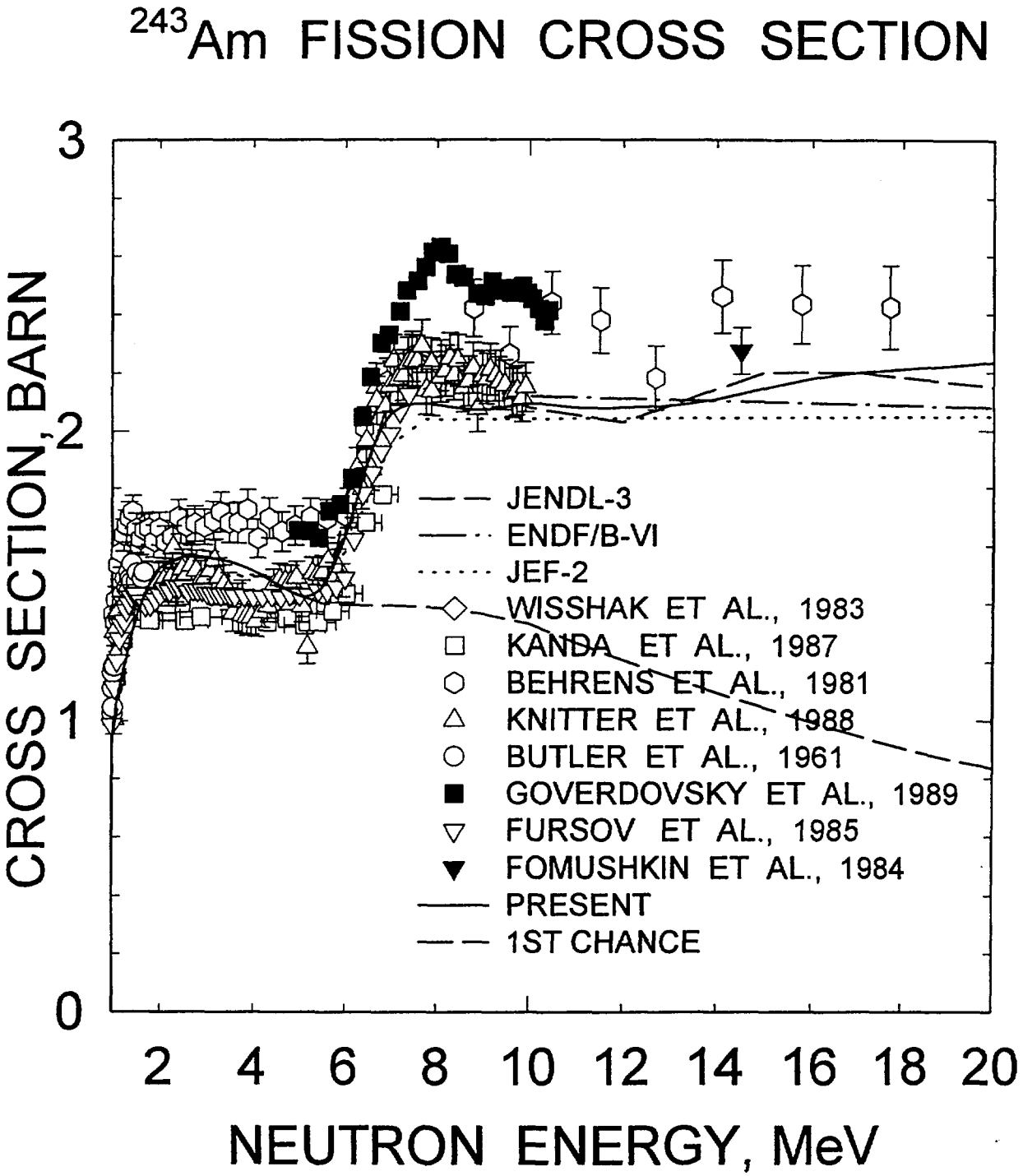
^{243}Am FISSION CROSS SECTION
CROSS SECTION, BARN
NEUTRON ENERGY, MeV
0
1
2
3
2
4
6
8
10
12
14
16
18
20
JENDL-3
ENDF/B-VI
JEF-2
WISSHAK ET AL., 1983
KANDA ET AL., 1987
BEHRENS ET AL., 1981
KNITTER ET AL., 1988
BUTLER ET AL., 1961
GOVERDOVSKY ET AL., 1989
FURSOV ET AL., 1985
FOMUSHKIN ET AL., 1984
PRESENT
1ST CHANCE

FIG. 56

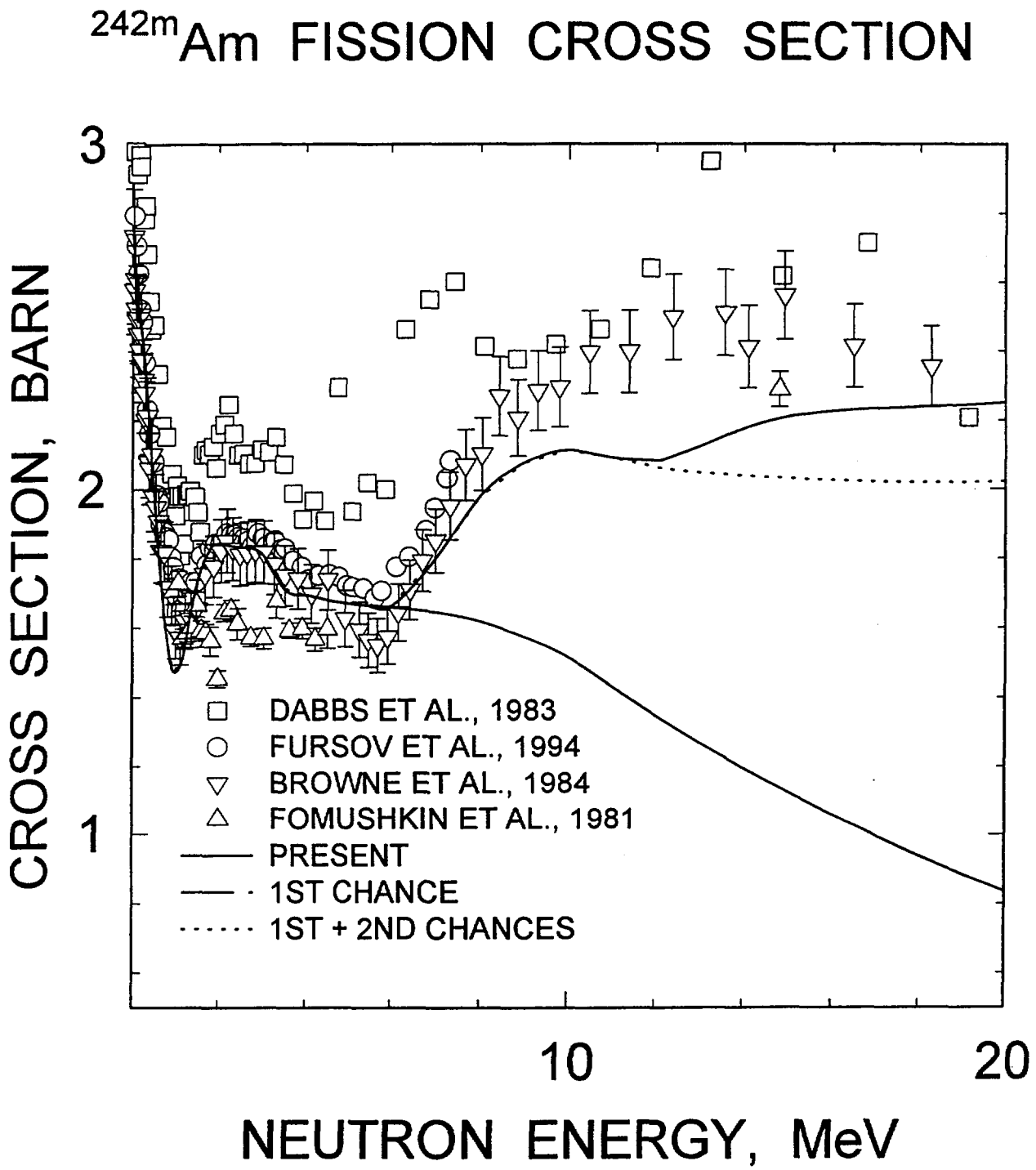
242mAm FISSION CROSS SECTION
CROSS SECTION, BARN
3
2
1
10
20
NEUTRON ENERGY, MeV
DABBS ET AL., 1983
FURSOV ET AL., 1994
BROWNE ET AL., 1984
FOMUSHKIN ET AL., 1981
PRESENT
1ST CHANCE
1ST + 2ND CHANCES

FIG. 57

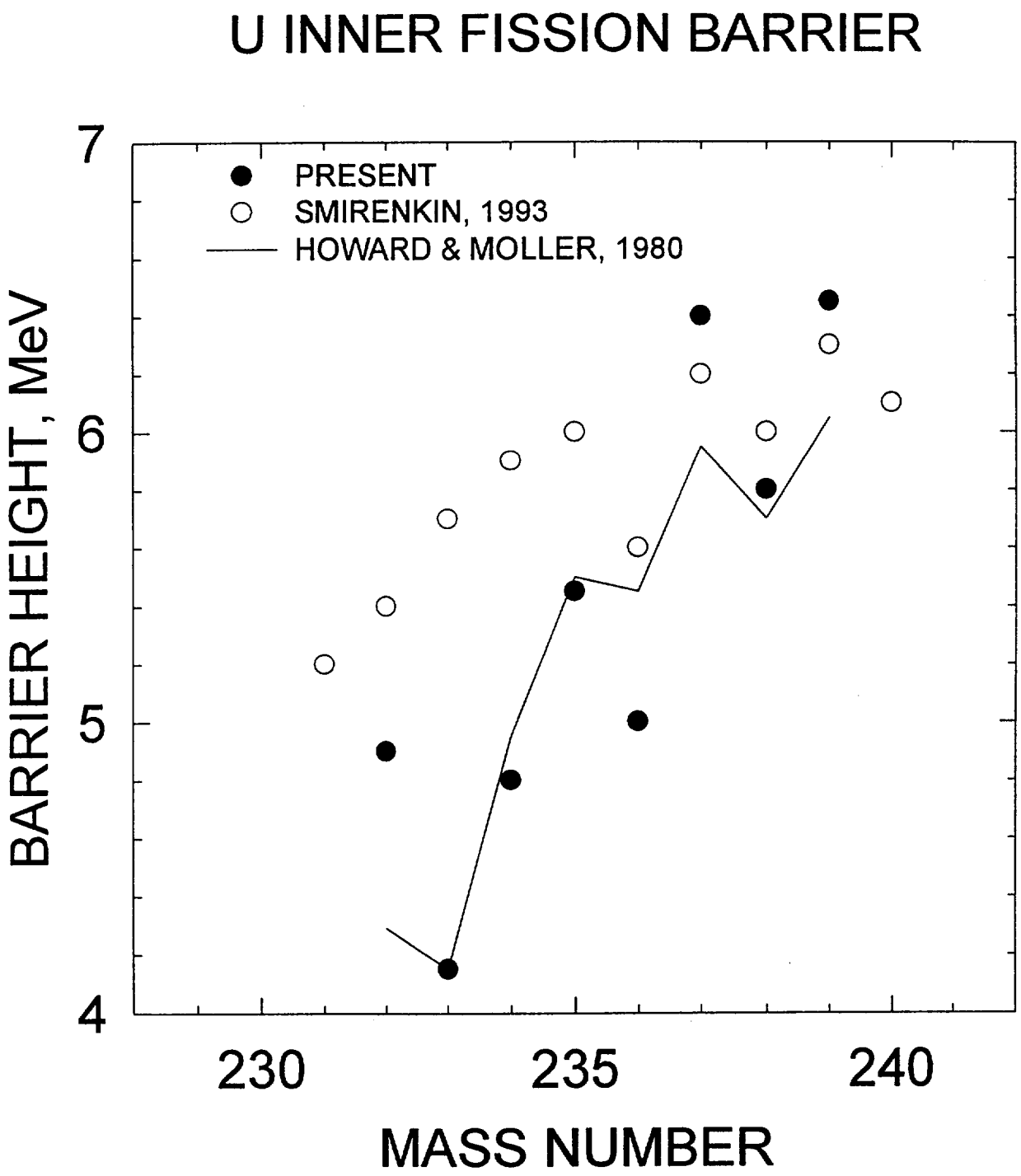
U INNER FISSION BARRIER
PRESENT
SMIRENKIN, 1993
HOWARD & MOLLER, 1980
BARRIER HEIGHT, MeV
7
6
5
4
230
235
240
MASS NUMBER

FIG. 58

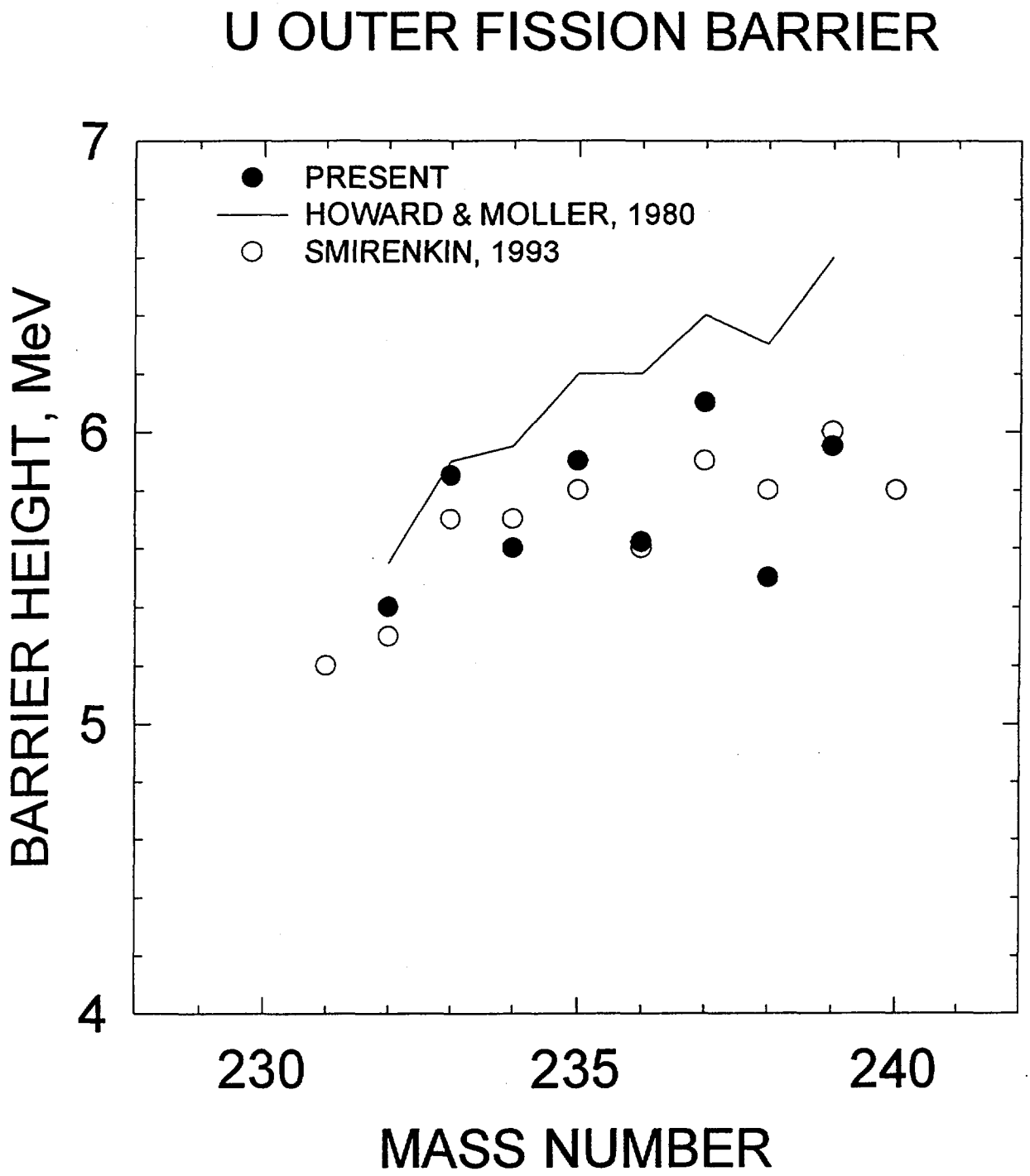
U OUTER FISSION BARRIER
PRESENT
HOWARD & MOLLER, 1980
SMIRENKIN, 1993
BARRIER HEIGHT, MeV
7
6
5
4
230
235
240
MASS NUMBER

FIG. 59

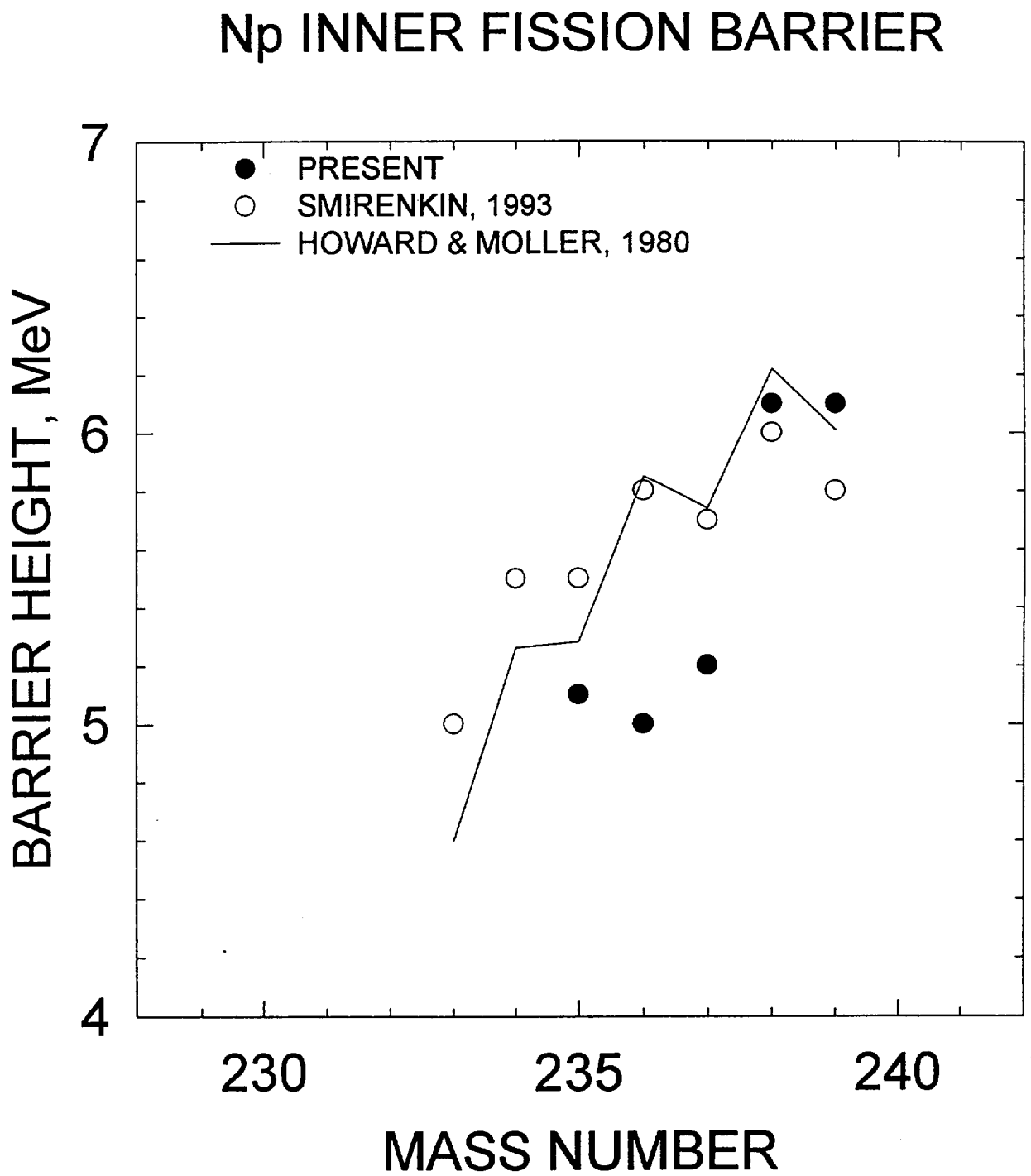
Np INNER FISSION BARRIER
PRESENT
SMIRENKIN, 1993
HOWARD & MOLLER, 1980
BARRIER HEIGHT, MeV
7
6
5
4
230
235
240
MASS NUMBER

FIG. 60

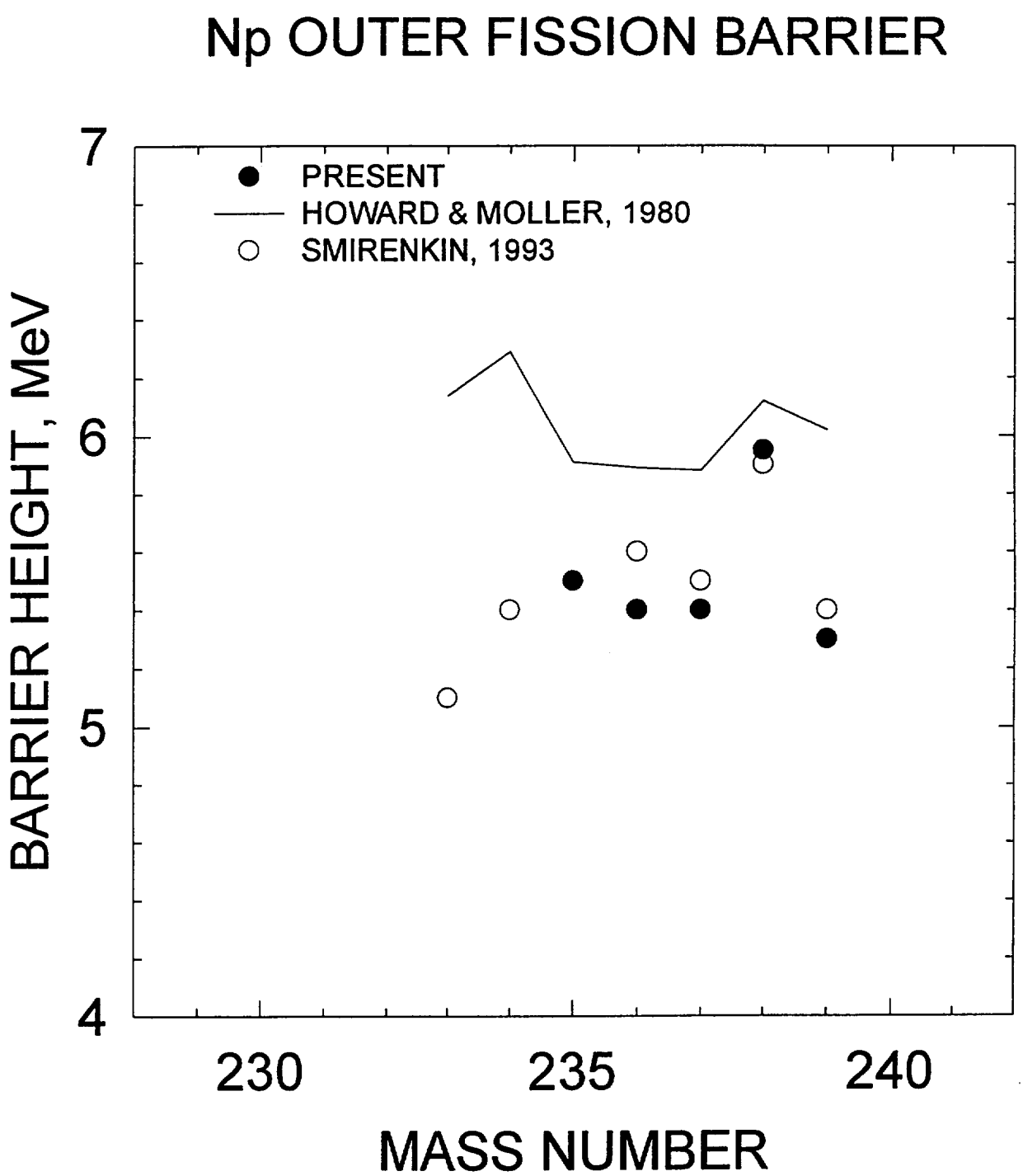
Np OUTER FISSION BARRIER
PRESENT
HOWARD & MOLLER, 1980
SMIRENKIN, 1993
BARRIER HEIGHT, MeV
7
6
5
4
230
235
240
MASS NUMBER

FIG. 61

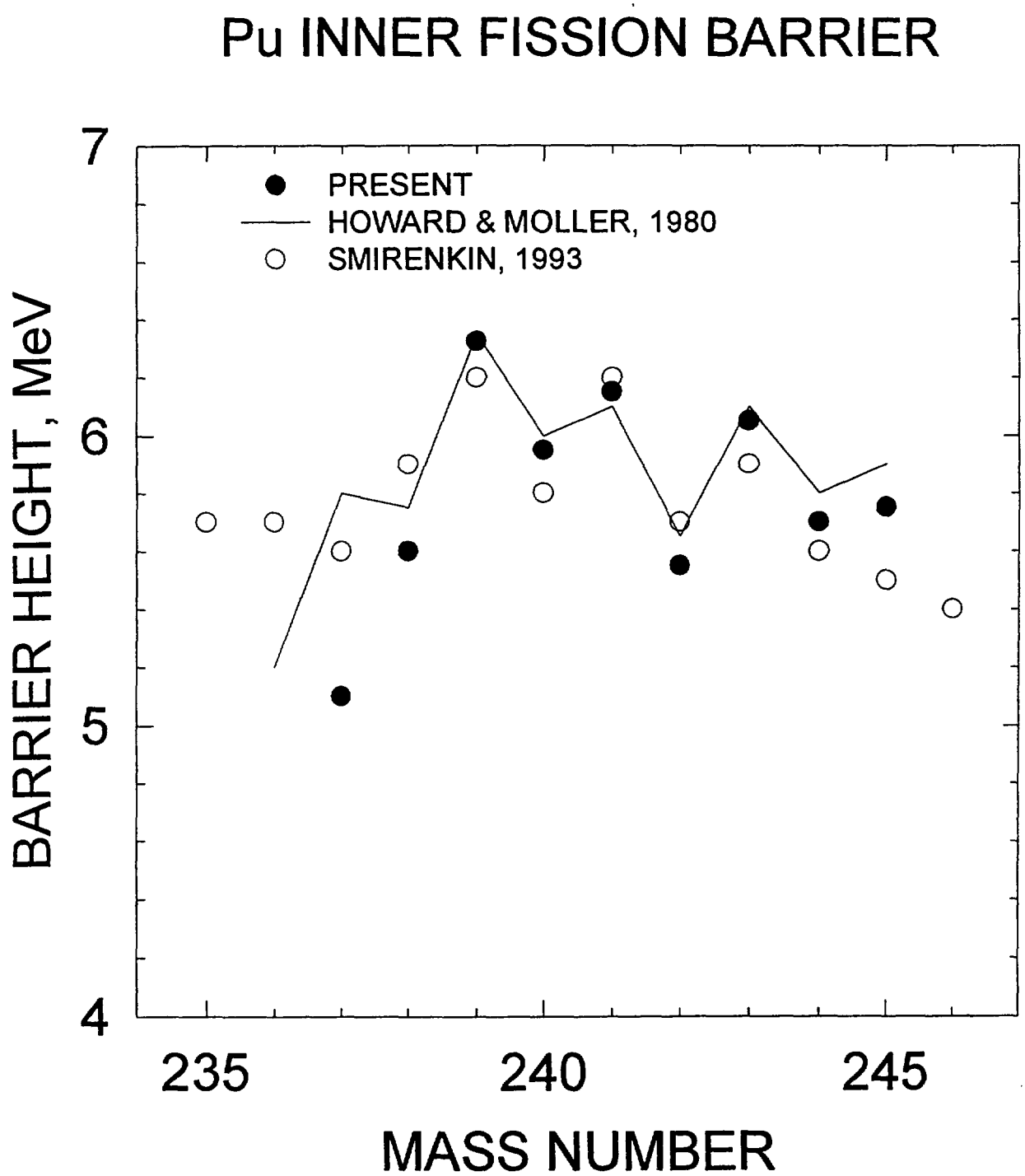
Pu INNER FISSION BARRIER
PRESENT
HOWARD & MOLLER, 1980
SMIRENKIN, 1993
BARRIER HEIGHT, MeV
7
6
5
4
235
240
245
MASS NUMBER

FIG. 62

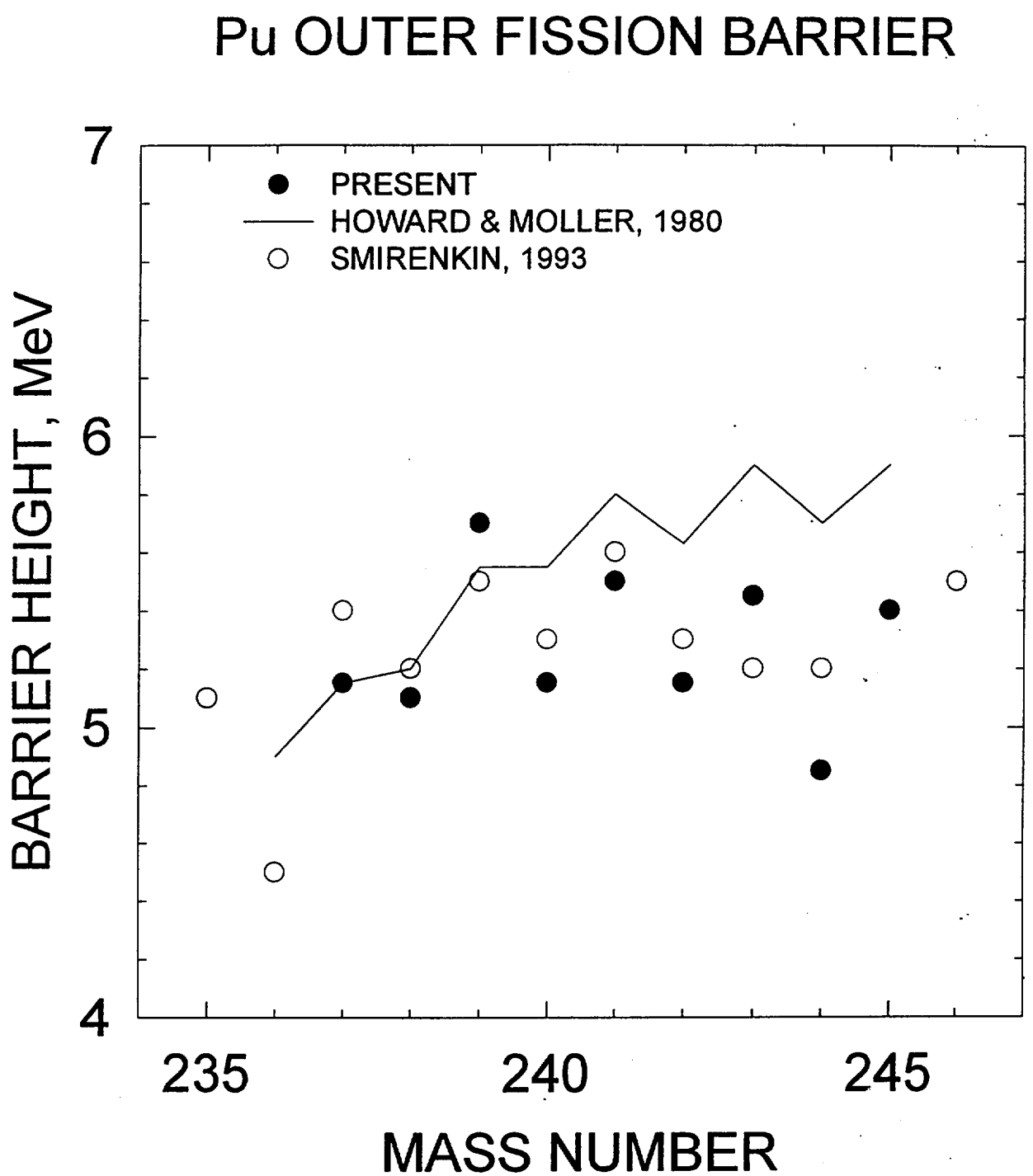
Pu OUTER FISSION BARRIER
PRESENT
HOWARD & MOLLER, 1980
SMIRENKIN, 1993
BARRIER HEIGHT, MeV
7
6
5
4
235
240
245
MASS NUMBER

FIG. 63

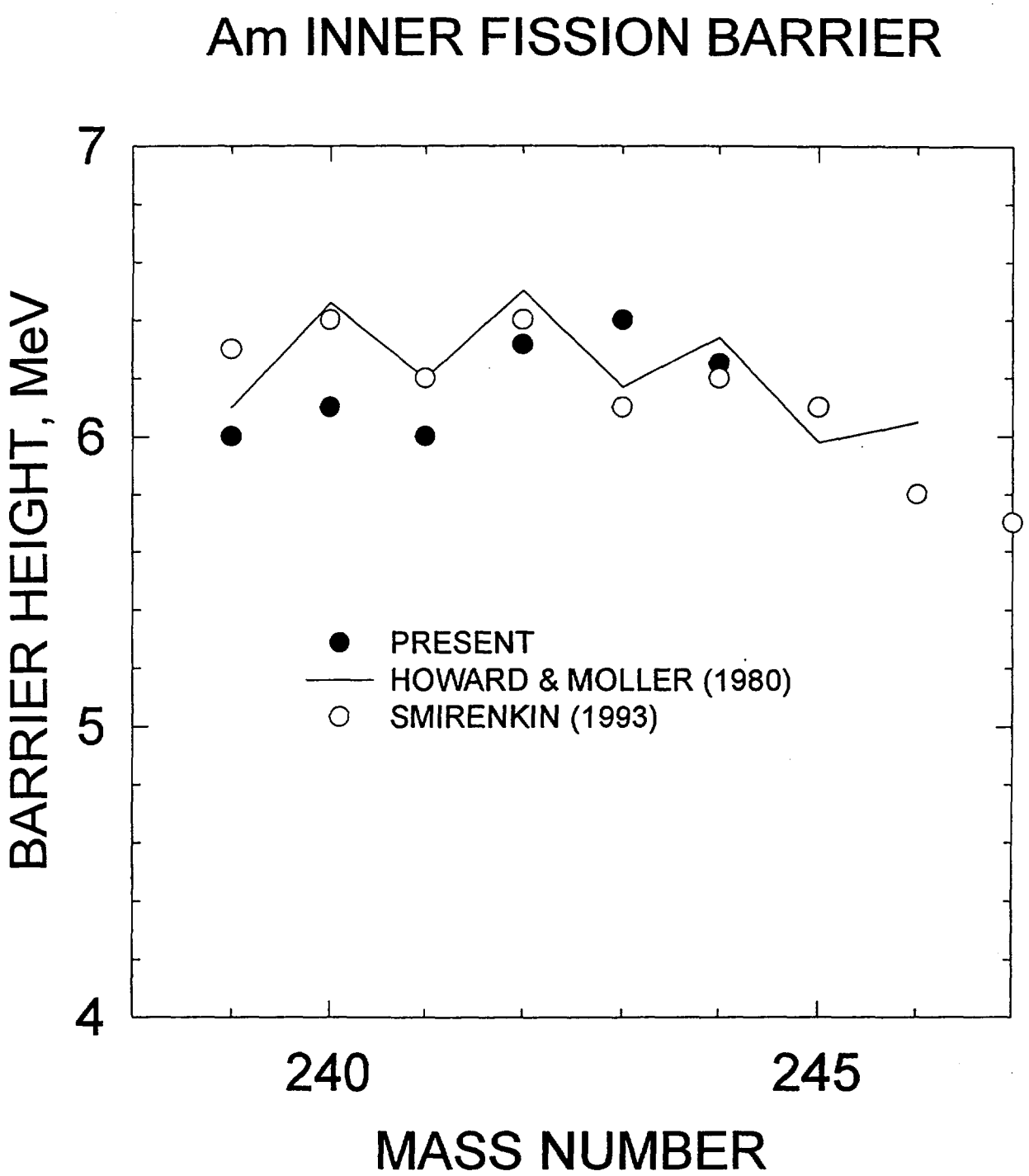
Am INNER FISSION BARRIER
BARRIER HEIGHT, MeV
7
6
5
4
240
245
MASS NUMBER
PRESENT
HOWARD & MOLLER (1980)
SMIRENKIN (1993)

FIG. 64

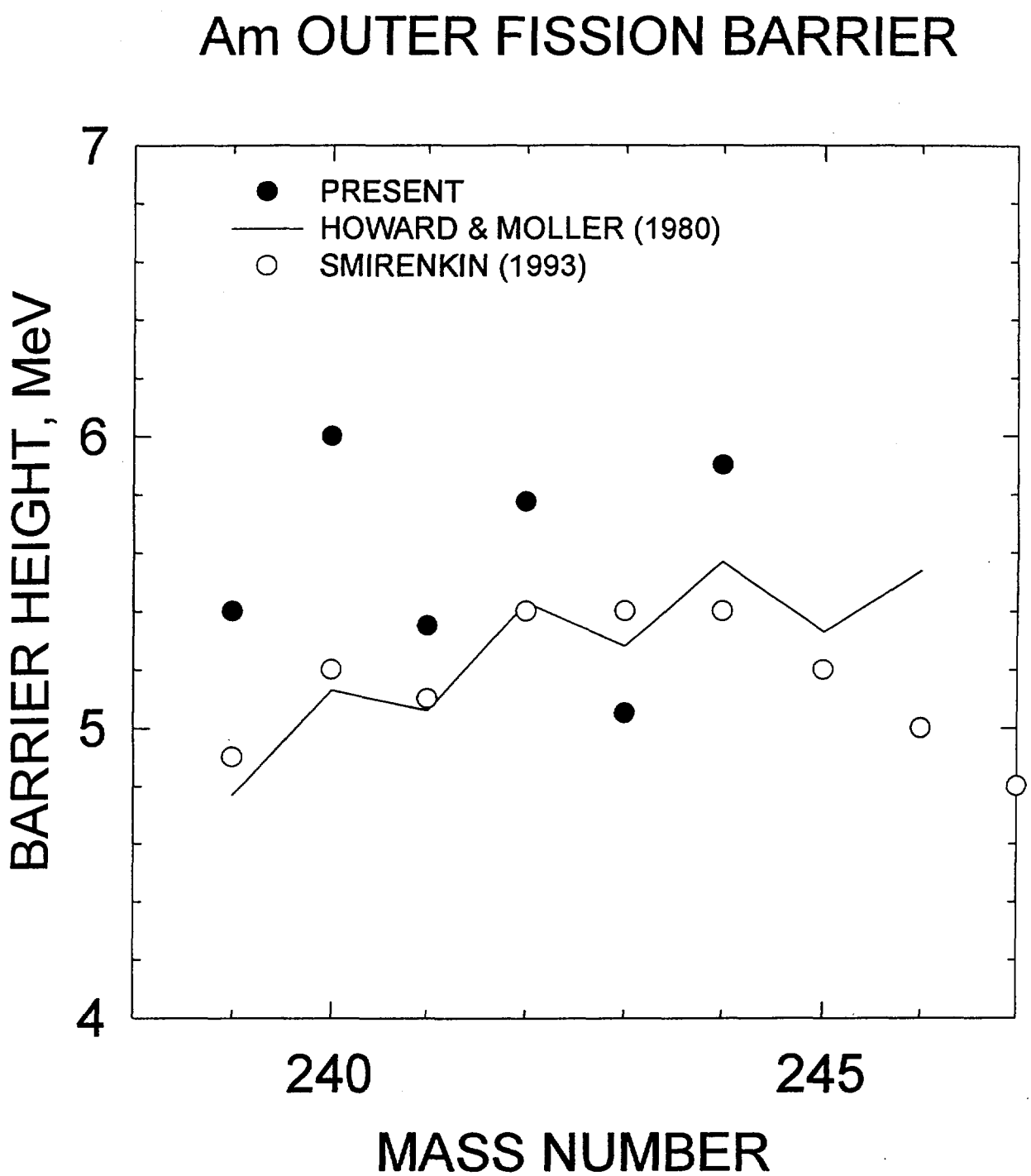
Am OUTER FISSION BARRIER
PRESENT
HOWARD & MOLLER (1980)
SMIRENKIN (1993)
BARRIER HEIGHT, MeV
7
6
5
4
240
245
MASS NUMBER

FIG. 65

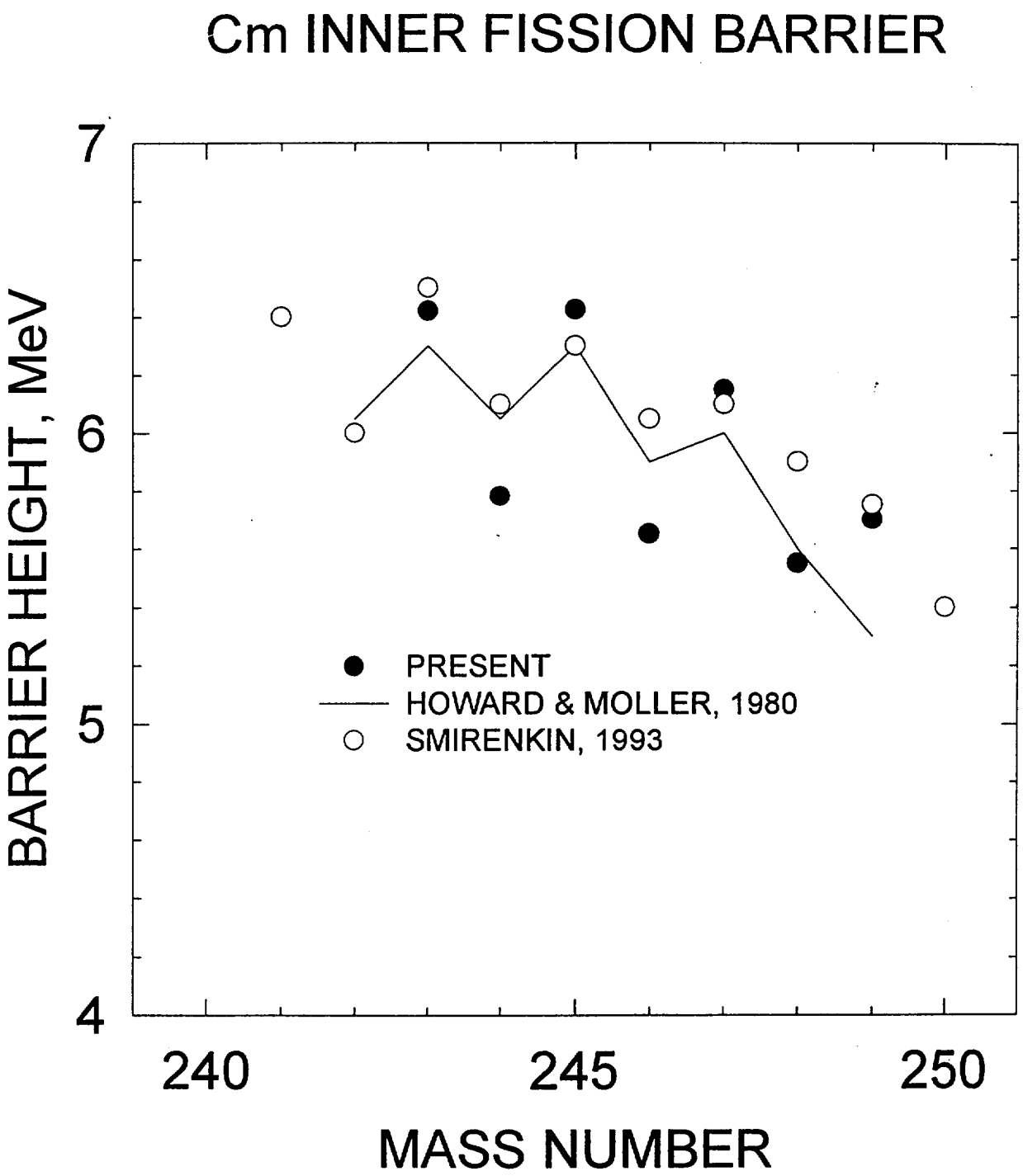
Cm INNER FISSION BARRIER
BARRIER HEIGHT, MeV
7
6
5
4
240
245
250
MASS NUMBER
PRESENT
HOWARD & MOLLER, 1980
SMIRENKIN, 1993

FIG. 66

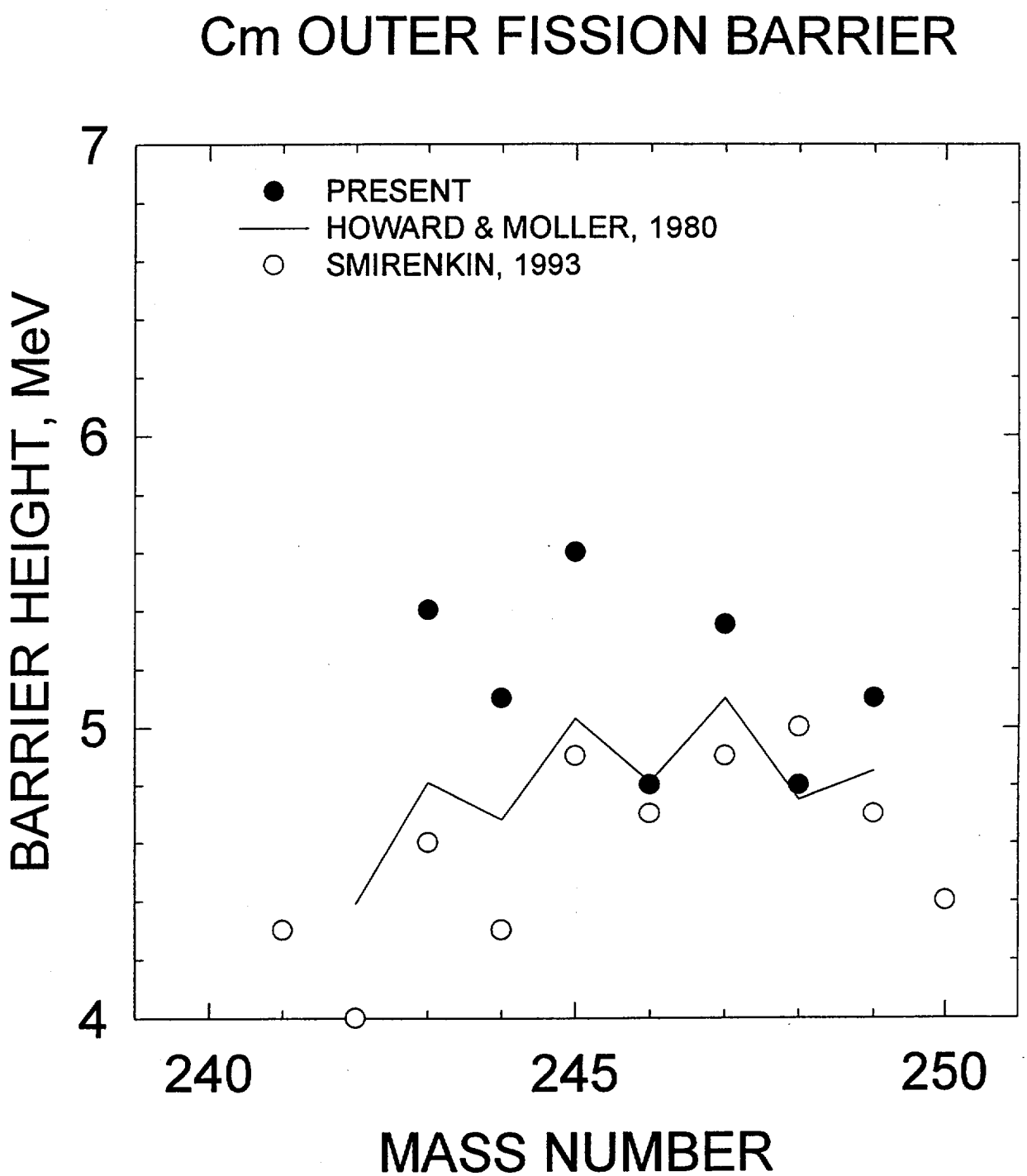
Cm OUTER FISSION BARRIER
PRESENT
HOWARD & MOLLER, 1980
SMIRENKIN, 1993
BARRIER HEIGHT, MeV
7
6
5
4
240
245
250
MASS NUMBER

FIG. 67

Nuclear Data Section
International Atomic Energy Agency
P.O. Box 100
A-1400 Vienna
Austria

e-mail: services@iaeand.iaea.or.at
fax: (43-1)26007
cable: INATOM VIENNA
telex: 1-12645 atom a
telephone: (43-1)2600-21710

online: TELNET or FTP: iaeand.iaea.or.at
username: IAEANDS for interactive Nuclear Data Information System
username: ANONYMOUS for FTP file transfer
username: FENDL for FTP file transfer of FENDL-1 files, FENDL2 for FENDL-2 files
For users with Web-browsers: http://www-nds.iaea.or.at